High Energy Resummation in Quantum Chromo–Dynamics

Simone Marzani

Thesis submitted for the degree of **Doctor of Philosophy**
The University of Edinburgh
2008

Abstract

In this thesis I discuss different aspects of high energy resummation in Quantum Chromo-Dynamics and its relevance for precision physics at hadron colliders. The high energy factorisation theorem is presented and discussed in detail, emphasizing its connections with standard factorisation of collinear singularities. The DGLAP and the BFKL equations are presented and leading twist duality relations between the evolution kernels are discussed.

High energy factorisation is used to compute resummed coefficient functions for hadronic processes relevant for LHC phenomenology. The case of heavy flavour production is analysed in some detail and results already present in the literature are confirmed. High energy effects can play an important role for such cross sections which are to be used as standard candles at the LHC, such as W/Z production. To this purpose Drell-Yan processes are studied in high energy factorisation.

The inclusive cross section for Higgs boson production via gluon-gluon fusion is analysed both in the heavy top limit and for finite values of the top mass. The different high energy behaviour of the two cases is studied, showing explicitly that the full theory exhibits single high energy logarithms in contrast to the infinite top mass limit. The correct high energy behaviour of the partonic cross section is then combined to the NNLO calculation performed in the heavy top limit, in order to obtain an improved coefficient function. Finite top mass effects at high energy on the hadronic cross section are moderate.

As far as parton evolution is concerned, an approximate expression for the NNLO contribution to the kernel of the BFKL equation is computed exploiting running coupling duality relations between DGLAP and BFKL. This result includes all collinear and anticollinear singular contributions and it is computed in various factorisation schemes. The collinear approximation is tested against the known LO and NLO kernels with the discrepancy being at the percent level. Therefore the approximate NNLO contribution is likely to be close to the as yet unknown complete result in the region relevant at leading twist.

Declaration

I do hereby declare that this thesis was composed entirely by myself and that the work described within is my own, except where explicitly stated otherwise.

The results presented in Chapter 5 are published in:
S. Marzani, R. D. Ball, V. Del Duca, S. Forte and A. Vicini,
Higgs production via gluon-gluon fusion with finite top mass beyond next-to-leading order,
Nuclear Physics B **800** (2008) 127 [arXiv:0801.2544 [hep-ph]].

The results presented in Chapter 6 are published in:
S. Marzani, R. D. Ball, P. Falgari and S. Forte,
BFKL at Next-to-Next-to-Leading Order,
Nuclear Physics B **783** (2007) 143 [arXiv:0704.2404 [hep-ph]].

Simone Marzani
October, 2008

Acknowledgements

First of all I would like to thank my supervisor Richard Ball for all I have learnt from him over these three years. I am also very grateful to Stefano Forte for his constant support and help. I would like to thank all the people in the Edinburgh PPT group, especially Thomas Binoth, Einan Gardi, Tilman Plehn, Luigi Del Debbio and Alberto Guffanti for many useful discussions and Tobias for reading this thesis. Thanks to all the physics PhD students, especially those I shared the office with: Ben, Tom, Dave, Maria, Chris, Eike and Matthew. I spent really good time with all of you. It has been a pleasure to work with Vittorio Del Duca, Alessandro Vicini and Pietro Falgari. These doctoral studies would not have been possible without the financial support of the Scottish Universities' Physics Alliance.

My most special thanks goes to Federica, who is always *here*, despite the distance. And of course also to my parents, my brother and my grandmother and all my family, whom I have always felt very close. I also want to mention all the people I left in Milan three years ago, whose friendship is still profound. This, like anything else, is for Caf.

This has been my first time in a foreign country and Edinburgh has been an amazing place to live in. It has not been easy from the beginning but now I can only be grateful for the many and so different experiences I had. People from other countries and with different cultures had opened my eyes to a world of possibilities, destroying my certainties, forcing me to discover things of myself I did not know before. But, most important, Edinburgh has been the place where I met new friends, which I would like to thank for the great time spent together. My flatmates at 25 WPT: Daria, Rupe, Sayaka, Ema, Raph, Shona and Claudia; but also Lucio, Fede, Cecile, Ana Arel, Sebastian, Nikos, Vasso, the Greeks and all the people I have randomly met around. Now it is time to leave, but I hope we shall find ways to keep in contact. *¡Qué lástima, pero adiós!*

Contents

Abstract i

Declaration ii

Acknowledgements iii

1 Introduction 3

2 Perturbative Quantum Chromo–Dynamics 6
- 2.1 QCD and the parton model . . . 6
  - 2.1.1 Deep inelastic scattering as an example . . . 7
  - 2.1.2 The DGLAP equations . . . 15
  - 2.1.3 Collinear factorisation theorem . . . 20
- 2.2 An Introduction to BFKL . . . 22
  - 2.2.1 Regge theory . . . 22
  - 2.2.2 The BFKL equation . . . 27
  - 2.2.3 BFKL kernel at next-to leading order . . . 32

3 High energy resummation 37
- 3.1 k_T-factorisation . . . 37
- 3.2 Duality . . . 46
  - 3.2.1 Duality beyond leading order . . . 46
  - 3.2.2 Small x resummed evolution . . . 53
- 3.3 Resummation of the coefficient function . . . 59

4 Hadronic processes at high energy 63
- 4.1 Heavy flavour production . . . 63
  - 4.1.1 The coefficient function at high energy . . . 63
  - 4.1.2 The N dependence of the impact factor . . . 67
- 4.2 Drell-Yan processes . . . 69
  - 4.2.1 The Drell-Yan cross section . . . 70
  - 4.2.2 The off-shell calculation . . . 72
  - 4.2.3 The coefficient function at high energy . . . 77
  - 4.2.4 Vector boson production . . . 79

5 Higgs boson production via gluon-gluon fusion **81**
5.1 Higgs boson at hadron colliders . . . 81
5.2 The $m_t \to \infty$ calculation in k_T-factorisation . . . 86
5.3 The finite top mass case . . . 90
5.3.1 The off-shell cross section . . . 90
5.3.2 The high energy behaviour . . . 94
5.4 Improvement of the NNLO coefficient function . . . 98

6 BFKL from DGLAP at next-to-next-to-leading order **107**
6.1 Factorisation schemes . . . 108
6.2 The collinear approximation . . . 111
6.2.1 The $\mathcal{R}$ factor . . . 114
6.2.2 Symmetrisation and results . . . 118

7 Conclusions and Outlook **127**
7.1 Drell-Yan and vector boson production . . . 127
7.2 Higgs production . . . 128
7.3 Approximate BFKL kernel . . . 129
7.4 Outlook . . . 129

A Kinematics of $2 \to 2$ processes **130**
A.1 d-dimensional two-body phase space . . . 130
A.2 Kinematics of off-shell processes . . . 131

B Form factors for $g^*g^* \to H$ **133**

C Explicit results for χ_2 **136**

Bibliography **139**

Chapter 1

Introduction

Hadron colliders such as the Tevatron at Fermilab and the Large Hadron Collider (LHC) at CERN test our understanding of particle physics at the smallest scales, trying to find deviations of the data from the Standard Model and hence discover new physics. In order to be able to separate a tiny fraction of interesting events from a huge background, the phenomenology of the Standard Model has to be understood with very high accuracy. The vast majority of Standard Model events are due to strong interactions.

The search for a theory of the strong force started in the Sixties of the past century with the main target of explaining the growing number of hadrons produced in experiments; one of the major breakthroughs was the quark model, proposed by Gell-Mann. This model describes the hadronic spectrum in terms of elementary constituents, the quarks; it also leads to the introduction of a new degree of freedom: the colour. Nowadays Quantum Chromo-Dynamics (QCD) is accepted as the theory of strong interactions. It is a non-Abelian gauge theory with gauge group $SU(3)_c$: it describes the interaction between fermionic and bosonic fields associated to quarks and gluons respectively (see for instance [1]-[3] and references therein). The Lagrangian of QCD is:

$$\mathcal{L} = -\frac{1}{4} G^A_{\mu\nu} G^{\mu\nu}_A + \sum_{flavours} \bar{\psi}_a (i\gamma_\mu D^\mu - m)_{ab} \psi_b \,, \tag{1.1}$$

where D^μ is the covariant derivative and $G^A_{\mu\nu}$ is the field strength, defined by:

$$G^A_{\mu\nu} = \partial_\mu A^A_\nu - \partial_\nu A^A_\mu - g_s f^{ABC} A^B_\mu A^C_\nu \,.$$

It is well known that the strong coupling $\alpha_s = g_s/4\pi$ is a decreasing function of the energy involved in the process. For this reason QCD has a low energy regime, in which the theory is strongly interacting and a high energy one, in which it is asymptotically free. This implies that strong processes are computable in perturbation

theory if a sufficiently high energy scale is involved. However, the computation of cross sections for hadronic processes always involves non-perturbative contributions, because the initial states are hadrons, which cannot be described in perturbation theory. Nevertheless factorisation enables one to separate the hard part of a process, computable in perturbation theory, from a low energy one, which is process-independent and can be taken as a phenomenological input. More details about factorisation are given in Chapter 2.

In order to improve the accuracy of theoretical predictions in QCD phenomenology, higher order terms in the perturbative expansion have been studied and cross sections have been computed at next-to-leading order (NLO) and, in some cases, also at next-to-next-to-leading order (NNLO). However, in certain regions of the phase space, the expansion in powers of the coupling constant α_s is no longer good. Cross sections contain terms proportional to the logarithm of some kinematical variable ω:

$$\sigma = \alpha_s a_0 \ln\omega + \alpha_s^2 \left(a_1 \ln^2\omega + b_0 \ln\omega\right) + \dots \tag{1.2}$$

If ω is very large or close to zero the logarithm is large and hence:

$$\alpha_s \ln\omega \sim 1, \tag{1.3}$$

even if the coupling is small; this clearly invalidates the perturbative expansion. In order to get reliable predictions, these logarithms have to be resummed to all orders. The perturbative expansion is reorganised as follows:

$$\sigma = \sum_k \left(\alpha_s \ln\omega\right)^{k+1} a_k + \alpha_s \sum_k \left(\alpha_s \ln\omega\right)^{k+1} b_k + \dots \tag{1.4}$$

The first term corresponds to a leading order resummation, while the second one to a next-to-leading order one. One may encounter different kinds of logarithms and different techniques have to be used to perform the resummation. For instance, the resummation of logarithms of the hard scale of the process ($\omega = Q^2/\mu^2$), due to the emission of collinear partons, is performed thanks to the DGLAP evolution equation. In this thesis the resummation of high energy logarithms is discussed in detail; in this case $\omega = x$, x being the ratio of the hard scale and the centre-of-mass energy. The high energy, or small x, behaviour of QCD is described by the BFKL evolution equation. Another important class of logarithms is given by $\omega = 1 - x$ and they are originated by soft radiation.

The LHC explores a region of the kinematic plane (x, Q^2) larger than any other collider before, reaching $x \sim 10^{-6}$, as shown in fig. 1.1. Very small values of x can be obtained at large rapidities y, which means that the produced particles are very close to the beam-pipe. This is the field of diffractive physics and small x resummation is

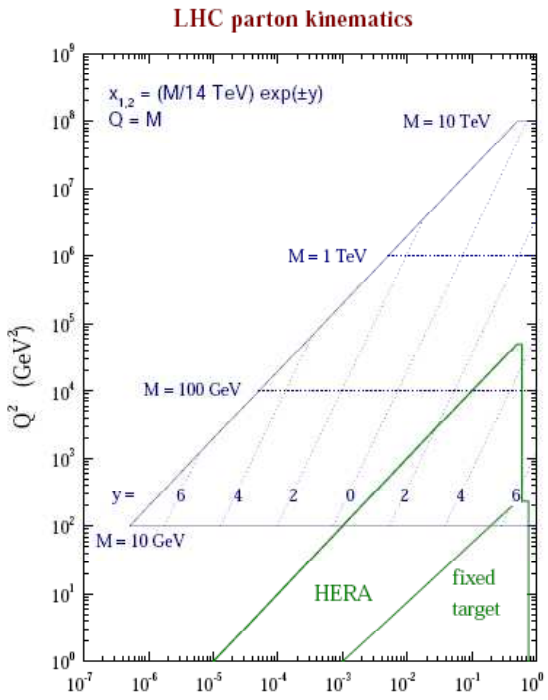

Figure 1.1: This plot shows the kinematical coverage of the LHC in the plane (x, Q^2), compared to previous colliders.

essential to describe diffraction [6]. However, high energy resummation is also relevant in the region of central rapidities $|y| \lesssim 2$. In this case $x \sim 10^{-3}$, so the small x behaviour is not the dominant one, but it may give corrections at the percent level to many important processes, such as the production of heavy quark pairs, vector and Higgs bosons. In recent years there has been important progress in understanding the resummation of parton evolution (for a review about the different approaches see [5]) so that now both collinear and high energy logarithms can be resummed simultaneously. In order to use these results for LHC phenomenology one needs resummed partonic cross sections for hadron-hadron collisions. An important part of this thesis (Chapters 4 and 5) is dedicated to the calculation of the resummed partonic coefficient functions for processes relevant to LHC phenomenology.

Finally, resummed results can be used to obtain approximate expressions to as yet unknown fixed order calculations. This can be done both for the coefficient functions and the evolution kernels. In Chapter 6 an approximate expression for the NNLO BFKL kernel is derived from the DGLAP anomalous dimension.

Chapter 2

Perturbative Quantum Chromo–Dynamics

In this chapter some features of perturbative QCD are discussed. Using deep inelastic scattering as an example the *collinear factorisation* theorem is introduced together with the DGLAP equations. Then the analysis is focused on the high energy limit of QCD and on the BFKL equation.

2.1 QCD and the parton model

The strong processes computable in perturbation theory are those which involve a high energy scale so that the coupling is sufficiently small. Some examples which will be discussed in this thesis are: deep inelastic scattering (DIS) of an electron off a proton, where the hard scale Q^2 is given by the transferred momentum, or the production of heavy particles, such as bottom quarks and Higgs bosons, where the hard scale is given by the mass of the produced particles. Even though QCD is asymptotically free the computation of cross sections for any strong process always involves non-perturbative contributions, because the initial states are not the fundamental degrees of freedom of the theory but compound states of quarks and gluons which cannot be described in perturbation theory. An important property of QCD is the *factorisation theorem*, which basically enables one to separate ("factorise") in every process a hard part, computable in perturbation theory, from a low energy one, which is process-independent and can be taken as a phenomenological input. The possibility of separating long and short distance effects largely explains the success of the *parton model*, a predecessor of QCD, introduced by Feynman and Bjorken in the late Sixties [7], [8]. The basic assumption of the parton model is that the interactions of hadrons are due to interactions of almost free constituents, called partons. The description of the hadron is given in terms of partonic distributions that, at leading order, represent the probability of having a particular

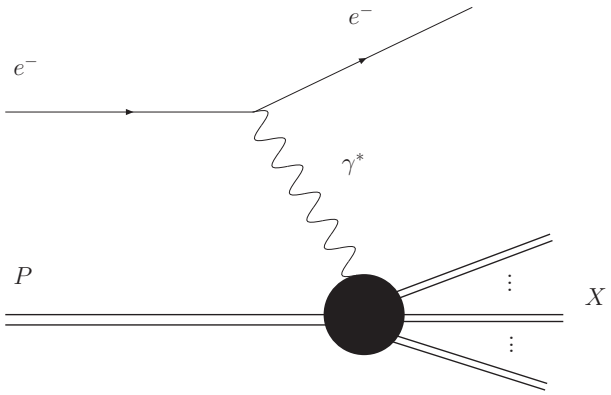

Figure 2.1: Deep inelastic electron - proton scattering.

parton which carries a fraction of the total longitudinal momentum. Nowadays the parton model is understood as the lowest order approximation of a perturbative QCD calculation.

In the following sub-sections the case of deep inelastic scattering (DIS) is discussed as an example in the framework of the parton model and then including QCD radiative corrections, showing how factorisation arises in the collinear limit. The choice of DIS is motivated by the fact that it involves only one hadron in the initial state and consequently the formulae are easier; these ideas are then generalised to hadronic processes. Finally the consequences of renormalization group invariance are investigated [3].

2.1.1 Deep inelastic scattering as an example

One of the most powerful tests of perturbative QCD is provided by the description of the inelastic scattering of a charged lepton off a hadronic target

$$e^- \, p \longrightarrow e^- \, X \, ,$$

where the lepton is an electron and the hadron a proton.

The incoming and the outgoing four-momenta of the electron are labelled l^μ and l'^μ respectively and P^μ is the momentum of the target proton. As shown in fig. 2.1 the scattering is mediated by the exchange of a vector boson with momentum $q^\mu = l^\mu - l'^\mu$.

DIS is usually described by the following kinematic variables

$$\begin{aligned} Q^2 &= -q^2 \\ x &= \frac{Q^2}{2P\cdot q} \qquad (2.1) \\ y &= \frac{q\cdot P}{l\cdot P} \\ \nu &= P\cdot q\,. \qquad (2.2) \end{aligned}$$

In the limit $Q^2 \ll m_Z^2$ the contribution arising from the exchange of a Z boson can be neglected and the Feynman amplitude which describes such process is

$$\mathcal{M} = i\,e\bar{u}(l')\gamma^\mu u(l)\frac{g_{\mu\nu}}{q^2}\langle X|J^\nu|P\rangle\,, \qquad (2.3)$$

where J^ν is the electro-magnetic current. The unpolarised cross section is proportional to this amplitude squared and summed over final polarisation states. The cross section can be factorised into a leptonic and a hadronic piece:

$$\sum_{pols}|\mathcal{M}|^2 = \frac{L^{\mu\nu}W_{\mu\nu}}{q^4}\,.$$

The leptonic tensor is then given by a straightforward QED calculation; neglecting the electron mass its expression is

$$L_{\mu\nu} = 4e^2\left(l_\mu l'_\nu + l_\nu l'_\mu - g_{\mu\nu}l\cdot l'\right)\,. \qquad (2.4)$$

The hadronic tensor instead contains all the information about the interaction of the electromagnetic current with the target proton; using the completeness relation among the final states it can be written as

$$W_{\mu\nu} = \frac{1}{4\pi}\sum_X \langle P|J^\dagger{}_\nu|X\rangle\langle X|J_\mu|P\rangle = \langle P|J^\dagger_\nu J_\mu|P\rangle\,. \qquad (2.5)$$

This tensor can depend only on P and q, it must be symmetric under the exchange of the two indices and respect the discrete symmetries of QCD: C, P and T. Because the electromagnetic current is conserved it also satisfies the condition

$$q_\mu W^{\mu\nu} = q_\nu W^{\mu\nu} = 0\,.$$

The most general tensor which respects the constraints above can be parametrised as

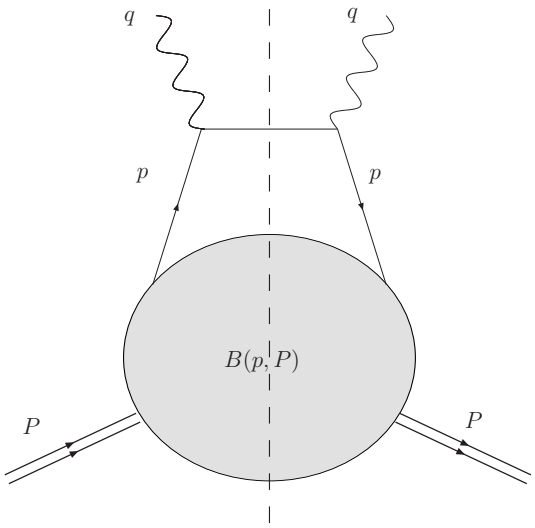

Figure 2.2: Deep inelastic electron - proton scattering: "handbag diagram".

follows

$$W_{\mu\nu}(P,q) = \left(-g_{\mu\nu} + \frac{q^\mu q^\nu}{q^2}\right) F_1(x,Q^2) + \\ + \left(P^\mu + \frac{q^\mu}{2x}\right)\left(P^\nu + \frac{q^\nu}{2x}\right)\frac{F_2(x,Q^2)}{P\cdot q}\,, \tag{2.6}$$

where F_1 and F_2 are two unknown functions called *structure functions*.

At the partonic level the scattering is due to the interaction between the virtual photon and a quark with momentum p. It is convenient to introduce Sudakov decomposition of the four momenta. The momentum of the quark can be written in terms of two lightlike vectors, P and η and of a spacelike one $\mathbf{p}$, whose only non-vanishing components are the transverse ones. The quark momentum on this basis is:

$$p^\mu = x_1 P^\mu + \frac{p^2+\mathbf{p}^2}{2x_1}\eta^\mu + \mathbf{p}^\mu\,. \tag{2.7}$$

In a fast moving frame, where the proton mass can be neglected, the momentum of the proton is lightlike

$$P = (P,0,0,P)\,,$$

and the four-vector η is defined by

$$\eta^2 = 0\,, \quad P\cdot\eta = 1 \quad \Longrightarrow \quad \eta = (\frac{1}{2P},0,0,-\frac{1}{2P})\,. \tag{2.8}$$

The hadronic tensor can be obtained, at lowest order, by the computation of the

diagram shown in figure 2.2:

$$W_{\mu\nu}(P,q) = e_q^2 \int \frac{d^4p}{(2\pi)^4} \left[\gamma_\mu(\not{p}+\not{q})\gamma_\nu\right]_{ij} \left[B(p,P)\right]_{ji} \delta((p+q)^2)\,, \tag{2.9}$$

where the function of $B(p,P)$ describes the non-perturbative physics. The assumption of the parton model is that the virtual photon interacts with an almost free quark whose momentum is proportional to the proton's one. This translates into the requirement that the function $B(p,P)$ has to be damped when the virtuality p^2 of the quark and its transverse momentum $|\mathbf{p}|^2$ are large. Such an assumption simplifies the integration in eq. (2.9); in particular the delta function becomes

$$\delta((p+q)^2) \simeq \delta(2x_1 P\cdot q - Q^2) = \frac{1}{2P\cdot q}\delta(x_1 - x)\,. \tag{2.10}$$

Hence, quite remarkably, a macroscopic parameter, namely the Bjorken variable x, controls the momentum of the parton involved in the process. The leading order contribution to structure function F_2 is easily obtained acting on the hadronic tensor with a suitable projector $\pi^{\mu\nu}$:

$$\begin{aligned} F_2(x,Q^2) &= 2P\cdot q\,\pi^{\mu\nu}W_{\mu\nu} = \\ &= e_q^2 x \int \frac{d^4p}{(2\pi)^4} \left[\Pi\right]_{ij} \left[B(p,P)\right]_{ji} \delta(x_1 - x) = e_q^2 x q(x)\,, \end{aligned} \tag{2.11}$$

where the quark distribution has been defined:

$$q(x) \equiv \int \frac{d^4p}{(2\pi)^4} \left[\Pi\right]_{ij} \left[B(p,P)\right]_{ji} \delta(x_1 - x)\,.$$

At this order the parton distribution has an appealing physical interpretation: it describes the probability to find a parton which carries a fraction of momentum x of the proton. According to eq. (2.11) the structure function does not depend on Q^2 but only on the dimensionless variable x. This result is known as *Bjorken scaling*:

$$F_2(x,Q^2) \longrightarrow F_2(x)\,.$$

Eq. (2.11) suggests to write the structure function F_2 as a convolution between a partonic coefficient function C_2 and the parton distribution function $q^{(0)}$:

$$F_2 = e_q^2\, C_2 \otimes q^{(0)} = e_q^2 \int_x^1 \frac{dx_1}{x_1} C_2\left(\frac{x}{x_1}\right) q^{(0)}(x_1)\,; \tag{2.12}$$

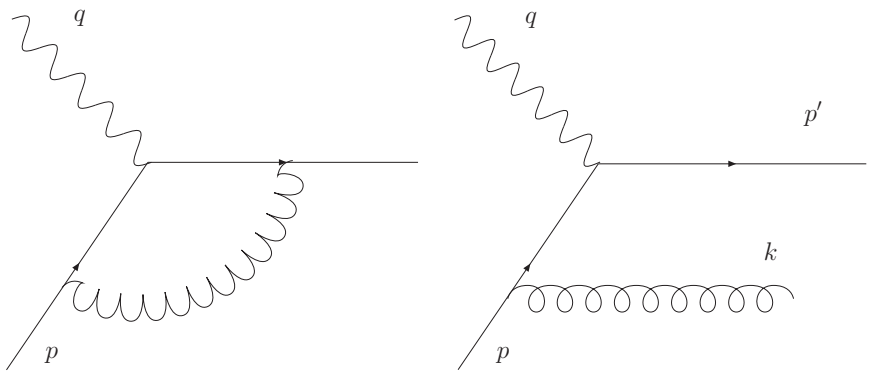

Figure 2.3: Virtual and real contributions to the coefficient function C_2 at next-to-leading-order

the leading order contribution to the coefficient function is a delta function:

$$C_2^{(0)} = x\delta(x_1 - x) = \delta(1 - z)\,, \tag{2.13}$$

where $z = \frac{x}{x_1}$ is often called partonic Bjorken variable.

The computation of the next-to-leading order (NLO) corrections is performed here in $d = 4 - 2\varepsilon$ dimension using dimensional regularisation. At $\mathcal{O}(\alpha_s)$ two classes of contributions appear; the interference between the one-loop correction and the tree-level amplitude has to be considered, together with the emission of one real gluon at tree level as shown in figure 2.3. The virtual contribution is given by

$$\left[C_2^{(1)}(x, Q^2, \varepsilon)\right]_{\text{virt}} = \frac{1}{8\pi} \int d\Phi^{(1)}\, \left[\mathcal{M}_l \mathcal{M}_0^* + \mathcal{M}_l^* \mathcal{M}_0\right], \tag{2.14}$$

where $\mathcal{M}_0$ and $\mathcal{M}_l$ are the tree-level and one-loop amplitudes respectively. The result is [4]

$$\begin{aligned}\left[C_2^{(1)}(z, Q^2, \varepsilon)\right]_{\text{virt}} &= -(Q^2)^{-\varepsilon}\,(4\pi)^{\varepsilon}\,\frac{C_{\text{F}}}{\pi}\,\frac{\Gamma(1+\varepsilon)\Gamma^2(1-\varepsilon)}{\Gamma(1-2\varepsilon)}\,\frac{1-\varepsilon}{1-2\varepsilon}\,\frac{1}{\varepsilon^2} \\ &\quad \left(1 + \frac{\varepsilon}{2} + \frac{3}{2}\varepsilon^2\right)\,\delta(1-z),\end{aligned} \tag{2.15}$$

where $C_{\text{F}} = 4/3$. The double pole in ε originates from the region of the loop integration where the exchanged virtual gluon is simultaneously soft and collinear to a massless quark line. This singularity is cancelled by an analogous contribution from the emission of one real gluon:

$$\gamma^*(q) + q(p) \to q(p') + g(k). \tag{2.16}$$

The corresponding contribution to the coefficient function is given by

$$\left[C_2^{(1)}(z,Q^2,\varepsilon)\right]_{\text{real}} = \frac{1}{8\pi}\int d\Phi^{(2)}(k,p')\ |\mathcal{M}_1|^2\ ; \tag{2.17}$$

details about the two-body phase space in d-dimensions can be found in Appendix A.1. The squared amplitude has the following structure:

$$|\mathcal{M}_1|^2 = 4\pi C_{\text{F}}\,\frac{R(z,y)}{p\cdot k\, p'\cdot k}, \tag{2.18}$$

where y is a function of the scattering angle: $y=(1+\cos\vartheta)/2$. The explicit expression of the function $R(z,y)$ is:

$$\begin{aligned} R(z,y) &= -\frac{2Q^4}{z}\big[2zy(2\varepsilon-3)(zy-z-y) \\ &\quad +(\varepsilon-1)(z+y)^2-6zy+2y+2z-2\big], \end{aligned} \tag{2.19}$$

Soft and collinear singularities arise from the denominators of eq. (2.18):

$$p\cdot k=\frac{Q^2}{2z}(1-y), \qquad p'\cdot k=\frac{Q^2}{2z}(1-z). \tag{2.20}$$

The contribution to the NLO coefficient function coming from emission of a real gluon is obtained integrating over the two body phase space:

$$\begin{aligned} \left[C_2^{(1)}(z,Q^2,\varepsilon)\right]_{\text{real}} &= (Q^2)^{-\varepsilon}\,\frac{C_{\text{F}}}{4\pi}\,\frac{(4\pi)^\varepsilon}{\Gamma(1-\varepsilon)}\,z^{2+\varepsilon}\,(1-z)^{-1-\varepsilon} \\ &\quad \frac{1}{Q^4}\int_0^1 dy\, y^{-\varepsilon}(1-y)^{-1-\varepsilon}\,R(z,y). \end{aligned} \tag{2.21}$$

The computation is greatly simplified if one expands the factor $(1-z)^{-1-\varepsilon}$ as

$$\frac{1}{(1-z)^{1+\varepsilon}} = -\frac{1}{\varepsilon}\delta(1-z)+\left[\frac{1}{1-z}\right]_+ -\varepsilon\left[\frac{\ln(1-z)}{1-z}\right]_+ +\mathcal{O}(\varepsilon^2), \tag{2.22}$$

where the + distributions are defined according to

$$\int_0^1 dz\ [f(z)]_+\ g(z) = \int_0^1 dz\, f(z)\ [g(z)-g(1)]\,. \tag{2.23}$$

The real contribution naturally splits into two terms

$$\left[C_2^{(1)}(z,Q^2,\varepsilon)\right]_{\text{real}} = \left[C_2^{(1)}(z,Q^2,\varepsilon)\right]_c + \left[C_2^{(1)}(z,Q^2,\varepsilon)\right]_l, \tag{2.24}$$

where the first term is proportional to $\delta(1-z)$ and hence has the same kinematical

structure as the virtual contribution; it is then natural to combine them together

$$\begin{aligned}\left[C_2^{(1)}(z,Q^2,\varepsilon)\right]_{\rm sv} &= \left[C_2^{(1)}(z,Q^2,\varepsilon)\right]_c + \left[C_2^{(1)}(z,Q^2,\varepsilon)\right]_{\rm virt}\\ &= (Q^2)^{-\varepsilon}\,(4\pi)^{\varepsilon}\,\frac{C_{\rm F}}{\pi}\,\frac{\Gamma(1-\varepsilon)}{\Gamma(1-2\varepsilon)}\,\frac{1-\varepsilon}{1-2\varepsilon}\,\frac{1}{\varepsilon^2}\\ &\quad\left[1-\frac{\varepsilon}{4}-\Gamma(1+\varepsilon)\Gamma(1-\varepsilon)\,\left(1+\frac{\varepsilon}{2}+\frac{3}{2}\varepsilon^2\right)\right]\,\delta(1-z).\end{aligned} \tag{2.25}$$

The double poles in ε cancel out as anticipated and the coefficient function is free of soft-collinear singularities. The residue of the simple pole can be computed by expanding eq. (2.25) in a Laurent series:

$$\begin{aligned}\alpha_0\,\left[C_2^{(1)}(z,Q^2,\varepsilon)\right]_{\rm sv} &= -\frac{C_{\rm F}\alpha_s}{2\pi}\,\left[\frac{1}{\varepsilon}-\gamma_E+\ln(4\pi)-\ln\frac{Q^2}{\mu^2}+\frac{2}{9}\,\pi^2+3\right]\\ &\quad\times\frac{3}{2}\,\delta(1-z),\end{aligned} \tag{2.26}$$

where $\alpha_0 = \mu^{2\varepsilon}\alpha_s$, as appropriate at next-to-leading order. The remaining term $\left[C_2^{(1)}(z,Q^2,\varepsilon)\right]_l$ can be computed expanding the factor $(1-y)^{-1-\varepsilon}$ in analogy with eq. (2.22):

$$\frac{1}{(1-y)^{1+\varepsilon}} = -\frac{1}{\varepsilon}\delta(1-y)+\left[\frac{1}{1-y}\right]_+ + \mathcal{O}(\varepsilon). \tag{2.27}$$

Some algebra leads to the expression

$$\begin{aligned}\alpha_0\,\left[C_2^{(1)}(z,Q^2,\varepsilon)\right]_l &= \frac{C_{\rm F}\alpha_s}{2\pi}\,z\left\{-\left[\frac{1}{\varepsilon}-\gamma_E+\ln(4\pi)-\ln\frac{Q^2}{\mu^2}\right]\,\frac{1+z^2}{(1-z)_+}\right.\\ &\quad-\frac{1+z^2}{1-z}\,\ln z+3+2z-\frac{3}{2}\left[\frac{1}{1-z}\right]_+\\ &\quad\left.+(1+z^2)\,\left[\frac{\ln(1-z)}{1-z}\right]_+\right\}.\end{aligned} \tag{2.28}$$

The final result is obtained adding the soft-virtual contribution, eq. (2.26), to eq. (2.28):

$$\begin{aligned}&\alpha_0\,C_2^{(1)}(z,Q^2,\varepsilon) = \frac{C_{\rm F}\alpha_s}{2\pi}\,z\left\{-\left[\frac{1}{\bar\varepsilon}-\ln\frac{Q^2}{\mu^2}\right]\,\left[\frac{1+z^2}{(1-z)_+}+\frac{3}{2}\,\delta(1-z)\right]\right.\\ &-\frac{1+z^2}{1-z}\,\ln z+3+2z+(1+z^2)\,\left[\frac{\ln(1-z)}{1-z}\right]_+-\frac{3}{2}\left[\frac{1}{1-z}\right]_+\\ &\left.-\left(\frac{9}{2}+\frac{\pi^2}{3}\right)\,\delta(1-z)\right\} = \frac{\alpha_s}{2\pi}\,z\,\left\{\left[\ln\frac{Q^2}{\mu^2}-\frac{1}{\bar\varepsilon}\right]\,P_{qq}(z)+C_2^q(z)\right\}\,.\end{aligned} \tag{2.29}$$

where according to the $\overline{\text{MS}}$ prescription

$$\frac{1}{\bar{\varepsilon}} = \frac{1}{\varepsilon} - \gamma_E + \ln(4\pi). \tag{2.30}$$

The function P_{qq} has also been introduced; it universally describes the splitting $q \to qg$.

In order to obtain the structure function F_2 one must convolute the coefficient function C_2 with the distribution $q^{(0)}$ of a quark in a proton and sum over the quark flavours:

$$\begin{aligned} F_2(x,Q^2) &= \sum_{q,\bar{q}} e_q^2 \int_x^1 \frac{dx_1}{x_1} C_2\left(\frac{x}{x_1}\right) q^{(0)}(x_1,\varepsilon) \\ &= x\sum_{q,\bar{q}} e_q^2 \Bigg\{ q^{(0)}(x) + \frac{\alpha_s}{2\pi}\int_x^1 \frac{dx_1}{x_1} q^{(0)}(x_1,\varepsilon) \\ &\quad \left[P_{qq}\left(\frac{x}{x_1}\right)\left[\ln\frac{Q^2}{\mu^2} - \frac{1}{\bar{\varepsilon}}\right] + C_2^q\left(\frac{x}{x_1}\right)\right] + ... \Bigg\}. \end{aligned} \tag{2.31}$$

One can regard $q^{(0)}(x,\varepsilon)$ as a d-dimensional bare distribution and therefore absorb the collinear pole into this unmeasurable quantity, defining a renormalised object as

$$q(x,\mu^2,\varepsilon) = q^{(0)}(x,\varepsilon) - \frac{\alpha_s}{2\pi}\int_x^1 \frac{dx_1}{x_1} q^{(0)}(x_1,\varepsilon)\left\{\frac{1}{\bar{\varepsilon}} P_{qq}\left(\frac{x}{x_1}\right) + \dots\right\} \tag{2.32}$$

Of course there is some arbitrariness in dealing with the finite contribution: different choices correspond to different factorisation schemes; in the $\overline{\text{MS}}$ scheme only the contribution proportional to $1/\bar{\varepsilon}$ is absorbed. The structure function is now free of collinear singularities. Thus one can take $\varepsilon \to 0$, obtaining:

$$\begin{aligned} F_2(x,Q^2) &= x\sum_{q,\bar{q}} e_q^2 \int_x^1 \frac{dx_1}{x_1} q(x_1,\mu^2) \\ &\quad \times\left\{\delta(1-\frac{x}{x_1}) + \frac{\alpha_s}{2\pi}\left[P_{qq}\left(\frac{x}{x_1}\right)\ln\frac{Q^2}{\mu^2} + C_2^q\left(\frac{x}{x_1}\right)\right]\right\} \end{aligned} \tag{2.33}$$

The distribution $q(x,\mu^2)$ cannot be determined from first principles, since it receives contribution from the non-perturbative regime of strong interactions.

In order to obtain a complete result at $\mathcal{O}(\alpha_s)$ one must consider the contribution coming form the process

$$\gamma^* + g \to q + \bar{q}\,,$$

in which the initial parton is a gluon that splits into two quarks, one of which scatters

off the virtual photon. The computation is similar to the previous case and the result is

$$\begin{aligned} F_2(x,Q^2) &= x\sum_{q,\bar{q}} e_q^2 \int_x^1 \frac{dx_1}{x_1} q(x_1,\mu^2) \\ &\quad \times\left\{ \delta(1-\frac{x}{x_1}) + \frac{\alpha_s}{2\pi}\left[P_{qq}\left(\frac{x}{x_1}\right)\ln\frac{Q^2}{\mu^2} + C_2^q\left(\frac{x}{x_1}\right)\right]\right\} \\ &+ x\sum_{q,\bar{q}} e_q^2 \int_x^1 \frac{dx_1}{x_1} g(x_1,\mu^2) \\ &\quad \times\left\{ \frac{\alpha_s}{2\pi}\left[P_{qg}\left(\frac{x}{x_1}\right)\ln\frac{Q^2}{\mu^2} + C_2^g\left(\frac{x}{x_1}\right)\right]\right\} + \mathcal{O}(\alpha_s^2)\,. \end{aligned} \tag{2.34}$$

where the gluon distribution g has been introduced together with the splitting function:

$$P_{qg}(z) = T_R\left[z^2 + (1-z)^2\right]\,, \tag{2.35}$$

with $T_R = \frac{1}{2}$ For the explicit expression of the coefficient function C_2^g see for example [3].

In this section it has been explicitly shown that at NLO in deep inelastic scattering one can separate contributions coming from non-perturbative QCD from perturbative ones. This is a fundamental feature of QCD which is known as *factorisation*. Parton distribution functions (PDFs) have been introduced in order to describe the physics of quarks and gluons in the proton. Presently non-perturbative methods such as lattice QCD [9] have not reached an accurate description of such objects. However, while the coefficient functions are process dependent, parton densities are universal and so can be taken as a phenomenological input from previous experiments. Moreover, even though PDFs are non-perturbative objects, their dependence on the factorisation scale μ^2 can be computed in perturbation theory, as described in the next section.

2.1.2 The DGLAP equations

In the previous section the structure function F_2 has been computed at next-to-leading order, considering the radiation of one parton and the one-loop virtual corrections. Eq. (2.34) explicitly shows that at $\mathcal{O}(\alpha_s)$ the Bjorken scaling is broken by logarithm of Q^2/μ^2. In the collinear limit this computation can be generalised to the radiation of n partons f_i

$$\gamma^* + q \to q + \sum_{i=0}^{n} f_i\,,$$

A more accurate analysis reveals that collinear divergences arise only from the region in which the transverse momenta of the radiated partons are strongly ordered:

$$|\mathbf{k}_n|^2 \gg |\mathbf{k}_{n-1}|^2 \gg ... \gg |\mathbf{k}_2|^2 \gg |\mathbf{k}_1|^2\,. \tag{2.36}$$

The computation of Feynman diagrams in the collinear limit leads to a squared amplitude proportional to:

$$|\mathcal{M}_n|^2 \sim \frac{(-1)^n}{n!}\left(\frac{\alpha_s}{2\pi}\right)^n \left(\frac{1}{\varepsilon}\left(\frac{Q^2}{\mu^2}\right)^{-\varepsilon}\right)^n P_{i_1,j_i} \otimes \cdots \otimes P_{i_n,j_n} \otimes C_2^{(0)} \tag{2.37}$$

Similarly to the case of single emission, the collinear divergences can be absorbed into renormalised quark and gluon distributions, leaving a logarithmic dependence:

$$F_2(x,Q^2) \sim \left(\frac{\alpha_s}{2\pi}\right)^n \ln^n \frac{Q^2}{\mu^2}\,. \tag{2.38}$$

This behaviour is potentially dangerous because Q^2 can be very large and hence the product $\alpha_s \ln \frac{Q^2}{\mu^2} \sim 1$. Formally subleading terms become important, invalidating the perturbative approach. Such collinear logarithms can be resummed using renormalization group techniques which lead to evolution equations for the parton distributions functions, as discussed in the following.

The factorisation of collinear singularities requires the introduction of an arbitrary energy scale μ^2, but physical observables such as hadronic structure functions cannot depend on this parameter:

$$\mu^2 \frac{d}{d\mu^2} F_2(x,Q^2) = 0\,. \tag{2.39}$$

The right-hand side of eq. (2.34) implies that the parton density $q(x,\mu^2)$ satisfies the equation:

$$\mu^2 \frac{\partial q(x,\mu^2)}{\partial \mu^2} = -\frac{\alpha_s}{2\pi}\int_x^1 \frac{dx_1}{x_1}\left[P_{qq}\left(\frac{x}{x_1}\right) q(x_1,\mu^2) + P_{qg}\left(\frac{x}{x_1}\right) g(x_1,\mu^2)\right]. \tag{2.40}$$

This is the well-known Dokshitzer- Gribov-Lipatov-Altarelli-Parisi equation [10]-[12]. The above derivation is valid only at the lowest order in perturbation theory, but an all-order proof is possible. The result is a $(2n_f+1)$-dimensional matrix equation in the space of quarks, antiquarks and gluons:

$$\begin{aligned}\frac{\partial}{\partial t}\begin{pmatrix} q_i(x,t) \\ g(x,t)\end{pmatrix} &= \frac{\alpha_s(t)}{2\pi}\sum_{q_j,\bar{q}_j}\int_x^1 \frac{dx_1}{x_1} \\ &\times \begin{pmatrix} P_{q_iq_j}\left(\frac{x}{x_1},\alpha_s(t)\right) & P_{q_ig}\left(\frac{x}{x_1},\alpha_s(t)\right) \\ P_{gq_j}\left(\frac{x}{x_1},\alpha_s(t)\right) & P_{gg}\left(\frac{x}{x_1},\alpha_s(t)\right)\end{pmatrix}\begin{pmatrix} q_j(x_1,t) \\ g(x_1,t)\end{pmatrix},\end{aligned} \tag{2.41}$$

where

$$t = \ln\frac{Q^2}{\mu^2}$$

and $\alpha_s(t)$ is the running coupling constant. Although the parton distribution functions are non-perturbative objects, the evolution kernels P_{ij} can be computed in perturbation theory:

$$P_{ij}(\alpha_s(t), z) = \sum_{n=0}^{\infty} \left(\frac{\alpha_s(t)}{2\pi}\right)^n P_{ij}^{(n)}(z)\,. \tag{2.42}$$

The DGLAP equations enable one to compute the scale dependence of the PDFs, hence they can be fitted from the data collected in a given experiment at some energy scale t_0 and used as a phenomenological input for a new experiment at a different energy scale t. The leading order expressions of the evolution kernel are:

$$\begin{aligned}
P_{qq}^{(0)}(z) &= C_F\Big[\frac{1+z^2}{(1-z)_+} + \frac{3}{2}\delta(1-z)\Big]\,,\\
P_{qg}^{(0)}(z) &= T_R\Big[z^2 + (1-z)^2\Big]\,,\\
P_{gq}^{(0)}(z) &= C_F\Big[\frac{1+(1-z)^2}{z}\Big]\,,\\
P_{gg}^{(0)}(z) &= 2C_A\Big[\frac{z}{(1-z)_+} + \frac{1-z}{z} + z(1-z)\Big] +\\
&\qquad \delta(1-z)\frac{(11C_A - 4n_f T_R)}{12\pi}\,,
\end{aligned} \tag{2.43}$$

where the plus distribution has been formerly defined. At this order the splitting functions $P_{ij}(z)$ have an attractive physical interpretation as the probabilities of finding a parton of type i in a parton of type j with a fraction z of the longitudinal momentum [12]. The splitting functions have been computed at next-to-leading order [13], [14] and more recently at next-to-next-to leading order [15], [16].

An efficient method to solve the DGLAP equations and hence compute the evolution of parton distributions, consists of defining particular linear combinations of the individual quark distributions u, d, c, s, t, b. It is possible to write eleven non-singlet flavour combinations which evolve independently [17]:

$$\begin{aligned}
V &= \sum_i q_i^-\,,\\
V_3 &= u^- - d^-\,,\\
V_8 &= u^- + d^- - 2s^-\,,\\
V_{15} &= u^- + d^- + s^- - 3c^-\,,\\
V_{24} &= u^- + d^- + s^- + c^- - 4b^-\,,\\
V_{35} &= u^- + d^- + s^- + c^- + b^- - 5t^-
\end{aligned} \tag{2.44}$$

$$
\begin{aligned}
T_3 &= u^+ - d^+ \,, \\
T_8 &= u^+ + d^+ - 2s^+ \,, \\
T_{15} &= u^+ + d^+ + s^+ - 3c^+ \,, \\
T_{24} &= u^+ + d^+ + s^+ + c^+ - 4b^+ \,, \\
T_{35} &= u^+ + d^+ + s^+ + c^+ + b^+ - 5t^+ \,,
\end{aligned} \tag{2.45}
$$

where

$$
q_i^{\pm} = q_i \pm \bar{q}_i \,. \tag{2.46}
$$

Then only one quark combination remains, it is the *singlet* one:

$$
\Sigma = \sum_i q_i^+ \equiv \sum_i (q_i + \bar{q}_i) \,, \tag{2.47}
$$

whose evolution is coupled to the gluon's one:

$$
\begin{aligned}
\frac{\partial}{\partial t} \begin{pmatrix} \Sigma(x,t) \\ g(x,t) \end{pmatrix} &= \frac{\alpha_s(t)}{2\pi} \int_x^1 \frac{dx_1}{x_1} \\
&\begin{pmatrix} P_{qq}\left(\frac{x}{x_1}, \alpha_s(t)\right) & 2n_f P_{qg}\left(\frac{x}{x_1}, \alpha_s(t)\right) \\ P_{gq}\left(\frac{x}{x_1}, \alpha_s(t)\right) & P_{gg}\left(\frac{x}{x_1}, \alpha_s(t)\right) \end{pmatrix} \begin{pmatrix} \Sigma(x_1,t) \\ g(x_1,t) \end{pmatrix} .
\end{aligned} \tag{2.48}
$$

In this thesis the singlet sector will be considered because it is the relevant one in the high energy limit. The singlet quark distribution and the gluon can be grouped into the vector

$$
\underline{G}(x,t) = \begin{pmatrix} G^{(1)}(x,t) \\ G^{(2)}(x,t) \end{pmatrix} = x \begin{pmatrix} \Sigma(x,t) \\ g(x,t) \end{pmatrix} \tag{2.49}
$$

Before solving the DGLAP equations it is useful to introduce a technical tool. The expression for a physical observable, such as the structure function F_2 given eq. (2.34), consists of a convolution between a hard coefficient function and parton distribution functions. Furthermore the DGLAP evolution is described by a set of coupled integro-differential equations (see eq. (2.41)). A theorem states that the convolution product f of two function g and h can be turned into an ordinary one by taking Mellin moments of the functions. Suppose one has

$$
f = g \otimes h \,, \tag{2.50}
$$

then

$$
\mathbb{M}[f] = \mathbb{M}[g] \times \mathbb{M}[h] \,, \tag{2.51}
$$

where $\mathbb{M}[f]$ is the Mellin transformed of the function f, defined by:

$$\mathbb{M}[f](n) = \int_0^1 \frac{d\alpha}{\alpha}\, \alpha^n f(\alpha)\,. \tag{2.52}$$

The proof is straightforward:

$$\begin{aligned}
\mathbb{M}[f](n) &= \int_0^1 \frac{d\alpha}{\alpha}\, \alpha^n \int_\alpha^1 \frac{d\beta}{\beta}\, g\left(\frac{\alpha}{\beta}\right) h(\beta) \\
&= \int_0^1 \frac{d\beta}{\beta} \int_0^\beta \frac{d\alpha}{\alpha}\, \alpha^n g\left(\frac{\alpha}{\beta}\right) h(\beta) \\
&= \int_0^1 \frac{d\beta}{\beta}\, \beta^n \int_0^1 \frac{d\omega}{\omega}\, \omega^n g(\omega) h(\beta) = \mathbb{M}[g](n)\, \mathbb{M}[h](n)\,.
\end{aligned} \tag{2.53}$$

In Mellin space the DGLAP equation for the singlet vector eq. (2.49) is

$$\begin{aligned}
\frac{\partial}{\partial t} \begin{pmatrix} G^{(1)}(N,t) \\ G^{(2)}(N,t) \end{pmatrix} = \begin{pmatrix} \gamma_{qq}(N,\alpha_s(t)) & 2n_f\gamma_{qg}(N,\alpha_s(t)) \\ \gamma_{gq}(N,\alpha_s(t)) & \gamma_{gg}(N,\alpha_s(t)) \end{pmatrix} \\
\times \begin{pmatrix} G^{(1)}(N,t) \\ G^{(2)}(N,t) \end{pmatrix},
\end{aligned} \tag{2.54}$$

where with some abuse of notation the function $\underline{G}(N,t)$ is the Mellin transformed of $\underline{G}(x,t)$. The elements of the matrix of the singlet anomalous dimension are defined as the Mellin moments of the splitting functions:

$$\gamma_{ij}(N,\alpha_s(t)) = \int_0^1 \frac{dz}{z} z^N z\, \frac{\alpha_s(t)}{2\pi} P_{ij}(z,\alpha_s(t))\,. \tag{2.55}$$

Note that with this definition the high partonic centre-of-mass energy limit $z \to 0$ corresponds to $N \to 0$ in Mellin space. In order to decouple the evolution in the singlet sector one diagonalises the anomalous dimension matrix. The eigenvalues are

$$\gamma^{(\pm)} = \frac{1}{2}\Big[\gamma_{gg} + \gamma_{qq} \pm \sqrt{(\gamma_{gg}-\gamma_{qq})^2 + 8n_f\gamma_{gq}\gamma_{qg}}\Big]\,, \tag{2.56}$$

and they admit the following perturbative expansion in powers of the strong coupling $\alpha_s(t)$:

$$\begin{aligned}
\gamma^{(\pm)}(\alpha_s(t),N) &= \alpha_s(t)\gamma_0^{(\pm)}(N) + \alpha_s(t)^2\gamma_1^{(\pm)}(N) + \alpha_s(t)^3\gamma_2^{(\pm)}(N) \\
&\quad + \mathcal{O}\left(\alpha_s(t)^4\right)\,.
\end{aligned} \tag{2.57}$$

The solution of the DGLAP equation in the singlet sector eq. (2.54) can be written on

the basis of the eigenvectors $G^{(\pm)}$:

$$G^{(\pm)}(N,t) = \exp\left[\int_{\alpha_s(t_0)}^{\alpha_s(t)} d\alpha \frac{\gamma^{(\pm)}(N,\alpha)}{\beta(\alpha)}\right] G^{(\pm)}(N,t_0)\,, \tag{2.58}$$

where the QCD β-function has been introduced. The solutions for the non-singlet case have the same form, but with different anomalous dimensions.

The specific form of eq. (2.58) solves the problem of large collinear logarithms which has been encountered in the computation of the structure function F_2, eq. (2.38). In fact all the leading logarithms of Q^2/μ^2 are resummed in the evolution factor if one considers the leading order anomalous dimension:

$$\begin{aligned}
&\exp\left[\int_{\alpha_s(0)}^{\alpha_s(t)} d\alpha \frac{\gamma(N,\alpha)}{\beta(\alpha)}\right] = \exp\left[\int_0^t dt' \gamma(N,\alpha_s(t'))\right] = \\
&\exp\left[\int_0^t dt'\, \alpha_s\, \gamma_0(N) + \ldots\right] = \exp\left[\alpha_s\, t\, \gamma_0(N)\right] = \\
&\sum_{n=0}^{\infty} \left(\alpha_s \ln \frac{Q^2}{\mu^2}\, \gamma_0(N)\right)^n\,,
\end{aligned} \tag{2.59}$$

where in the second line the running of the coupling has been neglected, as appropriate at LO. If higher terms in the perturbative expansion of the anomalous dimension are included, subleading logarithms can be resummed. The inclusion of γ_k enables to perform the resummation of $\mathrm{N}^k\mathrm{LO}$ logarithms:

$$(\alpha_s(t))^{k+n} \ln^n \frac{Q^2}{\mu^2}\,. \tag{2.60}$$

2.1.3 Collinear factorisation theorem

In the previous sections deep inelastic scattering at one-loop was discussed, showing how it is possible to absorb the singularities arising from the emission of collinear partons into a redefinition of the parton densities. It was also argued that one can compute the collinear behaviour to all orders in perturbation theory. The factorisation theorem of collinear singularities states that it possible to write the hadronic cross section as a convolution between a partonic, process dependent, coefficient function and universal parton distributions. Corrections to factorisation are suppressed by powers of Q^2. A rigorous proof of factorisation to all orders exists for deep inelastic scattering in the context of the operator product expansion (for a review see [18]). The plausibility of factorisation properties for processes with one incoming hadron can be seen from the following argument. As the centre-of-mass energy increases, the lifetime T of any virtual partonic state in the hadron is lengthened, while the time t which the electron takes to traverse the hadron is shortened because the hadron is Lorentz contracted.

When $t \ll T$ the hadron can be viewed as a single virtual state characterised by a definite number of partons during the entire time the electron takes to cross it. Since the partons do not interact during this time, each one may be thought of as carrying a definite fraction x of the momentum of the hadron. The electron interacts with partons of definite momentum, rather than with the hadron as a whole. In addition, if the momentum transfer is very high, the virtual photon is short-living and hence it cannot travel far. Therefore, if the density of the partons is not too high, the electron will be able to interact with only one single parton. Initial state interactions, which give rise to soft and collinear singularities, are too early relative to the short time scale of the hard scattering. Therefore it is appropriate that these singularities are included in the parton density describing the incoming hadrons rather than in the short-distance cross section. The proofs of factorisation confirm that this simple picture is in fact valid in perturbation theory for a large class of processes.

In hadron–hadron collisions, the analysis is more complicated since the question arises whether the partons in hadron h_1, through the influence of their colour fields, change the distribution of partons in hadron h_2, thus spoiling the simple parton picture. Factorisation of the cross section into a pure short-distance contribution, computable in perturbation theory and non-perturbative, but universal, parton distribution functions is more complicated because of these colour correlations. Nevertheless it can be proven to all orders [19]. The cross section for hadron–hadron collisions can be written as:

$$\begin{aligned} \sigma(\rho, Q^2) &= \sum_{j_1,j_2} \int_\rho^1 \frac{dx_1}{x_1} \int_\rho^1 \frac{dx_2}{x_2}\, \hat{\sigma}_{j_1,j_2}\left(\frac{\rho}{x_1 x_2}, Q^2, \alpha_s(\mu^2)\right) \\ &\quad \times f_{j_1}(x_1, \mu^2) f_{j_2}(x_2, \mu^2)\,, \end{aligned} \tag{2.61}$$

where ρ is the ratio between the hard scale of the process Q^2 and the centre-of-mass energy s.

2.2 An Introduction to BFKL

In this section the high energy limit of Quantum Chromo- Dynamics is discussed and the Balitsky-Fadin-Kuraev-Lipatov (BFKL) equation is introduced. Many concepts which are necessary in order to understand the framework of the BFKL equation come from a description of strong interactions at high energy prior to QCD, the so called *Regge theory*. A brief review of its basic ideas is provided, mainly following [6]. Afterwards the main features of the BFKL equation at leading order and beyond are discussed.

2.2.1 Regge theory

Before the advent of a complete field theoretical description of strong interactions, an attempt to describe the scattering of hadrons was carried out on the basis of few and very general assumptions on the scattering matrix, defined as the overlapping of *in* and *out* free particle states:

$$S_{\text{in,out}} = \langle \text{out} | \text{in} \rangle \,. \tag{2.62}$$

Three rather general postulates are assumed:

1. the S matrix is Lorentz invariant;
2. the S matrix is unitary;
3. the S matrix is an analytical function of its arguments, considered as complex variables.

The first hypothesis says that the S matrix can be written as a function of Lorentz invariant scalar products of the momenta of the incoming and outgoing particles. It is useful to consider the special case of the scattering of two particles into two particles:

$$a + b \to c + d \,.$$

The kinematics is described by the Mandelstam variables:

$$\begin{aligned} s &= (p_a + p_b)^2 \,, \\ t &= (p_a - p_c)^2 \,, \\ u &= (p_a - p_d)^2 \,. \end{aligned} \tag{2.63}$$

Energy-momentum conservation implies that

$$s + t + u = \sum_{i=a,b,c,d} m_i^2 \,,$$

so the scattering matrix element can be written as a function of two independent variables: s and t. The requirement of unitarity ensures the conservation of probability:

$$SS^\dagger = S^\dagger S = \mathbb{I}\,. \tag{2.64}$$

An important consequence of unitarity is the Cutkosky rule; introducing the scattering amplitude $\mathcal{A}$

$$S_{\mathrm{in,out}} = \delta_{\mathrm{in,out}} + i\,(2\pi)^4\delta^{(4)}(p_{\mathrm{in}} - p_{\mathrm{out}})\mathcal{A}_{\mathrm{in,out}}\,, \tag{2.65}$$

one can rewrite (2.64) in the following form:

$$2\,\mathrm{Im}\,\mathcal{A}_{\mathrm{in,out}} = (2\pi)^4\delta^{(4)}(p_{\mathrm{in}} - p_{\mathrm{out}})\sum_n \mathcal{A}_{\mathrm{in,n}}\mathcal{A}^*_{\mathrm{n,out}}\,. \tag{2.66}$$

Thus the imaginary part of an amplitude can be deduced from the scattering amplitudes of ingoing and outgoing particles, summed over the all possible intermediate states. A particular case of the Cutkosky rule is the *optical* theorem, which relates the imaginary part of the forward elastic scattering to the total cross section. For an elastic scattering initial and final states are the same and in the forward case $t = 0$:

$$2\,\mathrm{Im}\,\mathcal{A}(s,0) = (2\pi)^4\delta^{(4)}(p_{\mathrm{in}} - p_{\mathrm{out}})\sum_n |\mathcal{A}_{\mathrm{in}\,\to\,\mathrm{n}}|^2 = F\sigma_{\mathrm{TOT}}\,, \tag{2.67}$$

where F is the flux factor. The third postulate states that the S-matrix is analytic on the field of its complex arguments, with the exception of the singularities imposed by the unitarity condition. Moreover one can determine the structure of such singularities through the Cutkosky rule. According to eq. (2.66) the imaginary part of the amplitude receives new contributions when s crosses an intermediate particle threshold. In a region about the origin of the real s axis there are no contributions from the thresholds, so the amplitude is real. An analytic continuation of a function $A(s,t)$ with such properties is given by $\mathcal{A}(s,t) \equiv A(s^*,t)^*$ thanks to Schwartz reflection principle. In the whole domain of analyticity the following relation holds:

$$\mathcal{A}(s,t)^* = \mathcal{A}(s^*,t)\,.$$

Thus

$$\mathrm{Im}\,\mathcal{A}(s,t) = \frac{\mathcal{A}(s,t) - \mathcal{A}^*(s,t)}{2i} = \frac{\mathcal{A}(s,t) - \mathcal{A}(s^*,t)}{2i}\,, \tag{2.68}$$

hence a contribution to the imaginary part of the amplitude for real s may arise only through cuts along the real s axis with branch points at the n-particle thresholds ($n \geq 2$). A second useful consequence of analyticity is crossing symmetry, which relates

the amplitude of processes in different channels. For an s-channel process

$$a + b \to c + d\,,$$

$s > 0$ and $t, u < 0$ in the physical region. The scattering amplitude can be uniquely analytic continued in the region where $t > 0$ and $s, u < 0$. This corresponds to a t-channel scattering:

$$a + \bar{c} \to \bar{b} + d$$

and the relation between the amplitudes describing the two processes is:

$$\mathcal{A}_{a+\bar{c}\to\bar{b}+d}(s,t,u) = \mathcal{A}_{a+b\to c+d}(t,s,u) \tag{2.69}$$

An analogue relation can be found for u-channel processes. It is clear that the amplitude for a $t\,(u)$-channel scattering has cuts on the positive $t\,(u)$-axis as a consequence of physical thresholds and, because of crossing symmetry, cuts on the negative real axes as well.

The goal of *Regge theory* is to study scattering amplitudes in the high energy limit. More precisely the Regge limit is defined as:

$$s \gg |t| \tag{2.70}$$

It is convenient to start analysing a t-channel process because a *partial wave expansion* can be performed:

$$\mathcal{A}_{a+\bar{c}\to\bar{b}+d}(s,t) = \sum_{l=0}^{+\infty}(2l+1)a_l(s)P_l(\cos\vartheta)\,, \tag{2.71}$$

where $\cos\vartheta = 1 + \frac{2t}{s}$ is the scattering angle and P_l are Legendre polynomials. In this expansion the amplitude is seen as a superposition of contributions coming from the exchange of states with angular momentum l. Thanks to crossing symmetry it is straightforward to rewrite this expansion for an s-channel process:

$$\mathcal{A}_{a+b\to c+d}(s,t) = \sum_{l=0}^{+\infty}(2l+1)a_l(t)P_l\left(1+\frac{2s}{t}\right)\,. \tag{2.72}$$

An analytic continuation of this last expression in the plane of complex angular momenta l is provided by

$$\mathcal{A}(s,t) = \frac{1}{2i}\oint_C dl(2l+1)\frac{a(l,t)}{\sin(\pi l)}P\left(l, 1+\frac{2s}{t}\right)\,, \tag{2.73}$$

where the contour C goes along the real positive l axis and $P\left(l, 1+\frac{2s}{t}\right)$ is the analytic continuation of the Legendre polynomials. Note that the integrand has simple poles in correspondence of integer real values of l and thus eq. (2.72) is reproduced. The question that immediately arises is whether the function $a(l,t)$ is unique; it turns out to be not the case and one has to consider separately partial waves with even and odd angular momenta. Therefore the analytic continuation can be done in terms of two functions $a^{(\pm 1)}(l,t)$ and the integral representation takes the form:

$$\mathcal{A}(s,t) = \frac{1}{2i}\oint_C dl \frac{(2l+1)}{\sin(\pi l)} \sum_{\eta=\pm 1} \frac{\eta + e^{-i\pi l}}{2} a^{(\eta)}(l,t) P\left(l, 1+\frac{2s}{t}\right) , \tag{2.74}$$

where η is called the signature of the partial wave amplitude. In order to study the behaviour of this amplitude in the Regge limit eq. (2.70), it is convenient to deform the countour of integration C into $\tilde{C}$, such that the new one goes parallel to the imaginary axis at, for instance, $\mathrm{Re}\, l = -\frac{1}{2}$. In doing that one has to pick up all the contributions coming from poles and cuts in the complex plane one may encounter. In the following only the case of simple poles is considered for simplicity. Such singularities are called Regge poles and they occur at

$$l = \Omega^{n_\eta}(t) ,$$

as before η denotes the signature (even or odd) of the pole. The amplitude is written as the sum of two different contributions:

$$\mathcal{A}(s,t) = \mathcal{I}(s,t) + \mathcal{P}(s,t) . \tag{2.75}$$

The first contribution comes from the integral along $\mathrm{Re}\, l = -\frac{1}{2}$:

$$\begin{aligned} \mathcal{I}(s,t) &= \frac{1}{2i}\int_{-\frac{1}{2}-i\infty}^{-\frac{1}{2}+i\infty} dl \frac{(2l+1)}{\sin(\pi l)} \sum_{\eta=\pm 1} \frac{\eta + e^{-i\pi l}}{2} a^{(\eta)}(l,t) P\left(l, 1+\frac{2s}{t}\right) \\ &\quad \text{if } s \gg |t| \\ &\simeq \frac{1}{2i}\int_{-\frac{1}{2}-i\infty}^{-\frac{1}{2}+i\infty} dl \frac{(2l+1)}{\sin(\pi l)} \sum_{\eta=\pm 1} \frac{\eta + e^{-i\pi l}}{2} a^{(\eta)}(l,t) \frac{\Gamma(2l+1)}{\Gamma(l+1)^2} \left(\frac{s}{2t}\right)^l . \end{aligned} \tag{2.76}$$

Because the integral is along $\mathrm{Re}\, l = -\frac{1}{2}$, one can write $l = -\frac{1}{2} + ib$, obtaining

$$\left(\frac{s}{2t}\right)^l = \sqrt{\frac{2t}{s}} e^{ib\ln\left(\frac{s}{2t}\right)} .$$

So in the Regge limit:

$$\mathcal{I}(s,t) \to 0 , \text{ when } s \to \infty .$$

Hence the scattering amplitude is dominated by the contributions coming from the Regge poles, which can be computed thanks to the residue theorem:

$$\begin{aligned}\mathcal{P}(s,t) &= \sum_{\eta,n_\eta} \frac{(2l+1)\pi}{\sin(\pi l)} \frac{\eta + e^{-i\pi l}}{2} \mathrm{Res}\left[a^{(\eta)}(l,t)\right] P\left(l, 1+\frac{2s}{t}\right)\Big|_{l=\Omega^{n_\eta}(t)} \\ &\quad \text{if } s \gg |t| \\ &\simeq \sum_{\eta,n_\eta} \frac{(2l+1)\pi}{\sin(\pi l)} \frac{\eta + e^{-i\pi l}}{2} \mathrm{Res}\left[a^{(\eta)}(l,t)\right] \frac{\Gamma(2l+1)}{\Gamma(l+1)^2} \left(\frac{s}{2t}\right)^l \Big|_{l=\Omega^{n_\eta}(t)} .\end{aligned} \tag{2.77}$$

Moreover the leading energy behaviour for $s \to \infty$ is determined by the rightmost singularity:

$$\mathcal{A}(s,t) \simeq \frac{\eta + e^{-i\pi\Omega(t)}}{2} \beta(t)\, s^{\Omega(t)} , \tag{2.78}$$

where the function $\beta(t)$ contains the residue and the other coefficients. In the spirit of the partial wave expansion, eq. (2.78) can be interpreted in the following way: in the Regge limit the amplitude is dominated by an effective exchange in the t channel of an object with angular momentum $\Omega(t)$; because this number is not an integer (or a half-integer) this object cannot be a physical particle, it is called *reggeon*.

The theory developed so far predicts the Regge limit of a scattering amplitude: it behaves like a power of the centre of mass energy s. Unfortunately it does not say anything about the functional form of $\Omega(t)$. Information about it has to be extracted from experimental data. A particular t-channel scattering amplitude exhibits poles in correspondence of the exchange of physical particles with mass m and spin j such that $\Omega(m^2) = j$. The plot of these data in the (t, Ω) plane would show that they lay on a straight line called the *Regge trajectory*

$$\Omega(t) = \Omega^0 + \Omega' t\,,\ t > 0\,. \tag{2.79}$$

If this straight line is continued to negative values of t it provides information about the behaviour of the s-channel amplitude.

Through the optical theorem the intercept of the Regge trajectory Ω_0 determines the asymptotic behaviour of the total cross-section

$$\sigma_{TOT} = \frac{2}{F}\mathrm{Im}\,\mathcal{A}(s,t=0) \simeq \frac{1}{s}\mathrm{Im}\,\mathcal{A}(s,t=0) \sim s^{\Omega^0-1}\,. \tag{2.80}$$

A theorem due to Pomeranchuck, and revised afterwards in different forms, states that the total cross section for a given scattering process vanishes for large s unless it is dominated by the exchange of a state with quantum numbers of the vacuum. It is experimentally known that total cross sections slowly increase with s. If one was to

attribute this behaviour to a single reggeon exchange then, according to eq. (2.80), it must have intercept $\Omega_P^0 > 1$ and quantum numbers of the vacuum: this is called the *pomeron*. Studies of the total cross sections enable one to fit the value of the intercept [20], while the analysis of differential elastic cross sections determines the slope Ω'_P and establishes that the pomeron has even signature [21]:

$$\begin{aligned} \Omega_P^0 &\simeq 1.08 \\ \Omega'_P &\simeq 0.25\,\mathrm{GeV}\,. \end{aligned} \tag{2.81}$$

Deep inelastic scattering plays a crucial role in this analysis too. The Regge limit in this process is $s \gg Q^2$ and so $x \ll 1$. Analyses of the structure function F_2 show that at moderate values of the Bjorken variable ($10^{-2} < x < 10^{-1}$) the data are in good agreement with the pomeron picture. In the next section the high energy prediction of strongly interacting processes will be discussed in the framework of perturbative QCD. This will lead to a hard pomeron, as opposed to the soft one previously discussed, which has intercept $\omega^0 > \Omega_P^0$.

2.2.2 The BFKL equation

The leading contribution to the BFKL equation has been derived in different ways [22]-[25], and [26], [27]. In this sub-section a brief review is presented following the construction explained in [6]. The aim of the calculation is to compute the QCD pomeron by studying the behaviour of parton-parton scattering in the high energy limit. An important ingredient of the calculation is the *eikonal approximation*, which greatly simplifies the expressions of three-particle vertices when a soft gluon is emitted. In such an approximation if the incoming parton has momentum p and the soft gluon q the expressions for the vertices become:

$$\begin{aligned} qqg &: -2i\,g_s\,p^\mu\,\delta_{\lambda_1\lambda'_1}\,\tau^a_{ij} \\ ggg &: +2i\,g_s\,p^\mu\,g^{\nu\rho}\,T^A_{bc}\,, \end{aligned} \tag{2.82}$$

where λ_i are the quark helicities. The process to be considered is

$$q(p_1,\lambda_1) + q(p_2,\lambda_1) \longrightarrow q(p_1-q,\lambda'_1) + q(p_2+q,\lambda'_2)\,,$$

via the exchange of a colour singlet, to all orders in perturbation theory, keeping only the leading $\ln s$ term. Note that with this choice of kinematics $t = -\mathbf{q}^2$. The first contribution comes from the evaluation of one-loop diagrams as shown in fig. 2.4. The calculation can be performed using the Cutkosky rule. The lowest order amplitude

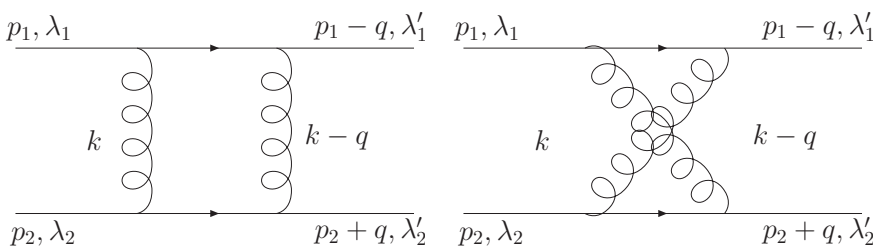

Figure 2.4: The lowest order contribution to quark-quark scattering via the exchange of a colour singlet.

turns out to be purely imaginary

$$\mathcal{A}_1 = 4i\,\alpha_s^2\,\delta_{\lambda_1\lambda_1'}\,\delta_{\lambda_2\lambda_2'}\frac{C_A^2-1}{4C_A^2}\int\frac{d^2\mathbf{k}}{\mathbf{k}^2(\mathbf{k}-\mathbf{q})^2}\,, \tag{2.83}$$

where on a Sudakov basis the momentum k has the expression:

$$k = yp_1 + zp_2 + \mathbf{k}\,, \tag{2.84}$$

and in the high energy limit $k^2 \simeq -\mathbf{k}^2$, $y = |z| \ll 1$. The next order in perturbation theory is the two-loop case. Diagrams can be classified into two classes: the ones which have a cut gluon line and the ones where the cut goes only through the quark lines. The first ones can be computed considering the amplitude for two quarks going into two quarks plus a gluon. The leading logarithmic contribution arises from the region where the longitudinal component of the momenta k_1 and k_2 of the internal lines are ordered:

$$y_2 \ll y_1 \ll 1\,, \quad |z_1| \ll |z_2| \ll 1\,, \tag{2.85}$$

while in contrast with the collinear case the magnitudes of the transverse momenta are all of the same order

$$|\mathbf{k}_1|^2 \simeq |\mathbf{k}_2|^2 \equiv |\mathbf{k}|^2 \ll s \tag{2.86}$$

The complete $2 \to 3$ amplitude can be expressed as the amplitude for the emission of a gluon along a vertical gluon line with the three-gluon coupling substituted by an effective vertex $\Gamma^{\sigma}_{\mu,\nu}(k_1, k_2)$. In order to compute the second class of diagrams one must consider the one-loop corrections to the process $qq \to qq$. Summing up the two classes

of contribution one obtains:

$$\mathrm{Im}\mathcal{A}_2 = -\frac{2C_A\alpha_s^3}{\pi^2}\,\delta_{\lambda_1\lambda_1'}\,\delta_{\lambda_2\lambda_2'}\,\frac{C_A^2-1}{4C_A^2}\ln\frac{s}{\mathbf{k}^2}\int d^2\mathbf{k}_1 d^2\mathbf{k}_2$$
$$\left[\frac{\mathbf{q}^2}{\mathbf{k}_1^2\mathbf{k}_2^2(\mathbf{k}_1-\mathbf{q})^2(\mathbf{k}_2-\mathbf{q})^2} - \frac{1}{2}\left(\frac{1}{\mathbf{k}_1^2(\mathbf{k}_1-\mathbf{k}_2)^2(\mathbf{k}_2-\mathbf{q})^2} + \mathbf{k}_1 \leftrightarrow \mathbf{k}_2\right)\right]. \tag{2.87}$$

Hence the two-loop amplitude contains a term for which the integrations over the transverse momenta factorise, leading to a contribution proportional to the one-loop amplitude.

The generalisation of such computation to n-loops is not an easy task even in the leading logarithmic approximation. Firstly diagrams describing $2 \to n+2$ processes have to be analysed in the kinematical region where

$$\frac{\mathbf{k}^2}{s} \ll y_{i+1} \ll y_i \ll 1\,, \quad \frac{\mathbf{k}^2}{s} \ll |z_i| \ll |z_{i+1}| \ll 1\,, \tag{2.88}$$

showing that such emissions can be still represented with a gluon ladder with the effective vertices $\Gamma^{\sigma}_{\mu,\nu}$. The picture still works and there are no leading logarithmic contributions coming from the emission of quarks. In the two-loop case there were diagrams for which the cut went only through the quark lines. These graphs can be seen themselves as the beginning of a ladder expansion and one can convince oneself that in order to compute the imaginary part of the n-loop amplitude, it is necessary to compute superpositions of gluon ladders. The effect of these superpositions is the *reggeization* of the gluon [6]. A particle with mass m and spin j is said to reggeize if the amplitude for a process which involves the t-channel exchange of the particle's quantum number behaves as $\mathcal{M} \sim s^{\omega(t)}$ and $\omega(m) = j$. In order to prove the reggeization of the gluon one has to perform a computation similar to the one for the pomeron but considering an octet exchange. Reggeization means that the propagator of the i^{th} vertical gluon has the form (in the Feynman gauge):

$$d_{\mu\nu} = \frac{ig_{\mu\nu}}{\mathbf{k}_i^2}\left(\frac{\rho_{i-1}}{\rho_i}\right)^{\epsilon_G(k_i^2)}\,, \tag{2.89}$$

where $\omega_G(-\mathbf{k}^2) = 1+\epsilon_G(-\mathbf{k}^2)$ is the gluon Regge trajectory, and its one-loop expression is:

$$\epsilon_G(-\mathbf{k}^2) = -\frac{\alpha_s C_A}{\pi}\int\frac{d^2\mathbf{k}'}{2\pi}\frac{\mathbf{k}^2}{\mathbf{k}'^2(\mathbf{k}^2-\mathbf{k}')^2}\,. \tag{2.90}$$

It is convenient to consider Mellin moments of the amplitude for singlet exchange, in order to unravel the nested integrals over the longitudinal momenta. Defining $x = \mathbf{k}^2/s$

one obtains

$$\int dx x^{N-1} \frac{\mathcal{A}(s,t)}{s} \equiv 4i\,\alpha_s^2\,\delta_{\lambda_1\lambda_1'}\,\delta_{\lambda_2\lambda_2'}\frac{C_A^2-1}{4C_A^2}\int \frac{d^2\mathbf{k}_1 d^2\mathbf{k}_2}{\mathbf{k}_2^2(\mathbf{k}_1-\mathbf{q})^2} f(N,\mathbf{k}_1,\mathbf{k}_2,\mathbf{q})\,, \tag{2.91}$$

The function f is closely related to the four-gluon Green's function and it is symmetric upon the exchange of the transverse momenta of the gluons at the top and at the bottom of the ladder ($\mathbf{k}_1 \leftrightarrow \mathbf{k}_2$). Henceforth only the case of zero momentum transferred $t = -\mathbf{q}^2 = 0$ will be considered; this choice greatly simplifies the equations and it is sufficient for the purposes of this thesis. The Green's function f admits a perturbative expansion in the strong coupling constant:

$$f(N,\mathbf{k}_1,\mathbf{k}_2) = \sum_{n=1}^{\infty}\left(\frac{\alpha_s C_A}{\pi}\right)^{n-1} f_n(N,\mathbf{k}_1,\mathbf{k}_2)\,, \tag{2.92}$$

whose first few coefficients are:

$$\begin{aligned} f_1(N,\mathbf{k}_1,\mathbf{k}_2) &= \frac{1}{N}\delta^{(2)}(\mathbf{k}_1-\mathbf{k}_2)\,, \\ f_2(N,\mathbf{k}_1,\mathbf{k}_2) &= \frac{\alpha_s C_A}{\pi}\frac{1}{N^2}\frac{1}{2\pi(\mathbf{k}_1-\mathbf{k}_2)^2}\,, \\ &\vdots \end{aligned} \tag{2.93}$$

Looking at the structure of such coefficients, it is possible to show that f can be obtained as the solution of an integral equation, the renowned BFKL equation:

$$N f(N,\mathbf{k}_1,\mathbf{k}_2) = \delta^{(2)}(\mathbf{k}_1-\mathbf{k}_2) + \alpha_s\left[\mathcal{K}_0\otimes f\right](N,\mathbf{k}_1,\mathbf{k}_2)\,, \tag{2.94}$$

where the action of the leading order kernel on f is given by

$$\begin{aligned} \alpha_s\left[\mathcal{K}_0\otimes f\right](N,\mathbf{k}_1,\mathbf{k}_2) &= \frac{\alpha_s C_A}{\pi}\int \frac{d^2\mathbf{k}'}{\pi(\mathbf{k}_1-\mathbf{k}')^2} \\ &\quad \left[-\frac{\mathbf{k}_1^2}{\mathbf{k}'^2+(\mathbf{k}_1-\mathbf{k}')^2} f(N,\mathbf{k}_1,\mathbf{k}_2) + f(N,\mathbf{k}',\mathbf{k}_2)\right]. \end{aligned} \tag{2.95}$$

The first contribution to the kernel comes from the one-loop Regge trajectory, while the second one describes the emission of one gluon along the ladder. The BFKL equation is schematically shown in fig. 2.5.

So far only partonic processes have been considered; in order to make contact between the BFKL equation and phenomenology, the coupling of the pomeron to hadrons must be described. The Mellin transform of the forward amplitude for hadron-

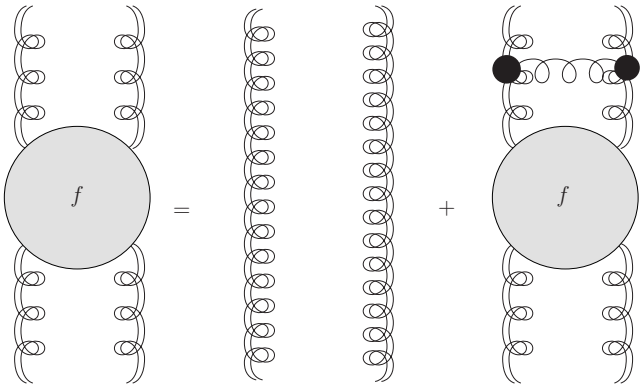

Figure 2.5: The BFKL equation for the gluon Green's function f. The vertical double lines represent reggeized gluons, while the black blobs are the effective vertices $\Gamma^{\sigma}_{\mu,\nu}$.

hadron scattering has the form

$$\mathcal{A}^{(\mathrm{hadr})}(N, t=0) = \mathcal{C} \int \frac{d^2\mathbf{k}_1}{(2\pi)^2} \frac{d^2\mathbf{k}_2}{(2\pi)^2} \frac{\Phi_1(\mathbf{k}_1)\Phi_2(\mathbf{k}_2)}{\mathbf{k}_1^2 \mathbf{k}_2^2} f(N, \mathbf{k}_1, \mathbf{k}_2)\,, \tag{2.96}$$

where $\mathcal{C}$ is the colour factor of the process. The pomeron-hadron coupling is parametrised by the functions Φ_i, which clearly depend on non-perturbative physics. The *unintegrated gluon density* is then defined as the hadronic scattering amplitude obtained when one of the hadron-pomeron couplings is replaced by a delta function, e.g. $\Phi_2(\mathbf{k}_2) = 2\pi\mathbf{k}_2^2\,\delta^{(2)}(\mathbf{k}_2 - \mathbf{k})$:

$$\mathcal{G}(N, \mathbf{k}) = \frac{1}{(2\pi)^3} \int \frac{d^2\mathbf{k}_1}{\mathbf{k}_1^2} \mathbf{k}^2 \Phi_1(\mathbf{k}_1) f(N, \mathbf{k}_1, \mathbf{k})\,. \tag{2.97}$$

In order to recover the parton distribution function which enters the DGLAP evolution eq. (2.58), this gluon density has to be integrated over the transverse momenta up to the relevant energy scale Q^2:

$$G(N, Q^2) \equiv \int \frac{d^2\mathbf{k}}{\pi\mathbf{k}^2}\, \Theta(Q^2 - \mathbf{k}^2)\mathcal{G}(N, \mathbf{k})\,. \tag{2.98}$$

The BFKL equation (2.94) can be cast in the form of an evolution equation in x for the unintegrated gluon density $\mathcal{G}$, inverting the N-Mellin and performing a second Mellin transform in order to turn the convolution integral into an ordinary product. The

Mellin transform of the evolution kernel is given by

$$\begin{aligned}\chi_0(M) &= \int d^2\mathbf{k}'\,\mathcal{K}_0(\mathbf{k}',\mathbf{k})\left(\frac{\mathbf{k}'^2}{\mathbf{k}^2}\right)^{M-1} \\ &= \frac{C_A}{\pi}\left[2\psi(1)-\psi(M)-\psi(1-M)\right], \end{aligned} \tag{2.99}$$

where ψ is the logarithmic derivative of the Euler Gamma function. The BFKL equation takes the form:

$$\frac{d}{d\xi}\mathcal{G}(\xi,M) = \alpha_s\chi_0(M)\mathcal{G}(\xi,M)\,, \quad \text{with} \quad \xi = \ln\frac{1}{x}\,. \tag{2.100}$$

It is clear from eq. (2.99) that the exchange symmetry $\mathbf{k}_1 \leftrightarrow \mathbf{k}_2$ in Mellin space becomes

$$M \leftrightarrow 1-M\,. \tag{2.101}$$

This property will be extensively used in this work. It is not difficult to solve eq. (2.100) at LO; the solution in (ξ,t) space has the form:

$$\mathcal{G}(\xi,t) = \int_{c-i\infty}^{c+i\infty}\frac{dM}{2\pi i}\exp\left[Mt+\alpha_s\chi_0(M)\xi\right]\mathcal{G}(0,M)\,. \tag{2.102}$$

The asymptotic behaviour of this function is determined, in the saddle point approximation, by the stationary point of the exponent; in the Regge limit $\frac{t}{\xi}\to 0$ and one obtains:

$$\mathcal{G}(\xi,t) \propto \exp\left[-\alpha_s\chi_0\left(\frac{1}{2}\right)\ln x\right] = x^{-(\omega^0-1)}\,. \tag{2.103}$$

This result is the hard pomeron prediction, which has been anticipated at the end of section 2.2.1:

$$c(\alpha_s) \equiv \omega^0 - 1 = \alpha_s\frac{C_A}{\pi}4\ln 2 > \Omega_P^0 - 1\,. \tag{2.104}$$

2.2.3 BFKL kernel at next-to leading order

The computation of the next-to-leading order correction to the BFKL kernel took almost ten years. The program was set up by Fadin and Lipatov in [28], where it was shown how to extend the computation previously described to the next-to-leading logarithmic accuracy. Firstly the two-loop gluon Regge trajectory is needed [29], [30]. Secondly the one-loop correction to the vertex $\Gamma^{\rho}_{\mu\nu}$ for the emission of one gluon along the ladder has to be considered [31]. Finally, at this accuracy, the tree level vertices for the emission of two gluons and for the production of a quark-antiquark pair along the ladder have to be included [32], [33]. The calculation of the BFKL pomeron in the next-to-leading approximation was completed by Fadin and Lipatov in [34] and by Camici and Ciafaloni in [35] and [36]. The evolution equation for the unintegrated

parton distribution at NLO can be written as:

$$\frac{d}{d\xi}\mathcal{G}(\xi,\mathbf{k}) = \left[\left(\alpha_s(\lambda^2)\mathcal{K}_0 + \alpha_s^2(\lambda^2)\mathcal{K}_1\right)\otimes\mathcal{G}\right](\xi,\mathbf{k})\,. \tag{2.105}$$

It is clear from the previous equation that the running of the coupling constant cannot be neglected beyond leading order. In particular working at this accuracy requires one to consider

$$\alpha_s(\lambda^2) = \frac{\alpha_s(\mu^2)}{1+\alpha_s(\mu^2)\beta_0\ln\frac{\lambda^2}{\mu^2}}\,, \tag{2.106}$$

where β_0 is the QCD β-function at one loop. A delicate issue has to be faced, namely the choice of the scale λ^2 for the running coupling. If one chooses $\lambda^2 = \mathbf{k}^2$ upon Mellin transform the BFKL equation becomes

$$\frac{d}{d\xi}\mathcal{G}(\xi,M) = \left(\hat{\alpha}_s\chi_0(M) + \hat{\alpha}_s^2\chi_1(M)\right)\mathcal{G}(\xi,M)\,, \tag{2.107}$$

while for $\lambda^2 = \mathbf{k}'^2$:

$$\frac{d}{d\xi}\mathcal{G}(\xi,M) = \left(\chi_0(M)\hat{\alpha}_s + \chi_1(M)\hat{\alpha}_s^2\right)\mathcal{G}(\xi,M)\,. \tag{2.108}$$

The differential operator $\hat{\alpha}_s$ represents the running coupling constant in Mellin space:

$$\hat{\alpha}_s = \frac{\alpha_s(\mu^2)}{1-\alpha_s(\mu^2)\beta_0\frac{\partial}{\partial M}}\,; \tag{2.109}$$

different arguments for the running coupling correspond to different orderings of the operators. In particular it is possible to compute contributions coming from the choice of the energy scale in an algebraic way:

$$\hat{\alpha}_s\chi_0 = \chi_0\hat{\alpha}_s + [\hat{\alpha}_s,\chi_0]\,. \tag{2.110}$$

These considerations are fundamental in order to understand *running coupling duality*, which will be introduced in the following chapter. The $\mathcal{O}\left(\alpha_s^2\right)$ contribution to the Mellin-transformed kernel in eq. (2.108) is given by:

$$\begin{aligned}\chi_1(M) \;=\; & -\left(\frac{C_A}{2\pi}\right)^2\Big[\left(\frac{11}{3}-\frac{2n_f}{3C_A}\right)\frac{1}{2}(\chi_0{}^2(M)-\psi'(M)+\psi'(1-M))\\ & -\left(\frac{67}{9}-\frac{\pi^2}{3}-\frac{10n_f}{9C_A}\right)\chi_0(M)-6\zeta(3)\\ & +\frac{\pi^2\cos(\pi M)}{\sin^2(\pi M)(1-2M)}\left(3+\left(1+\frac{n_f}{C_A{}^3}\right)\frac{2+3M(1-M)}{(3-2M)(1+2M)}\right)\\ & -\psi''(M)-\psi''(1-M)-\frac{\pi^3}{\sin(\pi M)}+4\phi(M)\Big]\,.\end{aligned} \tag{2.111}$$

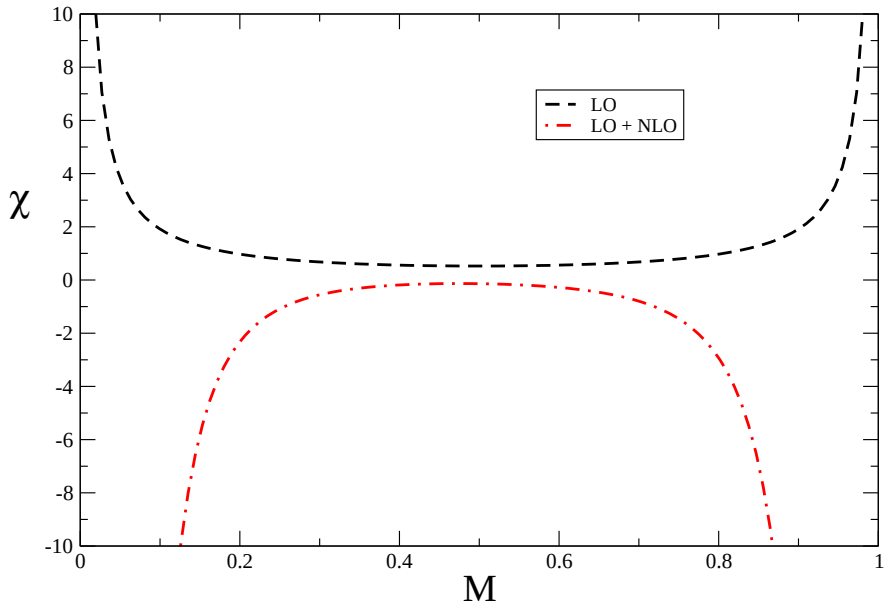

Figure 2.6: Plots of the BFKL kernel at leading order approximation (dashed line) and LO + NLO (dot-dashed line) with $\alpha_s = 0.2$ and $n_f = 4$. The perturbative expansion is unstable.

The function $\phi(M)$ is:

$$\begin{aligned}\phi(M) &= -\int_0^1 \frac{dx}{1+x}(x^{M-1}+x^{-M})\int_x^1 \frac{dt}{t}\ln(1-t) \\ &= \sum_{n=0}^{\infty}(-1)^n\Big[\frac{\psi(n+1+M)-\psi(1)}{(n+M)^2}+\frac{\psi(n+2-M)-\psi(1)}{(n+1-M)^2}\Big]\,.\end{aligned} \tag{2.112}$$

The above expression is not symmetric under the exchange $M \leftrightarrow 1-M$ in contrast to the LO case. Specifically the contribution which breaks the symmetry is $-\psi'(M)+\psi'(1-M)$. The origin of this term can be understood looking at eq. (2.110):

$$[\hat{\alpha}_s, \chi_0] = \hat{\alpha}_s^2\beta_0\chi_0'(M) = \hat{\alpha}_s^2\beta_0\frac{C_A}{\pi}\left(-\psi'(M)+\psi'(1-M)\right)+\mathcal{O}\left(\hat{\alpha}_s^3\right)\,. \tag{2.113}$$

In fig. 2.6 the kernel χ is plotted as a function of the variable M, between zero and one, at leading and next-to-leading order. It is clear that the perturbative expansion is not stable. The NLO corrections are large and they change the qualitative shape of the kernel even for reasonable values of α_s. This is mainly due to poles of increasing order and alternating sign in $M = 0$ and $M = 1$. For instance the Laurent expansions

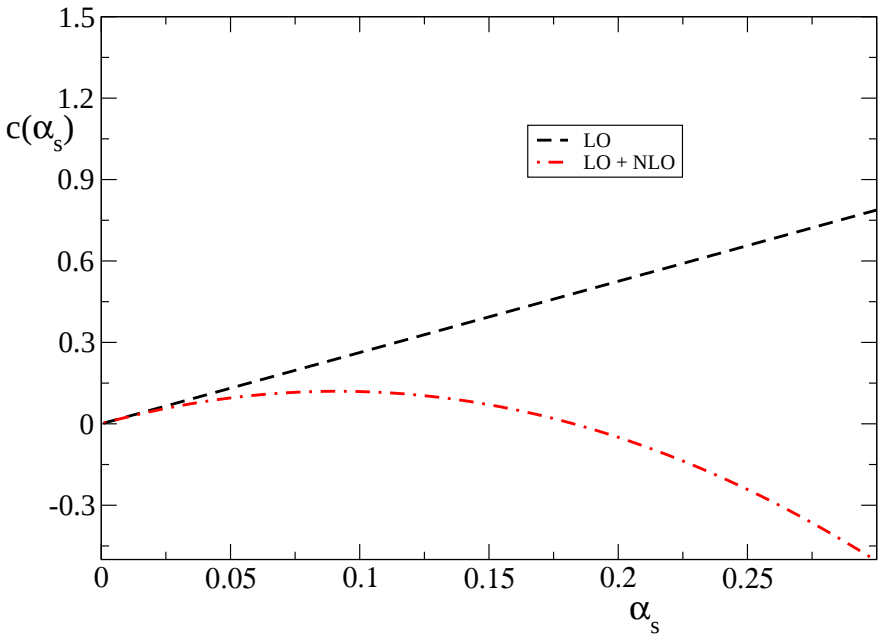

Figure 2.7: The pomeron intercept $c(\alpha_s) = \chi(\frac{1}{2}, \alpha_s)$, plotted as a function of the strong coupling constant.

about $M = 0$ of the LO and NLO kernels are:

$$\begin{aligned} \chi_0 &\sim \frac{1}{M} + \mathcal{O}\left(M^2\right) , \\ \chi_1 &\sim -\frac{1}{M^3} + \mathcal{O}\left(M^{-2}\right) . \end{aligned} \tag{2.114}$$

The slow convergence of the perturbative expansion can also be seen looking at the plot of the pomeron intercept $c(\alpha_s) = \chi(\frac{1}{2}, \alpha_s)$ in fig.2.7. The NLO curve sensibly departs from the LO one at very small values of the coupling constant ($\alpha_s \lesssim 0.05$). In order to perform reliable phenomenological predictions it is necessary to cure the perturbative instability of the kernel. This can be achieved by resumming to all orders the troublesome terms. In Chapter 3 it will be shown how the DGLAP anomalous dimension can be used in order to perform such a resummation. Alternatively one can try to compute higher order contributions to the kernel. However, beyond NLO the BFKL evolution presents various problems. A direct computation shows that the universality of the pomeron exchange is broken at NNLO [37]. Furthermore, a new class of contributions involving the t-channel exchange of four gluons enters at NNLO (see [38] and references therein). These are higher twist (power suppressed) contributions which can mix with the two-gluon operator, spoiling the ladder picture previously described. The form of the full BFKL equation at NNLO is thus different from that one at LO and NLO, in contrast to the DGLAP equation which has the same form

Progress has been recently made [39], [40] but a complete description of the BFKL at NNLO is not yet available. The computation of the collinear approximation of the BFKL kernel at $\mathcal{O}\left(\alpha_s^3\right)$ has been performed in [41]. The details of this computation are presented in Chapter 6.

Chapter 3

High energy resummation

The purpose of this chapter is to continue the analysis of perturbative QCD processes at high energy. This is particularly important in order to achieve a good understanding of the enormous background which characterises hadron colliders such as the LHC. In the high energy, or semi-hard, regime the following hierarchy of energy scales is realised:

$$\Lambda^2 \ll Q^2 \ll s\,; \tag{3.1}$$

Q^2 sets the scale of the coupling and so the first strong inequality ensures that perturbation theory is applicable as $\alpha_s(Q^2) \ll 1$. This scale can be identified, for instance, with the transferred momentum in deep inelastic scattering or with the mass of some heavy particles produced in the final states such as heavy quarks, Higgs boson or with the invariant mass of a lepton pair. The analysis of collinear factorisation carried out in the previous chapter enables one to resum large logarithms of the ratio Q^2/Λ^2 thanks to the DGLAP equation. However, the second strong inequality could destroy the reliability of this picture because both coefficient and splitting functions contain logarithms of the ratio Q^2/s, which become dangerous in the high energy limit. Because for deep inelastic scattering at high energy this ratio corresponds to the Bjorken variable x, the high energy regime is often called small x limit. In the previous chapter the high energy behaviour of QCD has been discussed, introducing the BFKL equation in order to resum high energy logarithms. In this chapter the general framework in which the high energy resummation of hard processes is performed is presented.

3.1 k_T-factorisation

The basic idea in this analysis consists of replacing the standard collinear factorisation eq. (2.34) and eq. (2.61) of hard coefficient functions and parton distributions with a corresponding high energy factorisation [44], [47]. This factorisation is k_T-dependent and enables one to resum leading high energy logarithms in the coefficient function

to all orders in perturbation theory. In order to simplify the formulae, the case of photon-hadron scattering (photoproduction) will be analysed in this section; this eases the connection with standard collinear factorisation discussed in the previous chapter for deep inelastic scattering. The generalisation to processes with two hadrons in the initial state will be presented afterwards. The k_T-factorisation theorem states that in the high energy limit the dimensionless hadronic cross section $\Sigma \equiv Q^2\sigma$ can be written as

$$\Sigma(\rho_h, Q^2) \;=\; \sum_j \int_{\rho_h}^1 \frac{dx_1}{x_1} \int \frac{d^2\mathbf{k}_1}{\pi \mathbf{k}_1^2} \hat{\Sigma}_j^{\text{off}} \left(\frac{\rho_h}{x_1}, \frac{\mathbf{k}_1}{Q}, \alpha_s(\mu^2) \right) \mathcal{F}_j(x_1, \mathbf{k}_1^2, \mu^2), \tag{3.2}$$

up to terms suppressed by powers of the hard scale Q^2; ρ_h is the ratio between the hard scale of the process Q^2 and the centre-of-mass energy s (the equivalent of the Bjorken variable for hadronic processes). The unintegrated parton distribution function $\mathcal{F}_j$ has been defined in eq. (2.97). Because the dominant contribution in the high energy limit is given by gluons, the summation over the parton index in (3.2) will be dropped in the following discussion and only the gluon distribution $\mathcal{G}$ will be considered. A full proof of eq. (3.2) would require a detailed analysis of gluon emission in the small x limit [42], [43]. Choosing an axial gauge multi-gluon exchange diagrams are subleading; it is then possible to show that initial soft gluon radiation can be factorised in the kinematic region where the longitudinal momenta are strongly ordered, building up the unintegrated distribution function $\mathcal{G}$. Then, what is left is the hard vertex of the process initiated by the photon and an off-shell gluon. Such a gluon is attached to an external parton with an eikonal vertex eq. (2.82), hence the off-shell cross section which enters the k_T-factorisation is:

$$\hat{\Sigma}_g^{\text{off}} \left(\frac{\rho_h}{x_1}, \frac{\mathbf{k}_1}{Q} \right) = \frac{\rho_h}{2x_1} \frac{2x_1^2 p_1^\mu p_1^\nu}{\mathbf{k}_1^2} \mathcal{A}_{\mu\nu}(k_1, k_2)\,, \tag{3.3}$$

where the obvious dependence on the strong coupling has been dropped. A detailed description of the kinematics of processes with initial off-shell partons is reported in Appendix A.2. In eq. (3.3) the momentum p_1 in the numerator comes from the eikonal vertex; $\mathcal{A}$ is the contribution coming from the relevant hard process to the imaginary part of the $\gamma g \to \gamma g$ amplitude. A more careful analysis at the level of the matrix element can simplify the structure of eq. (3.3), as shown in the following. The off-shell

matrix element saturated with the eikonal coupling is

$$\begin{aligned}\mathcal{M}^{\text{off}}(k_1,k_2;p_3,p_4) &= \frac{\sqrt{2}x_1\,p_1^\mu}{|\mathbf{k}_1|}\mathcal{M}_\mu(k_1,k_2;p_3,p_4)\\ &= \frac{\sqrt{2}x_1\,p_1^\mu}{|\mathbf{k}_1|}d_{\mu\nu}(k_1)\widehat{\mathcal{M}}^\nu(k_1,k_2;p_3,p_4)\,,\end{aligned} \tag{3.4}$$

where the polarisation tensor $d_{\mu\nu}$ comes from the off-shell gluon. This object is gauge dependent and one might wonder about the gauge invariance of $\mathcal{M}^{\text{off}}$. All the derivation is performed in an axial gauge, so the polarisation tensor has the form:

$$d_{\mu\nu}(k) = -g_{\mu\nu} + \frac{n_\mu k_\nu + k_\mu n_\nu}{n\cdot k} - n^2\frac{k_\mu k_\nu}{(n\cdot k)^2}\,, \tag{3.5}$$

with, for instance, $n = ap_1 + bp_2$. A straightforward calculation gives:

$$p_1^\mu d_{\mu\nu}(k_1) = \frac{\mathbf{k}_{1\,\nu}}{x_1}\,, \tag{3.6}$$

so that the gauge dependence cancels out and the off-shell matrix element becomes:

$$\mathcal{M}^{\text{off}} = \sqrt{2}\frac{\mathbf{k}_1^\mu}{|\mathbf{k}_1|}\widehat{\mathcal{M}}^\mu\,. \tag{3.7}$$

If hadron-hadron processes are considered, then the matrix element $\widehat{\mathcal{M}}$ itself contains gauge-dependent contributions, because of the non-Abelian diagrams. Nevertheless it is possible to check for specific processes that it is gauge invariant too because the eikonal couplings induce physical polarisation for the initial gluons, despite being off-shell [44]. Therefore the hard cross section which enters the k_T-factorisation theorem is gauge invariant and it is given by the leading order diagrams of the relevant process computed with initial off-shell gluons whose polarisation vectors are given by eq. (3.7); the squared matrix element has to be averaged over colour and polarisations of the initial particles. It is then integrated over the final state phase space with flux factor given by the longitudinal contribution to the centre of mass energy $\nu = 2x_1p_1\cdot p_2$:

$$\hat{\Sigma}_g^{\text{off}} = \frac{Q^2}{2\nu}\int d\Phi\,\left|\overline{\mathcal{M}}^{\,\text{off}}\right|^2\,. \tag{3.8}$$

The convolutions over transverse and longitudinal momenta in eq. (3.2) can be turned into ordinary products by taking the Mellin transforms with respect

to ρ_h and Q^2:

$$\Sigma(N,M) = \int_0^1 \frac{d\rho_h}{\rho_h}\rho_h^N \int_0^\infty \frac{dQ^2}{Q^2}\left(\frac{Q^2}{\mu^2}\right)^{-M} \Sigma(\rho_h, Q^2)\,, \tag{3.9}$$

so that the factorisation formula becomes:

$$\Sigma(N,M) = \hat{\Sigma}_g^{\rm off}(N,M)\mathcal{G}(N,M)\,, \tag{3.10}$$

where on the right-hand side of the equation the double Mellin transformed of the off-shell cross section and of the gluon density have been introduced. The factorisation formula eq. (3.10) is valid in the high energy limit ($N \to 0$) and in the collinear limit ($M \to 0$). In order to make contact with standard collinear factorisation it is better to deal with integrated parton distributions, rather than unintegrated ones

$$G(x,Q^2) = \int_0^{Q^2} \frac{dk^2}{k^2}\mathcal{G}(x,k^2)\,, \tag{3.11}$$

which in double Mellin space (N,M) becomes

$$G(N,M) = \frac{1}{M}\,\mathcal{G}(N,M) \tag{3.12}$$

It is convenient to define an impact factor $h(N,M)$ by multiplying the Mellin transformed of the off-shell cross section by the factor M, coming from the parton densities:

$$\begin{aligned} h(N,M) &= M\hat{\Sigma}_g^{\rm off}(N,M) \\ &= M\int_0^1 \frac{d\rho}{\rho}\rho^N \int \frac{d^2\mathbf{k}_1}{\pi\mathbf{k}_1^2}\left(\frac{\mathbf{k}_1^2}{Q^2}\right)^M \hat{\Sigma}_g^{\rm off}\left(\rho, \frac{\mathbf{k}_1}{Q}\right)\,, \\ &\qquad \text{with} \quad \rho = \frac{\rho_h}{x_1}\,. \end{aligned} \tag{3.13}$$

The physical cross section is then obtained inverting the Mellin transforms:

$$\begin{aligned} \Sigma(\rho_h, Q^2) &= \int_{c-i\infty}^{c+i\infty} \frac{dN}{2\pi i}e^{\xi N}\int_{c-i\infty}^{c+i\infty}\frac{dM}{2\pi i}e^{tM}h(N,M)G(N,M)\,, \\ &\qquad \text{with} \quad \xi = \ln\frac{1}{\rho_h}\,, \quad t = \ln\frac{Q^2}{\mu^2}\,. \end{aligned} \tag{3.14}$$

Here N and M have to be considered as complex variables. The two contours of integration have to be kept to the right of the singularities of the integrand near $N = 0$ and $M = 0$. The purpose of this discussion is the resummation of the collinear and high

energy logarithms, which contaminate the coefficient function evaluated at fixed order in perturbation theory. In Mellin space such logarithms correspond to inverse powers of M and N respectively. It turns out that these logarithms are single logarithms: at each order in perturbation theory there is at most one extra logarithm of each type for every power of the strong coupling. Hence a typical contribution to integrand in eq. (3.14) has the form $\alpha_s^l M^{-m} N^{-n}$, with $m, n \leq l$. In order to obtain meaningful results such contributions have to be factored into the gluon distribution $G(N, M)$ and resummed by solving the DGLAP and BFKL evolution equations (2.54) and (2.100) respectively. Taking the double Mellin transform both equations simplify to pure algebraic ones; neglecting the running of the coupling the two equations become:

$$\begin{aligned} MG(N,M) &= G_0(N) + \gamma(N,\alpha_s)G(N,M)\,, \\ NG(N,M) &= \bar{G}_0(M) + \chi(M,\alpha_s)G(N,M)\,, \end{aligned} \tag{3.15}$$

where $G_0(N)$ and $\bar{G}_0(M)$ are non-perturbative initial conditions and, unless stated differently, $\gamma = \gamma^{(+)}$ is the larger eigenvalue of the anomalous dimension matrix in the singlet sector. The two evolution equations admit the simple solution:

$$G(N,M) = \frac{1}{M - \gamma(N,\alpha_s)} G_0(N) = \frac{1}{N - \chi(M,\alpha_s)} \bar{G}_0(M)\,. \tag{3.16}$$

The leading twist solution is determined by the pole in the perturbative factors:

$$M = \gamma(N,\alpha_s)\,, \quad N = \chi(M,\alpha_s)\,. \tag{3.17}$$

Hence the evolution kernels must satisfy the consistency conditions:

$$\begin{aligned} M &= \gamma(\chi(M,\alpha_s),\alpha_s) \\ N &= \chi(\gamma(N,\alpha_s),\alpha_s)\,. \end{aligned} \tag{3.18}$$

These are called duality relations [52], [53], [55] and they state that the two evolution kernels are one the inverse of the other one. Therefore χ determines the high energy ($N = 0$) singularities of the DGLAP anomalous dimension and γ the collinear poles ($M = 0$) of the BFKL kernel. Further implications of duality, its extension beyond the fixed coupling approximation and the resummation of the kernels will be investigated in section 3.2. Fixed coupling (or naive) duality can be also used to perform the resummation of the logarithms which contaminate the hard coefficient functions. Factorisation states that all the collinear and high energy logarithms can be factored into the gluon distribution, hence the impact factor $h(N, M)$ in eq. (3.14) is a regular function of its arguments in a neighbourhood of the origin. The singularity close to the origin is thus determined by $G(N, M)$ and eq. (3.16) can be used to

perform, via the residue theorem, one of the Mellin inversions in eq. (3.14). Usually the M-inverse Mellin transform is performed in this way, while the contour integral over N is computed numerically. According to eq. (3.17), the singularity close to the origin is at $M = \gamma(N, \alpha_s)$, so the hadronic cross section evaluated at the pole becomes

$$\Sigma(\rho_h, Q^2) = \int_{c-i\infty}^{c+i\infty} \frac{dN}{2\pi i} e^{\xi N} e^{t\gamma(N,\alpha_s)} h(N, \gamma(N, \alpha_s)) G_0(N)\,. \tag{3.19}$$

The anomalous dimension computed from naive duality, eq. (3.18), contains itself resummed poles in N:

$$\gamma(N, \alpha_s) = \gamma_s\left(\frac{\alpha_s}{N}\right) = \sum_{k=1}^{\infty} g_k^{(s)} \left(\frac{\alpha_s}{N}\right)^k\,, \tag{3.20}$$

so the leading high energy logarithms in the hard coefficient function are effectively resummed. The first few terms of the series in eq. (3.20) are

$$\gamma_s\left(\frac{\alpha_s}{N}\right) = \frac{C_A}{\pi}\frac{\alpha_s}{N} + 2\zeta_3\left(\frac{C_A}{\pi}\frac{\alpha_s}{N}\right)^4 + 2\zeta_5\left(\frac{C_A}{\pi}\frac{\alpha_s}{N}\right)^6 + \ldots \tag{3.21}$$

It is important to notice that with this procedure it is straightforward to extract from the impact factor the leading high energy singularities of the fixed order coefficient function $C(N, \alpha_s)$. The perturbative expansion of the standard coefficient function, computed from collinear factorisation is

$$C(N, \alpha_s) = \sum_{n=0}^{\infty} \alpha_s^n C^{(n)}(N)\,. \tag{3.22}$$

On the other hand, the explicit N dependence of the impact factor can be neglected because it is subleading: $h(N, M)$ is free of the high energy poles. One can set $N = 0$ and Taylor expand the impact factor with respect to M:

$$h(0, M) = \sum_{m=0}^{\infty} \alpha_s\, h_m M^m\,. \tag{3.23}$$

In order to get leading high energy singularities of the coefficient function it is sufficient to use the pole condition eq. (3.17), substituting as $\gamma(N, \alpha_s)$ the small N limit of the fixed order expansion of the anomalous dimension $\gamma(N, \alpha_s) = \sum_{k=0}^{\infty} \alpha_s^{k+1}\gamma_k(N)$ or, equivalently, the resummed expression eq. (3.20) truncated at the appropriate

perturbative order. One obtains:

$$\begin{aligned} C(N,\alpha_s) &= \sum_{n=0} \alpha_s^n C^{(n)}(N) \\ &= \alpha_s \sum_m h_m \left[\sum_k g_k^{(s)} \left(\frac{\alpha_s}{N}\right)^k \right]^m (1+\mathcal{O}(N)) \,. \end{aligned} \tag{3.24}$$

Thanks to this observation the matching between resummed results and fixed order calculations is under control.

However, some care has to be taken in comparing results from collinear and high energy factorisation beyond leading order. It was shown in [46] that the parton density defined from collinear factorisation and the gluon Green's function extracted from high energy factorisation have different normalisations; the ratio of the two distributions is a universal factor. This result is obtained considering the dimensional regularised version of k_T-factorisation eq. (3.2):

$$\Sigma(N,Q^2) = \int d^{2-2\varepsilon}\mathbf{k}_1 \, \hat{\Sigma}^{\text{off}} \left(N, \frac{\mathbf{k}_1}{Q}, \left(\frac{Q^2}{\mu^2}\right)^{\varepsilon}, \varepsilon \right) f^{\text{bare}}(N,\mathbf{k}_1,\alpha_s,\mu,\varepsilon) G^{\text{bare}}(N,\mu,\varepsilon) \,, \tag{3.25}$$

where f^{bare} is the bare gluon Green's function and G^{bare} is the bare gluon density. In the case of a collinear safe process, the off-shell cross section is free of collinear poles and can be computed in four dimensions. All the ε poles are in the Green's function and they can be factorised through a universal transition function. In the $\varepsilon \to 0$ limit, one obtains [46]:

$$f^{\text{bare}} = \frac{\gamma_{gg}(N,\alpha_s)}{\pi \mathbf{k}^2} \, R \left(\frac{\mathbf{k}^2}{\mu^2}\right)^{\gamma_{gg}} \Gamma_{gg} \,, \tag{3.26}$$

where the $\overline{\text{MS}}$ transition function is defined as:

$$\Gamma_{gg} = \exp\left(\frac{1}{\varepsilon} \int_0^{\alpha_s e^{-\varepsilon(\ln 4\pi - \gamma_E)}} \frac{d\alpha}{\alpha} \gamma_{gg}(N,\alpha) \right) . \tag{3.27}$$

In the high energy limit

$$\gamma_{gg}(N,\alpha_s) = \gamma_s\left(\frac{\alpha_s}{N}\right) + \mathcal{O}\left(\alpha_s \left(\frac{\alpha_s}{N}\right)^k\right) . \tag{3.28}$$

As before the anomalous dimension $\gamma_s = \gamma_s\left(\frac{\alpha_s}{N}\right)$ is the naive dual to leading order BFKL kernel χ_0 and R gives the normalisation mismatching between collinear and high energy factorisation. The poles are then absorbed into the bare gluon distribution

$$G(N,\mu^2) = \Gamma_{gg} G^{\text{bare}} \,. \tag{3.29}$$

More details about the functional form of R will be discussed in Chapter 6. The mismatch in the normalisation can be regarded as a difference in the factorisation schemes. Traditionally the factorisation scheme related to high energy factorisation is called Q_0, so the relative normalisation of the gluon in the two schemes is given by:

$$R(N,t) = \frac{G^{Q_0}(N,t)}{G^{\overline{\rm MS}}(N,t)}\,. \tag{3.30}$$

The impact factor computed so far is in Q_0, while the $\overline{\rm MS}$ result is given by

$$h^{\overline{\rm MS}}(N,M) = h(N,M)R(N,M)\,, \tag{3.31}$$

so that eq. (3.19) becomes:

$$\Sigma(\rho_h,Q^2) = \int_{c-i\infty}^{c+i\infty}\frac{dN}{2\pi i}e^{\xi N}e^{t\gamma_s}R(0,\gamma_s)h(0,\gamma_s)G_0(N)\,, \tag{3.32}$$

with

$$\begin{aligned} R\left(0,\gamma_s\left(\frac{\alpha_s}{N}\right)\right) &= 1+\frac{8}{3}\zeta_3\left(\frac{C_A}{\pi}\right)^3\left(\frac{\alpha_s}{N}\right)^3-\frac{3}{4}\zeta_4\left(\frac{C_A}{\pi}\right)^4\left(\frac{\alpha_s}{N}\right)^4 \\ &\quad+\frac{22}{5}\zeta_5\left(\frac{C_A}{\pi}\right)^5\left(\frac{\alpha_s}{N}\right)^5+\mathcal{O}\left(\left(\frac{\alpha_s}{N}\right)^6\right). \end{aligned} \tag{3.33}$$

The normalisation factor induces a scheme dependence on the anomalous dimension as it will be explicitly shown in the next section.

So far k_T-factorisation for photoproduction processes has been discussed. However the main purpose of this thesis is to discuss collider phenomenology and thus processes with two hadrons in the initial state must be considered. The factorisation formula eq. (3.2) generalises to:

$$\begin{aligned} \Sigma(\rho_h,Q^2) &= \sum_{j_1,j_2}\int_{\rho_h}^1\frac{dx_1}{x_1}\int_{\rho_h}^1\frac{dx_2}{x_2}\int\frac{d^2\mathbf{k}_1}{\pi\mathbf{k}_1^2}\int\frac{d^2\mathbf{k}_2}{\pi\mathbf{k}_2^2} \\ &\quad\hat{\Sigma}^{\rm off}_{j_1,j_2}\left(\frac{\rho_h}{x_1x_2},\frac{\mathbf{k}_1}{Q},\frac{\mathbf{k}_2}{Q},\alpha_s(\mu^2)\right)\mathcal{F}_{j_1}(x_1,\mathbf{k}_1^2,\mu^2)\mathcal{F}_{j_2}(x_2,\mathbf{k}_2^2,\mu^2)\,, \end{aligned} \tag{3.34}$$

The partonic cross section is computed as in the photoproduction case, eq. (3.8) but

with two initial off-shell gluons. The impact factor is defined as

$$\begin{aligned} h(N,M_1,M_2) &= M_1M_2\hat{\Sigma}^{\text{off}}_{gg}(N,M_1,M_2) \\ &= M_1M_2\int_0^1\frac{d\rho}{\rho}\rho^N\int\frac{d^2\mathbf{k}_1}{\pi\mathbf{k}_1^2}\left(\frac{\mathbf{k}_1^2}{Q^2}\right)^{M_1}\int\frac{d^2\mathbf{k}_2}{\pi\mathbf{k}_2^2}\left(\frac{\mathbf{k}_2^2}{Q^2}\right)^{M_2} \\ &\quad\times\hat{\Sigma}^{\text{off}}_{gg}\left(\rho,\frac{\mathbf{k}_1}{Q},\frac{\mathbf{k}_2}{Q}\right), \quad \text{with} \quad \rho=\frac{\rho_h}{x_1x_2}, \end{aligned} \tag{3.35}$$

and the high energy singularities can be computed as discussed in the previous case.

Finally, the quark contributions have to be considered. At the leading logarithmic accuracy the splitting of a quark into a gluon has to be considered $\gamma_{gq}\sim C_F/C_A\gamma_{gg}$ while the other splittings are subleading $\gamma_{qg}=\gamma_{qq}=0$. The unintegrated quark parton density can be written as

$$\mathcal{F}^q(N,\mathbf{k})=\frac{C_F}{C_A}\left[\mathcal{G}(N,\mathbf{k})-\delta^{(2)}(\mathbf{k})\right]. \tag{3.36}$$

It is then possible to compute the impact factors for quarks in terms of the one for gluons; the results in $\overline{\text{MS}}$ are

$$\begin{aligned} h^{gq}(N,M_1,M_2) &= \frac{C_F}{C_A}\Big[h(0,M_1,M_2)R(0,M_1)R(0,M_2)-h(0,M_1,0)R(0,M_1)\Big] \\ &\quad+\mathcal{O}(N). \\ h^{qq}(N,M_1,M_2) &= \left(\frac{C_F}{C_A}\right)^2\Big[h(0,M_1,M_2)R(0,M_1)R(0,M_2) \\ &\quad-h(0,M_1,0)R(0,M_1) \\ &\quad-h(0,0,M_2)R(0,M_2)+h(0,0,0)\Big]+\mathcal{O}(N). \end{aligned} \tag{3.37}$$

Many studies about the high energy resummation of hadronic processes rely on the described procedure [44]-[50]. The prediction is a strong but unstable growth in the cross section due to singularities at positive values of M_i. This problem has been investigated in [51] where a way to correctly treat these singularities has been found. This procedure is summarised in section 3.3.

High energy factorisation not only provides a way to resum leading logarithms to all order in perturbation theory but also can be used to improve fixed order results. For instance, in the case of the cross section for the production of a Higgs boson via gluon gluon fusion, k_T-factorisation can be used to compute the exact high energy behaviour of the partonic cross section and improving the NNLO order calculation performed in the heavy top limit. This computation is discussed in detail in Chapter 5.

3.2 Duality

In this section duality relations eq. (3.18) are investigated more in depth, looking at their extension beyond the leading logarithmic accuracy. In addition the small x resummation proposed by Altarelli, Ball and Forte (ABF) is presented in detail. The result of this construction is a perturbatively stable evolution for the parton densities at next-to-leading-logarithmic accuracy.

3.2.1 Duality beyond leading order

It has been already shown that at small x and large Q^2 the mutual consistency of the DGLAP and BFKL equations implies that the evolution kernels must satisfy:

$$M = \gamma(\chi(M, \alpha_s), \alpha_s)\,, \tag{3.38}$$

$$N = \chi(\gamma(N, \alpha_s), \alpha_s)\,. \tag{3.39}$$

Such relations can be expanded order by order in perturbation theory, for instance considering eq. (3.39), one gets

$$N = \alpha_s \chi_0(\gamma_s + \alpha_s \gamma_{ss}) + \alpha_s^2 \chi_1(\gamma_s) + \mathcal{O}(\alpha_s^3)\,, \tag{3.40}$$

where

$$\gamma(N, \alpha_s) = \gamma_s(\alpha_s/N) + \alpha_s \gamma_{ss}(\alpha_s/N) + \ldots \tag{3.41}$$

The second term γ_{ss} contains the sum of the subleading singularities. Fixed coupling duality expanded up to $\mathcal{O}(\alpha_s^2)$ reads as

$$\begin{aligned} \chi_0\left(\gamma_s\left(\alpha_s/N\right)\right) &= \frac{N}{\alpha_s}\,, \\ \gamma_{ss}\left(\alpha_s/N\right) &= -\frac{\chi_1\left(\gamma_s(\alpha_s/N)\right)}{\chi_0'\left(\gamma_s(\alpha_s/N)\right)}\,. \end{aligned} \tag{3.42}$$

Before introducing the running of the coupling a few comments on the function χ_1 are due. It is known [34] that this function cannot be immediately identified with the NLO contribution to the BFKL kernel eq. (2.111). The reason for this discrepancy is the choice of kinematical variables (x, Q^2). In the context of semi-hard processes there is one hard scale Q^2 and consequently the dimensionless variable is defined as $x = Q^2/s$. Conversely in the derivation of the BFKL equation $\mathbf{k}_1 \simeq \mathbf{k}_2 \simeq \mathbf{k}$ and so the definition $x_s = \mathbf{k}^2/s$ reflects the symmetry $\mathbf{k}_1 \leftrightarrow \mathbf{k}_2$. The difference between x and a symmetric choice such as $x_s = \sqrt{Q^2 k^2}/s$ results into a reshuffling of the Mellin

variables N and M:

$$\begin{aligned} x^N \left(\frac{Q^2}{k^2}\right)^{-M} &= \left(\frac{Q^2}{s}\right)^N \left(\frac{Q^2}{k^2}\right)^{-M} = \left(\frac{\sqrt{Q^2 k^2}}{s}\right)^N \left(\frac{Q^2}{k^2}\right)^{-M+\frac{N}{2}} \\ &= x_s^N \left(\frac{Q^2}{k^2}\right)^{-M+\frac{N}{2}} . \end{aligned} \tag{3.43}$$

The kernel which enters duality is related to the one computed by Fadin and Lipatov (χ^{FL}) through the shift in the Mellin variable $M \to M - \frac{N}{2}$:

$$\chi(M, \alpha_s) = \chi^{FL}\left(M - \frac{N}{2}, \alpha_s\right) , \tag{3.44}$$

or, using duality, through the implicit relation

$$\chi(M, \alpha_s) = \chi^{FL}\left(M - \frac{1}{2}\chi(M, \alpha_s), \alpha_s\right) . \tag{3.45}$$

The previous equation can be expanded in powers of the strong coupling, obtaining an expression which relates the kernels in different variables, order by order in perturbation theory

$$\begin{aligned} \chi_0(M) &= \chi_0^{FL}(M) \\ \chi_1(M) &= \chi_1^{FL}(M) - \frac{1}{2}\chi_0'(M)\chi_0(M) , \end{aligned} \tag{3.46}$$

where the prime denotes the derivative with respect to M. It is clear that the LO contribution is not affected by the choice of kinematical variables. The effect on the NLO contribution is to remove the third order pole at $M = 0$ eq. (2.114), so that χ_1 in asymmetric variables has a double pole in the origin. The calculation of the $\mathcal{O}\left(\hat{\alpha}_s^3\right)$ contribution is described in Chapter 6; in that case the computation is more subtle because the running of the coupling can no longer be neglected.

It has been already shown that the running coupling constant in Mellin space becomes a differential operator, therefore the DGLAP and the BFKL equations in double Mellin space, eq. (3.15), are no longer simple algebraic equations:

$$\begin{aligned} MG(N, M) &= G_0(N) + \gamma(N, \hat{\alpha}_s)G(N, M) , \\ NG(N, M) &= \bar{G}_0(M) + \chi(M, \hat{\alpha}_s)G(N, M) . \end{aligned} \tag{3.47}$$

Running coupling duality states that given the BFKL kernel χ computed to some accuracy in α_s there exists a function γ such that the solutions of the eqs. (3.47) coincide at leading twist once Mellin inverted in the (x, Q^2) space. Conversely, given γ, there exists a function χ with such property. The proof of this statement was

first performed in [56] using a perturbative construction. In that approach the running coupling BFKL equation is solved at a given accuracy in the (N, M) space; the solution is then transformed into the (N, t) space and it is compared to the solution of the DGLAP equation at the same order. The anomalous dimension is then determined as the lower order one plus some running coupling corrections. Subsequently in [62] an all-order proof of duality was given, based on an operator approach, which will be described in the following. The solution to the DGLAP equation can be written as

$$G(N, M) = [M - \gamma(N, \hat{\alpha}_s)]^{-1} G_0(N)\,; \tag{3.48}$$

collinear factorisation ensures that all the non-perturbative physics is factorised into the initial condition G_0. The leading twist solution is determined by the position of the perturbative pole of eq. (3.48) in the M space:

$$MG(N, M) = \gamma(N, \hat{\alpha}_s)G(N, M)\,. \tag{3.49}$$

The statement of running coupling duality in this approach is then that such equation can be inverted at the pole:

$$NG(N, M) = \chi(M, \hat{\alpha}_s)G(N, M)\,. \tag{3.50}$$

The two operators $\chi(M, \hat{\alpha}_s)$ and $\gamma(N, \hat{\alpha}_s)$ then satisfy

$$MG(N, M) = \gamma(\chi(M, \hat{\alpha}_s), \hat{\alpha}_s)G(N, M)\,, \tag{3.51}$$

$$NG(N, M) = \chi(\gamma(N, \hat{\alpha}_s), \hat{\alpha}_s)G(N, M)\,. \tag{3.52}$$

It is important to emphasise the different meaning of these two equation with respect to naive duality eq. (3.18). At the running coupling level eqs. (3.51) state that the operator M and $\gamma(M, \hat{\alpha}_s)$ (or similarly N and $\chi(M, \hat{\alpha}_s)$) act in the same way on the solution $G(N, M)$, despite being in general different operators. From now on the proof proceeds very similarly to the fixed coupling case; the expansion of eq. (3.48) about a generic N_0 gives:

$$G(N, M) = \left[M - \gamma(N_0, \hat{\alpha}_s) - \gamma'(N_0, \hat{\alpha}_s)(N - N_0) + \dots\right]^{-1} (G_0(N_0) + \dots)\,. \tag{3.53}$$

Then N_0 is chosen as the position of the perturbative pole in the N plane for given M: $N_0 = \chi(M, \hat{\alpha}_s)$. Using eq. (3.51) one gets

$$\begin{aligned} G(N, M) &= [N - \chi(M, \hat{\alpha}_s)]^{-1} \left[-\gamma'(\chi(M, \hat{\alpha}_s), \hat{\alpha}_s)\right]^{-1} G_0(\chi(M, \hat{\alpha}_s)) + \dots \\ &\equiv [N - \chi(M, \hat{\alpha}_s)]^{-1} \bar{G}_0(M) + \dots\,. \end{aligned} \tag{3.54}$$

This is the solution of the running coupling BFKL equation, with kernel obtained from duality. At leading twist, the all-order factorisation of the solution into a non-perturbative boundary condition and a evolution factor is a direct consequence of all-order factorisation of the DGLAP equation. Of course the existence of an operator-valued function $\chi(M, \hat{\alpha}_s)$ which is the running coupling dual of the DGLAP kernel is not obvious; nevertheless a constructive proof exists.

The problem can be formalised as follows: given an operator equation of the form

$$\hat{p}\, G = \hat{q}\, G \tag{3.55}$$

and given a function $f(\hat{q})$, determine the function $g(\hat{p})$ such that

$$f(\hat{q})\, G = g(\hat{p})\, G\,. \tag{3.56}$$

As a matter of fact, if one considers $\hat{p} = \hat{\alpha}_s^{-1} N$ and $\hat{q} = \hat{\alpha}_s^{-1}\chi(M, \hat{\alpha}_s)$, then eq. (3.55) is clearly the same as the pole condition eq. (3.50). One can choose f as the function γ_s which is the naive dual to the leading order BFKL kernel:

$$\gamma_s(\chi_0(M)) = M \tag{3.57}$$

and then in eq. (3.56) the function g is the running coupling dual $\gamma(N, \hat{\alpha}_s)$ of the initial $\chi(M, \hat{\alpha}_s)$

$$MG = g(\hat{p})G = \gamma(N, \hat{\alpha}_s)G\,. \tag{3.58}$$

For operators with non-vanishing commutation relations the determination of the function g in eq. (3.56) is not trivial, but it can be obtained by using the Baker-Campbell-Hausdorff formula for a pair of operators A and B. This relation to cubic order is [65]:

$$e^A e^B = \exp\{A + B + \tfrac{1}{2}[A, B] + \tfrac{1}{12}([A, [A, B]] + [B, [B, A]]) + ...\}. \tag{3.59}$$

Letting $A = \hat{q}$ and $B = \hat{p} - \hat{q}$ one gets

$$\begin{aligned} e^{\hat{q}} e^{\hat{p}-\hat{q}} \;\; = \;\; & \exp\{\hat{p} - \tfrac{1}{2}[\hat{p}, \hat{q}] + \tfrac{1}{6}[\hat{q}, [\hat{q}, \hat{p}]] + \tfrac{1}{12}[\hat{p}, [\hat{p}, \hat{q}]] + \tfrac{1}{24}[\hat{q}, [\hat{q}, [\hat{q}, \hat{p}]]] \\ & + \tfrac{1}{24}[\hat{q}, [\hat{p}, [\hat{p}, \hat{q}]]] + ...\}. \end{aligned} \tag{3.60}$$

Multiplying the right-hand side by the identity $e^{\hat{p}} e^{-\hat{p}} = 1$ on the left, and using the Baker-Campbell-Hausdorff formula again with $A = -\hat{p}$ and B set equal to the exponent

on the r.h.s., the equation can be written as

$$\begin{aligned} e^{\hat{q}}e^{\hat{p}-\hat{q}} &= e^{\hat{p}}\exp\{-\tfrac{1}{2}[\hat{p},\hat{q}]+\tfrac{1}{6}[\hat{q},[\hat{q},\hat{p}]]+\tfrac{1}{3}[\hat{p},[\hat{p},\hat{q}]]+\tfrac{1}{24}[\hat{q},[\hat{q},[\hat{q},\hat{p}]]] \\ &\quad +\tfrac{1}{8}[\hat{q},[\hat{p},[\hat{p},\hat{q}]]]-\tfrac{1}{8}[\hat{p},[\hat{p},[\hat{p},\hat{q}]]]+...\}. \end{aligned} \tag{3.61}$$

This expression can be further simplified because according to eq. (3.55) one has

$$(\hat{p}\,-\hat{q}\,)G=0 \quad \Rightarrow \quad e^{\hat{p}\,-\hat{q}}\,G=G\,. \tag{3.62}$$

Hence eq. (3.61) relates the action of the exponential of two operators which act in the same way on physical states. This result can be generalised to any function f by observing that

$$f(\hat{q})=e^{\hat{q}\frac{d}{d\lambda}}f(\lambda)\big|_{\lambda=0}\,. \tag{3.63}$$

Rescaling the operators $\hat{p}$ and $\hat{q}$ by letting $\hat{p}\to\hat{p}\frac{d}{d\lambda}$, $\hat{q}\to\hat{q}\frac{d}{d\lambda}$, eq. (3.61) becomes

$$\begin{aligned} f(\hat{q})G &= e^{\hat{p}\frac{d}{d\lambda}}\exp\Big\{-\tfrac{1}{2}[\hat{p},\hat{q}]\tfrac{d^2}{d\lambda^2}+\tfrac{1}{6}[\hat{q},[\hat{q},\hat{p}]]\tfrac{d^3}{d\lambda^3}+\tfrac{1}{3}[\hat{p},[\hat{p},\hat{q}]]\tfrac{d^3}{d\lambda^3} \\ &\quad +\tfrac{1}{24}[\hat{q},[\hat{q},[\hat{q},\hat{p}]]]\tfrac{d^4}{d\lambda^4}+\tfrac{1}{8}[\hat{q},[\hat{p},[\hat{p},\hat{q}]]]\tfrac{d^4}{d\lambda^4}-\tfrac{1}{8}[\hat{p},[\hat{p},[\hat{p},\hat{q}]]]\tfrac{d^4}{d\lambda^4}+...\Big\} \\ &\quad f(\lambda)\big|_{\lambda=0}G\,. \end{aligned} \tag{3.64}$$

The expansion of the exponential on the r.h.s. leads to an expression in terms of $f(\hat{p})$, its derivatives and multiple commutators of $\hat{p}$ and $\hat{q}$

$$\begin{aligned} f(\hat{q})G &= \big\{f(\hat{p})-\tfrac{1}{2}f''(\hat{p})\,[\hat{p},\hat{q}]+\tfrac{1}{6}f'''(\hat{p})\,[\hat{q},[\hat{q},\hat{p}]] \\ &\quad +\tfrac{1}{3}f'''(\hat{p})\,[\hat{p},[\hat{p},\hat{q}]]+\tfrac{1}{8}f''''(\hat{p})[\hat{p},\hat{q}]^2+\ldots)\big\}G \\ &\equiv g(\hat{p})G\,, \end{aligned} \tag{3.65}$$

where the expansion in the commutators is justified because, as it will be shown in the following, it corresponds to an expansion in powers of $\hat{\alpha}_s$. Eq. (3.65) is the result aimed for, because it gives an expression for the function g in terms of the function f. More specifically, if f is chosen to be the naive dual as in eq. (3.57) then the anomalous dimension $\gamma(N,\hat{\alpha}_s)$, which is the running coupling dual to a given kernel $\chi(M,\hat{\alpha}_s)$, can be written as the fixed coupling dual γ_s, plus running coupling contributions. Such corrections simply involve derivatives of the naive dual and commutators of the operators $\hat{p}=\hat{\alpha}_s^{-1}N$ and $\hat{q}=\hat{\alpha}_s^{-1}\chi(M,\hat{\alpha}_s)$.

The commutators which are relevant in order to compute the running coupling corrections can be easily calculated from the basic one:

$$\big[\hat{\alpha}_s^{-1}N,\chi_0(M)\big]=-N\beta_0\chi_0'(M)\,, \tag{3.66}$$

where the running coupling has been considered at one loop accuracy, i.e. including only β_0 terms. Because $\mathcal{O}(N) = \mathcal{O}(\hat{\alpha}_s)$ the expansion in the commutators in eq. (3.65) is justified. Thanks to this result eq. (3.58) can be written as

$$\begin{aligned} MG &= \big\{\gamma_s(\hat{\alpha}_s^{-1}N) - \tfrac{1}{2}\gamma_s''(\hat{\alpha}_s^{-1}N)\left(-N\beta_0\chi_0'(M)\right) \\ &\quad +\tfrac{1}{3}\gamma_s'''(\hat{\alpha}_s^{-1}N)\left((N\beta_0)^2\chi_0''(M)\right) + \tfrac{1}{8}\gamma_s''''(\hat{\alpha}_s^{-1}N)\left(-N\beta_0\chi_0'(M)\right)^2 \\ &\quad +O(\hat{\alpha}^3)\big\}G\,, \end{aligned} \tag{3.67}$$

where the prime always denotes the derivative of a function with respect to its entire argument. Eq. (3.67) cannot be seen yet as a DGLAP-type equation because of the residual dependence on M in the evolution factor through χ_0 and its derivatives. However, such a dependence can be perturbatively removed by solving the equation at the lowest order and back-substituting the result to determine the next order solution, and so on. Some care has to be taken in the back-substitution because non-commuting operators are involved; for instance given $MG = \gamma_s(\hat{\alpha}_s^{-1}N)G$, then

$$\chi_0'(M) = \left\{\chi_0'(\gamma_s(\hat{\alpha}_s^{-1}N)) - \tfrac{1}{2}\chi_0'''(\gamma_s(\hat{\alpha}_s^{-1}N))[M, \gamma_s(\hat{\alpha}_s^{-1}N)] + \dots\right\}. \tag{3.68}$$

Performing the back-substitutions and expressing the derivatives of γ_s in terms of derivatives of χ_0 eq. (3.67) can be written as resummed DGLAP evolution equation:

$$MG = \left\{\gamma_s(\hat{\alpha}_s^{-1}N) + \hat{\alpha}_s\beta_0\Delta\gamma_{ss} + (\hat{\alpha}_s\beta_0)^2\Delta\gamma_{sss}^{(0)} + \mathcal{O}\left(\hat{\alpha}_s^3\right)\right\}G\,, \tag{3.69}$$

where the running coupling corrections are

$$\begin{aligned} \Delta\gamma_{ss}(\hat{\alpha}_s^{-1}N) &= -\chi_0\frac{\chi_0''}{2\chi_0'^2}\bigg|_{M=\gamma_s(\hat{\alpha}_s^{-1}N)} \\ \Delta\gamma_{sss}^{(0)}(\hat{\alpha}_s^{-1}N) &= -\chi_0^2\frac{15\chi_0''^3 - 16\chi_0'\chi_0''\chi_0''' + 3\chi_0'^2\chi_0'''}{24\chi_0'^5}\bigg|_{M=\gamma_s(\hat{\alpha}_s^{-1}N)} \end{aligned} \tag{3.70}$$

A complete calculation of running coupling duality at the considered accuracy should include the NLO contribution to the BFKL kernel and the QCD β-function at two loops:

$$\beta(\alpha_s) = -\beta_0\alpha_s^2(1 + \alpha_s\beta_1 + \dots)\,; \tag{3.71}$$

the running coupling operator at this accuracy becomes:

$$\hat{\alpha}_s^{-1} = \frac{1}{\alpha_s} - \beta_0\frac{\partial}{\partial M} + \beta_1\left(-\alpha_s\beta_0\frac{\partial}{\partial M} - \frac{1}{2}(\alpha_s\beta_0)^2\frac{\partial^2}{\partial M^2}\right) + \mathcal{O}\left(\hat{\alpha}_s^3\right)\,. \tag{3.72}$$

Moreover, at higher orders, one should rearrange eq. (3.65) in such a way that $f(\hat{p})$ acts

directly on the physical state G. Higher-order running coupling duality was investigated in [66] and [67] and the results were published in [41]. The complete NNLO running coupling corrections are

$$\Delta\gamma_{sss} = \Delta\gamma_{sss}^{(0)} + \tfrac{1}{\beta_0}\Delta\gamma_{sss}^{(1)} + \tfrac{\beta_1}{\beta_0}\Delta\gamma_{ss}\,, \tag{3.73}$$

where

$$\Delta\gamma_{sss}^{(1)} = \left(\tfrac{1}{2}\chi_0\chi_0'\gamma_{ss}'' + \tfrac{1}{2}\chi_0\chi_1'\gamma_s'' + \tfrac{1}{2}\chi_0'\chi_1\gamma_s'' + \tfrac{1}{2}\chi_0'\chi_0''\gamma_s''\gamma_{ss}\right)\Big|_{M=\gamma_s(\hat{\alpha}_s^{-1}N)}\,. \tag{3.74}$$

The choice of the kinematical variables and running coupling contributions are not the only effects that must be taken into account beyond leading order. As already mentioned in section 2.2, the BFKL equation naturally describes the evolution of the unintegrated gluon density $\mathcal{G}$, while the usual parton distribution G, which enters DGLAP evolution is integrated over the transverse momenta. The relation between integrated and unintegrated distributions in Mellin space is given in eq. (3.12). It follows that if $\mathcal{G}$ satisfies a BFKL equation with kernel $\chi(M,\hat{\alpha}_s)$, then the evolution of G is described by a different kernel

$$\chi^i(M,\hat{\alpha}_s) = M^{-1}\chi(M,\hat{\alpha}_s)M\,. \tag{3.75}$$

Therefore the anomalous dimension which describes the evolution of G must be computed through duality from the kernel $\chi^i(M,\hat{\alpha}_s)$. The perturbative expansion of eq. (3.75) in powers of $\hat{\alpha}_s$ shows that the LO kernel is not affected, while the NLO one receives a contribution proportional to β_0

$$\begin{aligned}\chi^i(M,\hat{\alpha}_s) &= \hat{\alpha}_s\chi_0 + \hat{\alpha}_s^2\chi_1 + \left[M^{-1},\hat{\alpha}_s\right]\chi_0 M + \mathcal{O}\left(\hat{\alpha}_s^3\right)\\ &= \hat{\alpha}_s\chi_0 + \hat{\alpha}_s^2\left(\chi_1 + \beta_0\tfrac{\chi_0}{M}\right) + \mathcal{O}\left(\hat{\alpha}_s^3\right)\,.\end{aligned} \tag{3.76}$$

It has already been discussed that there is a normalisation mismatching between collinear and high energy factorisation eq. (3.30); beyond leading order it is necessary to specify the scheme in which both the impact factor eq. (3.31) and the evolution kernel are computed. The anomalous dimension obtained through running coupling duality from the usual BFKL kernel is in the Q_0 scheme. The function which describes the scheme change to $\overline{\text{MS}}$ can be computed exponentiating the R factor:

$$\gamma^{Q_0} = \gamma^{\overline{\text{MS}}} + \frac{d}{dt}\ln R(N,t)\,. \tag{3.77}$$

3.2.2 Small x resummed evolution

The resummation of high energy logarithms have always faced the fact that collider data show little evidence for such effects. For instance global parton distributions fits obtained with standard NLO DGLAP evolution describe the experimental DIS data from the HERA collider in a wide kinematic region [68], even where low x effects were supposed to be significant. On the contrary the most direct implementation of LO BFKL resummation predicts a fairly strong growth at small x as described by eq. (2.103). Moreover the calculation of the NLO kernel χ_1 shows that the perturbative expansion behaves badly. On the other hand the recently determined NNLO DGLAP splitting functions exhibit a small x instability, requiring a treatment of high energy logarithms. The puzzle of a correct inclusion of high energy resummation has been studied in the past years by different groups: ABF, CCS(S) [69]-[72] and Thorne–White [73]. In this section the ABF resummation is summarised. For simplicity only the case of a pure Yang-Mills theory is considered. In order to consider full QCD with $n_f \neq 0$ and the resummation of the different entries of the anomalous dimension matrix some subtleties have to be addressed. These issues have been recently solved in [64] where the full resummation with quarks has been performed. However the most important features of the resummation are present in the pure gluonic case.

The first key element to understand is conservation of longitudinal momentum, which implies for the anomalous dimension [54]

$$\left.\begin{array}{c}\gamma_{gq}(1,\alpha_s)+\gamma_{qq}(1,\alpha_s)=0\\ 2n_f\,\gamma_{qg}(1,\alpha_s)+\gamma_{gg}(1,\alpha_s)=0\end{array}\right\}\Rightarrow \gamma(1,\alpha_s)=0\,, \tag{3.78}$$

where γ is the larger eigenvalue of the anomalous dimension matrix. Duality relations then constrain the all-order behaviour of the BFKL kernel in the collinear region $M=0$:

$$\chi(\gamma(N,\alpha_s),\alpha_s)=N\big|_{N=1}\Rightarrow \chi(0,\alpha_s)=1\,, \tag{3.79}$$

up to subleading running coupling corrections. Thus the BFKL kernel is regular and the alternating-sign poles which characterise the fixed order expansion resums to one:

$$\chi_s\sim\frac{\alpha_s}{\alpha_s+M}=\frac{\alpha_s}{M}-\frac{\alpha_s^2}{M^2}+\frac{\alpha_s^3}{M^3}+\dots \tag{3.80}$$

The kernel χ_s, which is the fixed coupling dual of γ_0, is free of collinear poles, therefore the instability of the BFKL kernel can be cured reorganising the perturbative series into a double leading expansion (DL) [57]:

$$\chi_{DL}=\chi_{DL\,LO}+\alpha_s\chi_{DL\,NLO}+\dots \tag{3.81}$$

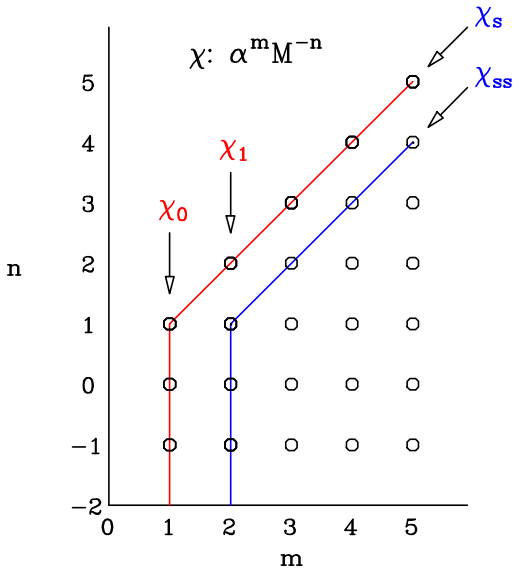

Figure 3.1: Graphical representation of different expansions of χ: vertical lines correspond to terms of the same fixed order in α_s, while contributions along a diagonal line are of the same order in α_s at fixed α_s/M. Following a line of a given colour one finds all terms contained in the double leading expansion at a given order.

The DL expansion is pictorially shown in fig. 3.1. The LO term is the sum of the leading order BFKL kernel χ_0 and χ_s:

$$\chi_{DL\,LO}(M,\alpha_s) = \alpha_s\chi_0(M) + \chi_s\left(\frac{\alpha_s}{M}\right) - \frac{C_A\alpha_s}{\pi M}\,, \tag{3.82}$$

where the last term avoids double counting. At NLO one has to subtract three double counting terms

$$\chi_{DL\,NLO}(M,\alpha_s) = \alpha_s\chi_1(M) + \chi_{ss}\left(\frac{\alpha_s}{M}\right) - \alpha_s\left(\frac{f_2}{M^2}+\frac{f_1}{M}\right) - f_0\,, \tag{3.83}$$

with

$$f_0 = 0\,,\quad f_1 = 0\,,\quad f_2 = \tfrac{11C_A^2}{12\pi^2}\,,\quad \text{in the}\quad n_f = 0\quad \text{case}\,. \tag{3.84}$$

The functions χ_s and χ_{ss} are the analogous of eq. (3.42)

$$\begin{aligned}\gamma_0\left(\chi_s\left(\alpha_s/M\right)\right) &= \frac{M}{\alpha_s}\,,\\ \chi_{ss}\left(\alpha_s/M\right) &= -\frac{\gamma_1\left(\chi_s(\alpha_s/M)\right)}{\gamma_0'\left(\chi_s(\alpha_s/M)\right)}\,.\end{aligned} \tag{3.85}$$

The DL expansion of the BFKL kernel is now perturbatively stable in the collinear

region, however the instability in the anticollinear region $M \sim 1$ has still to be cured. This is particularly bad when one includes the NLO correction: at $M = 0$ the kernel is regular and positive, while it has a pole in $M = 1$ with negative coefficient. It follows that there is no minimum and hence the high energy behaviour cannot be predicted as in eq. (2.103). This problem can be solved exploiting the symmetry of the BFKL kernel eq. (2.101), which enables one to construct a double leading expansion also in the anticollinear region [74], [63]. However, as previously discussed, this symmetry is realised only for the BFKL kernel written in terms of Mellin variable M, which corresponds to a symmetric choice of the kinematic variables eq. (3.45). The DL kernel eq. (3.81) can be written in symmetric variables shifting $M \to M + \frac{N}{2}$; it is then symmetrised using $M \leftrightarrow 1 - M$ and finally it is brought back to asymmetric variables. For instance, indicating with χ_σ the kernel in symmetric variables and with χ_Σ the one in asymmetric variables, the symmetrisation of the χ_s term in eq. (3.82) is

$$\begin{aligned} \bar{\chi}_\sigma(M, N, \alpha_s) &= \chi_s\left(\tfrac{\alpha_s}{M+\frac{N}{2}}\right) + \chi_s\left(\tfrac{\alpha_s}{1-M+\frac{N}{2}}\right), \\ \bar{\chi}_\Sigma(M, N, \alpha_s) &= \chi_s\left(\tfrac{\alpha_s}{M}\right) + \chi_s\left(\tfrac{\alpha_s}{1-M+N}\right). \end{aligned} \tag{3.86}$$

The kernel $\bar{\chi}(M, N, \alpha_s)$ can be viewed as an "off-shell" continuation of the usual kernel $\chi(M, \alpha_s)$. The latter can be found putting on-shell the N dependence, i.e. solving the implicit equation

$$\chi(M, \alpha_s) = \bar{\chi}(M, \chi(M, \alpha_s), \alpha_s). \tag{3.87}$$

In Ref. [63] a full symmetrised double leading off-shell BFKL kernel has been computed

$$\bar{\chi}_{\sigma\, DL}(M, N, \alpha_s) = \bar{\chi}_{\sigma\, LO}(M, N, \alpha_s) + \alpha_s \bar{\chi}_{\sigma\, NLO}(M, N, \alpha_s) + \dots \tag{3.88}$$

The leading and next-to-leading contributions are

$$\begin{aligned} \bar{\chi}_{\sigma\, LO}(M, N, \alpha_s) &= \chi_s\left(\tfrac{\alpha_s}{M+\frac{N}{2}}\right) + \chi_s\left(\tfrac{\alpha_s}{1-M+\frac{N}{2}}\right) + \alpha_s \chi_0(M, N) \\ &\quad + \chi_{\rm mom}(N), \\ \bar{\chi}_{\sigma\, NLO}(M, N, \alpha_s) &= \chi_{ss}\left(\tfrac{\alpha_s}{M+\frac{N}{2}}\right) + \chi_{ss}\left(\tfrac{\alpha_s}{1-M+\frac{N}{2}}\right) + \alpha_s \chi_1(M, N) \\ &\quad + \chi_{\rm mom}(N), \end{aligned} \tag{3.89}$$

where $\chi(M, N)$ is the off-shell continuation of the fixed order expansion of the BFKL kernel and $\chi_{\rm mom}$ enforces momentum conservation. The double leading on-shell kernel is shown in fig. 3.2: it is clear that the symmetrisation ensures the presence of a minimum. Moreover, while the fixed order perturbative expansion is pathological, the double leading one is very stable. The kernel in asymmetric variables can be obtained

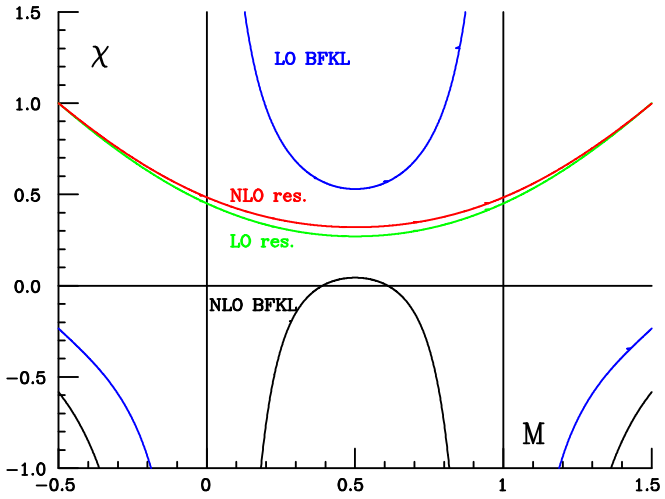

Figure 3.2: Plot of different kernels χ in symmetric variables [63]. The fixed order BFKL kernel are $\alpha_s\chi_0$ (blue) and $\alpha_s\chi_0 + \alpha_s^2\chi_1$ (black). The resummed DL expansion kernels χ_σ at LO (green) and NLO (red) both on-shell. All curves are determined with $\beta_0 = 0$ (fixed coupling), $\alpha_s = 0.2$ and $n_f = 0$. Note that $\chi(0, \alpha_s) = 1$ implies $\chi_\sigma(-\frac{1}{2}, \alpha_s) = \chi_\sigma(\frac{3}{2}, \alpha_s) = 1$.

through the relation

$$\bar{\chi}_{\Sigma\, DL}(M, N, \alpha_s) = \bar{\chi}_{\sigma\, DL}(M - \tfrac{N}{2}, N, \alpha_s)\,. \tag{3.90}$$

Once a stable on-shell BFKL kernel in asymmetric variables has been constructed one would like to compute from it a resummed anomalous dimension using running coupling duality:

$$\chi_\Sigma(\gamma_\Sigma(N, \hat{\alpha}_s), \hat{\alpha}_s) = N\,. \tag{3.91}$$

It has already been shown in eq. (3.69) that a perturbative treatment of running coupling effects leads to the following result

$$\gamma_\Sigma^{pert}(N, \alpha_s(t)) = \tilde{\gamma}_\Sigma(N, \alpha_s(t)) + \alpha_s(t)\beta_0\,(\Delta\gamma_{ss} + 1)\ , \tag{3.92}$$

where the tilde stands for an anomalous dimension obtained from naive duality. The running coupling correction $\Delta\gamma_{ss}$ was defined in eq. (3.70) and the last term avoids double counting. Unfortunately this perturbative treatment of the running coupling effects introduces a new source of instability [56]. This is due to unphysical singularities in the small x region. Because χ_0 has a minimum at $M = \frac{1}{2}$, its first derivative has a zero, thus the lowest order running coupling correction, as a function of M, has a pole. Moreover, at each order in perturbation theory, the running coupling corrections contain

increasing inverse powers of χ_0'. Such strong singularities dominate the Mellin inversion at small x, so that formally subleading running coupling corrections overwhelm the leading contribution. Therefore, running coupling corrections cannot be considered order by order in the strong coupling but they must be resummed. In order to achieve this the running coupling BFKL equation has to be solved in a closed form rather than perturbatively. This is possible if one considers a quadratic approximation to the LO kernel about its minimum $M_0 = \frac{1}{2}$

$$\chi^q(M, \hat{\alpha}_s) = c(\hat{\alpha}_s) + \tfrac{1}{2}\kappa(\hat{\alpha}_s)(M - M_0)^2 + \dots \tag{3.93}$$

In the case of intercept and curvature linear in α_s the BFKL equation can be solved in terms of Airy functions [75]; however, in the symmetrised case, the kernel to be considered is the quadratic approximation to the one obtained by solving eq. (3.87) and hence the two parameters c and κ have a non-trivial dependence upon α_s. At leading logarithmic level the BFKL equation can still be solved in terms of Bateman functions [63]. The Bateman anomalous dimension is then defined in the usual way by taking the logarithmic derivative of the solution

$$\gamma^B(N, \alpha_s) = \frac{d}{dt} \ln G_B(N, t)\,. \tag{3.94}$$

The resummed anomalous dimension at NLO is then obtained adding the Bateman result to the anomalous dimension obtained solving perturbatively running coupling duality, eq. (3.92)

$$\begin{aligned} \gamma_\Sigma^{res}(N, \alpha_s(t)) &= \gamma_\Sigma^{pert}(N, \alpha_s(t)) + \gamma^B(N, \alpha_s(t)) \\ &- \left[\gamma_s^B\left(\tfrac{\alpha_s}{N}\right) + \alpha_s(t)\gamma_{ss}^B\left(\tfrac{\alpha_s}{N}\right)\right] \\ &+ \gamma_{\rm mom}(N, \alpha_s(t)) + \gamma_{\rm match}(N, \alpha_s(t))\,. \end{aligned} \tag{3.95}$$

The terms in square brackets cancel the double counting between the Bateman anomalous dimension and the one obtained from running coupling duality. The terms in the last line are subleading corrections which enforce exact momentum conservation and exact matching to the fixed order NLO anomalous dimension at large N. The final result for the resummed anomalous dimension as obtained in [63] is plotted in fig. 3.3 and the correspondent splitting function in fig. 3.4. The NLO resummed splitting function is very close to the standard DGLAP case also for very small values of x; the rise starts only for $x < 10^{-6}$. The BFKL regime is softened by the resummation, explaining the success of standard NLO fits to HERA data.

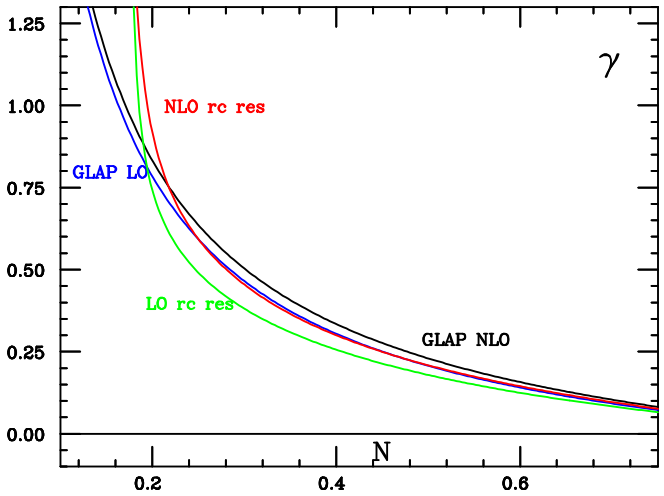

Figure 3.3: The fixed order DGLAP anomalous dimensions (blue and black) are compared to the resummed ones eq. (3.95) (green and red); the resummed results are very stable.

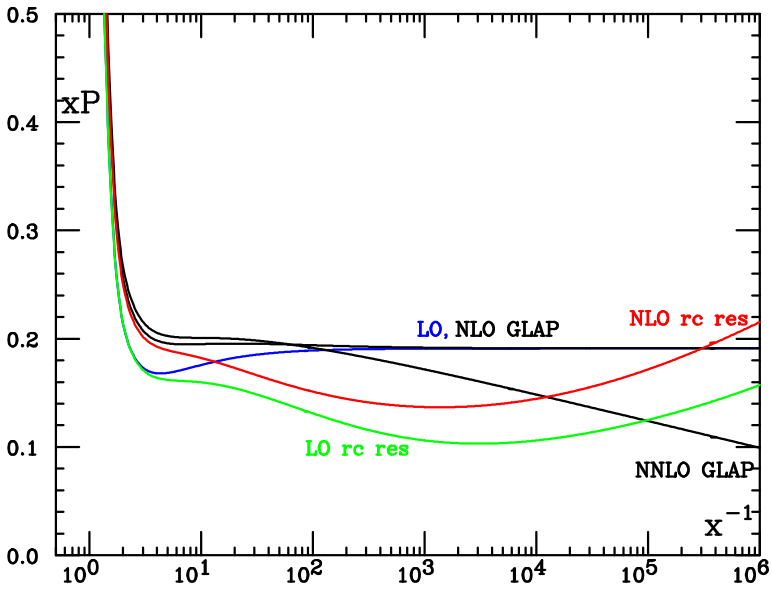

Figure 3.4: The LO and NLO resummed splitting function, obtained by Mellin transformation of the anomalous dimension are compared to fixed order DGLAP at LO, NLO and NNLO.

3.3 Resummation of the coefficient function

In section 3.1 a procedure to compute and resum the high energy logarithms has been derived. One of the key-points of the calculation was the fixed-coupling pole condition eq. (3.17), which enables one to perform the M_i-Mellin transforms analytically. However in the previous section it was shown that naive duality fails to describe the correct behaviour of the PDFs at high energy. For this reason one might expect a similar inadequacy of the fixed coupling approximation for the resummation of the partonic cross section too. Moreover, as the position of the pole in the evolution factor moves away from the origin, the inverse-Mellin contour of integration may encounter new singularities. Indeed the impact factor $h(N, M_1, M_2)$ as defined in eq. (3.13) usually has a rather complicated structure of singularities. Firstly, one finds poles at negative values of M_1 and M_2 which lead, upon Mellin inversion, to negative powers of Q^2. These are higher twist contributions which are not relevant in this discussion. More worrying are infrared singularities which show up as poles at positive values of the Mellin variables and lines of singularities such as

$$M_1 + M_2 = n\,, \quad n > 0\,. \tag{3.96}$$

For instance the line of singularities at $n = 1$ correspond to an s-channel gluon going on-shell. In the case of heavy flavour production [44], [48] such a singularity is touched by the contour integration of the Mellin inversion, resulting into a strong but unstable enhancement of the cross section. A way to perform the inverse Mellin in a more reliable way has been discussed in [51] and it is presented in the following.

It is often convenient in collider phenomenology to introduce the gluon-gluon luminosity:

$$\mathcal{L}(z, t_1, t_2) = \int_{\rho_h}^1 \frac{dx_1}{x_1} \int_{\rho_h}^1 \frac{dx_2}{x_2}\, \delta(z - x_1 x_2) G(x_1, t_1) G(x_2, t_2)\,, \tag{3.97}$$

which in Mellin space becomes

$$\mathcal{L}(N, M_1, M_2) = G(N, M_1) G(N, M_2)\,. \tag{3.98}$$

Then the dimensionless hadronic cross section in (N, Q^2) space can be written as

$$\begin{aligned} \Sigma(N, Q^2) \;\; = \;\; & \alpha_s^2 \sum_{m_1=0}^{\infty} \sum_{m_2=0}^{\infty} h_{m_1,m_2}(N) \int_{c-i\infty}^{c+i\infty} \frac{dM_1}{2\pi i} \frac{dM_2}{2\pi i}\, e^{t(M_1+M_2)} \\ & M_1^{m_1} M_2^{m_2} \mathcal{L}(N, M_1, M_2)\,, \end{aligned} \tag{3.99}$$

where the impact factor $h(N, M_1, M_2)$ has been Taylor expanded about the origin.

The M_i-Mellin inversions can be performed observing that the first term of the series $m_1 = m_2 = 0$ is trivial because it simply gives the gluon luminosity $\mathcal{L}(N,t)$ and subsequent powers of M_i can be seen as derivative with respect to t

$$\Sigma(N,Q^2) = \alpha_s^2 \sum_{m_1=0}^{\infty} \sum_{m_2=0}^{\infty} h_{m_1,m_2}(N) \frac{\partial^{m_1+m_2}}{\partial t_1^{m_1} \partial t_2^{m_2}} \mathcal{L}(N,t_1,t_2)\Big|_{t_1=t_2=t} . \tag{3.100}$$

In this derivation no assumptions on the running of the coupling have been made. For this reason, provided that the series converges, the previous equation generalises the pole approximation. This is even more explicit if one writes the derivatives of the gluon luminosity in terms of the anomalous dimension. For instance one finds

$$\begin{aligned} \frac{\partial}{\partial t_1} \mathcal{L}(N,t_1,t_2)\Big|_{t_1=t_2=t} &= \gamma(N,\alpha_s(t)) \mathcal{L}(N,t) , \\ \frac{\partial^2}{\partial t_1 \partial t_2} \mathcal{L}(N,t_1,t_2)\Big|_{t_1=t_2=t} &= \gamma^2(N,\alpha_s(t)) \mathcal{L}(N,t) . \end{aligned} \tag{3.101}$$

These expressions are as the ones one would obtain from the pole approximation $M_i = \gamma(N,\alpha_s)$. However, the anomalous dimension depends on t through the running coupling and hence it leads to subleading corrections

$$\frac{\partial^2}{\partial t_1^2} \mathcal{L}(N,t_1,t_2)\Big|_{t_1=t_2=t} = \left(\gamma^2(N,\alpha_s(t)) + \frac{\partial}{\partial t} \gamma(N,\alpha_s(t)) \right) \mathcal{L}(N,t) \tag{3.102}$$

The previous argument suggests a way of dealing with the infrared singularities too. Suppose the impact factor has a line of n^{th}-order singularities at $M_1 + M_2 = 1$. The following relation holds [76]

$$\frac{1}{(1-M_1-M_2)^n} = \frac{1}{n!} \int_0^{\infty} d\tau \tau^{n-1} e^{-\tau(1-M_1-M_2)} . \tag{3.103}$$

The dimensionless cross section behaves like

$$\begin{aligned} \Sigma(N,Q^2) &= \int_{c-i\infty}^{c+i\infty} \frac{dM_1}{2\pi i} \frac{dM_2}{2\pi i} e^{t(M_1+M_2)} \frac{1}{(1-M_1-M_2)^n} \mathcal{L}(N,M_1,M_2) \\ &= \frac{1}{n!} \int_0^{\infty} d\tau \tau^{n-1} e^{-\tau} \\ &\quad \times \int_{c-i\infty}^{c+i\infty} \frac{dM_1}{2\pi i} \frac{dM_2}{2\pi i} e^{(t+\tau)(M_1+M_2)} \mathcal{L}(N,M_1,M_2) \\ &= \frac{1}{n!} \int_0^{\infty} d\tau \tau^{n-1} e^{-\tau} \mathcal{L}(N,t+\tau) . \end{aligned} \tag{3.104}$$

The previous result can be Taylor expanded in τ and hence written as a series of

derivatives of the gluon luminosity in analogy with eq. (3.100)

$$\begin{aligned}\Sigma(N,Q^2) &= \int_0^\infty d\tau \sum_{m=0}^{\infty} \frac{\tau^{m+n-1}}{n!m!} e^{-\tau} \frac{\partial^m}{\partial t^m} \mathcal{L}(N,t) \\ &= \sum_{m=0}^{\infty} \frac{(n+m)!}{n!m!} \frac{\partial^m}{\partial t^m} \mathcal{L}(N,t)\,. \end{aligned} \tag{3.105}$$

In order to understand the effect of the running of the coupling one can consider an impact factor which is simply given by

$$h^{\rm toy}(N,M_1,M_2) = \frac{\alpha_s^2}{1-M_1-M_2}\,. \tag{3.106}$$

At fixed coupling

$$\mathcal{L}(N,t) = e^{2\gamma(N,\alpha_s)t}\mathcal{L}_0(N) \tag{3.107}$$

and eq. (3.104) gives the same result as the pole approximation:

$$\Sigma(N,Q^2) = \int_0^\infty d\tau\ e^{-\tau} e^{2\gamma(N,\alpha_s)(t+\tau)}\mathcal{L}_0(N) = \frac{1}{1-2\gamma(N,\alpha_s)}\mathcal{L}(N,t)\,. \tag{3.108}$$

As a consequence there is a new singularity in the N plane which enhances the growth of the cross section; if one consider the LO anomalous dimension $\gamma_0 \sim \alpha_s/N$, the Mellin inversion gives

$$\begin{aligned}\Sigma(\rho_h,Q^2) &= \int_{c-i\infty}^{c+i\infty} \tfrac{dN}{2\pi i} e^{\xi N} \tfrac{1}{1-2\gamma_0}\mathcal{L}(N,t) \sim \int_{c-i\infty}^{c+i\infty} \tfrac{dN}{2\pi i} e^{\xi N} \tfrac{N}{N-2\alpha_s}\mathcal{L}(N,t) \\ &\sim e^{2\alpha_s\xi}\mathcal{L}(\xi,t) = \rho_h^{-2\alpha_s}\mathcal{L}(\rho_h,Q^2). \end{aligned} \tag{3.109}$$

Thus the cross section at low ρ_h grows faster than the parton luminosity. However eq. (3.104) is valid at the running coupling level as well. If one considers $\alpha_s(t) = 1/\beta_0 t$ then $\mathcal{L}(N,t) = t^{2\gamma_0/\beta_0}\mathcal{L}_0(N)$ and the τ integral can be still performed analytically

$$\begin{aligned}\Sigma(N,t) &= \int_0^\infty d\tau\ e^{-\tau}(t+\tau)^{2\gamma_0(N)/\beta_0}\mathcal{L}_0(N) \\ &= t^{-2\gamma_0(N)/\beta_0} e^t \Gamma(1+2\beta_0^{-1}\gamma_0(N),t)\mathcal{L}(N,t)\,. \end{aligned} \tag{3.110}$$

The result is given in terms of the incomplete Γ function, which has no singularities for $t > 0$, therefore the asymptotic behaviour of the cross section is given by the evolution of the parton luminosity. The strong enhancement observed in the previous case is smoothed by the running coupling. This observation suggests a way to perform the high energy resummation of the coefficient functions. Rather than using the pole approximation, one performs running coupling resummation, dealing separately the

infrared singularities. More precisely, one Taylor expands the impact factor in powers of M_i about the origin, keeping the infrared singularities unexpanded. Then the powers of M_i are dealt with eq. (3.100), while the inverse Mellin of the infrared singularities are performed using eq. (3.104) or eq. (3.105). This procedure smooths out the strong enhancement predicted by the pole approximation; as a consequence the high energy growth of the cross sections is universal, driven by the parton distributions.

Chapter 4

Hadronic processes at high energy

In this chapter two different hadronic processes are studied in the framework of k_T-factorisation. Firstly the production of a pair of heavy quarks, specifically $b\bar{b}$ is considered. Secondly Drell-Yan processes are studied and a resummed partonic coefficient function is computed.

4.1 Heavy flavour production

Heavy flavour production has been widely studied in the literature, both at fixed order and resummed level. The production of $b\bar{b}$ pairs at LHC is one of the perturbative process with the lowest hard scale and hence the one which is likely to show important high energy corrections:

$$Q^2 = 4m^2 \ll s\,, \tag{4.1}$$

where m is the mass of the b-quark and as usual s is the centre-of-mass energy. The LHC has a dedicated experiment, LHCb, on the physics of b quarks; moreover many background studies rely on an accurate prediction for the total cross section $\sigma_{b\bar{b}}$. Historically the production of heavy quarks was the first process to be studied in k_T-factorisation [44], [47]. In this section the calculation of the leading high energy singularities is performed and the result is in full agreement with the one published in the literature [48], [49].

4.1.1 The coefficient function at high energy

The LO cross section for the hadroproduction of heavy quarks is collinear safe, hence the calculation of the high energy behaviour is a straightforward application of the method described in the previous chapter. More specifically the reduced cross section

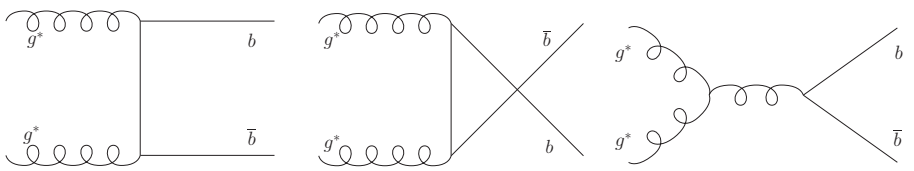

Figure 4.1: Diagrams for heavy quark hadroproduction $g^*g^* \to b\overline{b}$. The Abelian contribution is on the left and in the centre, while non-Abelian one on the right.

$\Sigma = m^2\sigma$ obeys a factorisation formula like eq. (3.34), where in this case

$$\rho = \frac{\rho_h}{x_1 x_2} = \frac{4m^2}{\nu}\,, \tag{4.2}$$

and the partonic cross section $\hat{\Sigma}^{\rm off}_{gg}$ is computed considering the process

$$g^*(k_1) + g^*(k_2) \to b(p_3) + \overline{b}(p_4)\,. \tag{4.3}$$

The kinematics of this kind of processes is described in Appendix A.2, eq. (A.14). The cross section can be written as

$$\begin{aligned}\hat{\Sigma}^{\rm off}_{gg} &= \hat{\Sigma}_{\rm Ab} + \hat{\Sigma}_{\rm non-Ab} = \frac{1}{2n_c}\mathcal{A}^{\rm Ab} + \frac{n_c}{2(n_c^2-1)}\mathcal{A}^{\rm non-Ab} = \\ &= \frac{1}{2(n_c^2-1)}\left[n_c\left(\mathcal{A}^{\rm Ab} + \mathcal{A}^{\rm non-Ab}\right) - \frac{1}{n_c}\mathcal{A}^{\rm Ab}\right] = \hat{\Sigma}_0 + \hat{\Sigma}_1\,.\end{aligned} \tag{4.4}$$

The leading and subleading colour contributions to the off-shell cross section are determined integrating over the phase space eq. (A.16) the squared matrix element obtained from the three diagrams in figure 4.1:

$$\hat{\Sigma}_i\left(\rho, \frac{\mathbf{k}_1}{m^2}, \frac{\mathbf{k}_2}{m^2}\right) = \frac{\alpha_s^2 m^2}{2(n_c^2-1)}\int d\Phi^{(2)} W_i(\mathbf{k}_1, \mathbf{k}_2, z_1, z_2, \mathbf{p}, m^2)\,, \tag{4.5}$$

where

$$\begin{aligned}W_1 &= n_c\left[\frac{1}{s}\left(\frac{1}{m^2-t} - \frac{1}{m^2-u}\right)(1-z_1-z_2) - \frac{B^2+C^2}{\mathbf{k}_1^2\mathbf{k}_2^2}\right. \\ &\quad + \frac{2(B-C)}{\mathbf{k}_1^2\mathbf{k}_2^2\, s}\left((1-z_2)\mathbf{k}_1^2 + (1-z_1)\mathbf{k}_2^2 - \mathbf{k}_1\cdot\mathbf{k}_2\right) \\ &\quad \left. + \frac{2}{\nu s} - \frac{2}{\mathbf{k}_1^2\mathbf{k}_2^2}\frac{\left((1-z_2)\mathbf{k}_1^2 + (1-z_1)\mathbf{k}_2^2 - \mathbf{k}_1\cdot\mathbf{k}_2\right)^2}{s^2}\right]. \\ W_2 &= \frac{1}{n_c}\left[\frac{-1}{(m^2-u)(m^2-t)} + \frac{(B+C)^2}{\mathbf{k}_1^2{\mathbf{k}_2}^2}\right],\end{aligned} \tag{4.6}$$

and

$$
\begin{aligned}
B &= \frac{1}{2} - \frac{(1-z_1)(1-z_2)\nu}{m^2-u} + \frac{\nu(1-z_1-z_2)}{2s} + \frac{(\mathbf{p}-\mathbf{k}_2)\cdot(\mathbf{k}_1-\mathbf{k}_2)}{s}\,, \\
C &= \frac{1}{2} - \frac{z_1 z_2 \nu}{m^2-t} - \frac{\nu(1-z_1-z_2)}{2s} - \frac{(\mathbf{p}-\mathbf{k}_2)\cdot(\mathbf{k}_1-\mathbf{k}_2)}{s}\,.
\end{aligned} \tag{4.7}
$$

The Mandelstam variables are

$$
\begin{aligned}
s &= (k_1+k_2)^2\,, \\
t &= (k_1-p_3)^2\,, \\
u &= (k_1-p_4)^2\,.
\end{aligned} \tag{4.8}
$$

It turns out that it is better to perform the Mellin transforms before doing the phase space integrals. Thus one considers the impact factor

$$
\begin{aligned}
h(N,M_1,M_2) &= M_1 M_2 \frac{\alpha_s^2 m^2}{2(n_c^2-1)} \int d\nu \frac{d^2\mathbf{k}_1}{\pi \mathbf{k}_1^2} \frac{d^2\mathbf{k}_2}{\pi \mathbf{k}_2^2} dz_1 dz_2 d^2\mathbf{p} \\
&\quad \left(\frac{4m^2}{\nu}\right)^N \left(\frac{\mathbf{k}_1^2}{m^2}\right)^{M_1} \left(\frac{\mathbf{k}_2^2}{m^2}\right)^{M_2} \\
&\quad \nu\delta((1-z_2)z_1\nu - |\mathbf{p}|^2)\delta((1-z_1)z_2\nu - |\mathbf{k}_1+\mathbf{k}_2-\mathbf{p}|^2)\left[W_1+W_2\right]\,,
\end{aligned} \tag{4.9}
$$

and one performs the N Mellin exploiting one of the delta functions; the second delta is used to fix the value of one of the longitudinal momenta, either z_1 or z_2. For instance

$$
z_2 = \frac{|\mathbf{k}_1+\mathbf{k}_2-\mathbf{p}|^2}{\nu(1-z_1)}\,. \tag{4.10}
$$

Despite a great amount of effort has been put into, it has not been possible to compute the remaining Mellin moments and phase space integrals keeping the full N dependence. If one sets $N=0$, then the result can be expressed in terms of Euler Gamma functions. The impact factor $h(0,M_1,M_2)$ is enough to compute the leading logarithmic behaviour, as previously discussed. However, for future phenomenological studies, it would be important to keep the N dependence, in order to have a better control of the singularities [51]. This issue will be discussed more in detail in section 4.1.2. The calculation of the impact factor is not straightforward because of the presence of scalar products between the transverse components of the momenta in the denominators, through the Mandelstam variables s, t and u, which leads to complicated angular

integrations. It is useful to combine the denominators with Feynman parameters:

$$\begin{aligned}\frac{1}{AB} &= \int_0^1 d\alpha \frac{1}{[A\alpha + (1-\alpha)B]^2}\,, \\ \frac{1}{A^2B^2} &= \frac{\partial^2}{\partial A \partial B}\frac{1}{AB} = \int_0^1 d\alpha \frac{6\alpha(1-\alpha)}{[A\alpha + (1-\alpha)B]^4}\,,\end{aligned} \tag{4.11}$$

where $A, B = s, t, u$. Because the denominators now only contain linear combinations of the Mandelstam invariants, one can complete the squares shifting the integration variable $\mathbf{p} \to \mathbf{l}$, which leads to denominators of the form:

$$D = \mathbf{l}^2 + \Delta\,, \tag{4.12}$$

where Δ does not contain scalar products between the vectors $\mathbf{l}$ and $\mathbf{k}_i$; hence the angular dependence appears only in the numerators. Using this trick the integrals in eq. (4.9) can be performed. The calculation is lengthy, especially for the non-Abelian contributions, but the results is rather simple:

$$\begin{aligned}h(0, M_1, M_2) = {} & \frac{\alpha_s^2 \pi}{n_c^2 - 1}\Gamma(1+M_1)\Gamma(1-M_1)\Gamma(1+M_2)\Gamma(1-M_2) \\ & \Big[4n_c \frac{(\Gamma(3-M_1-M_2))^2}{(1-M_1-M_2)\Gamma(6-2(M_1+M_2))}\Big(1 + \Big(\frac{\Gamma(1-M_1-M_2)}{\Gamma(1-M_1)\Gamma(1-M_2)}\Big)^2\Big) \\ & -\frac{2}{n_c}(7 - 5(M_1+M_2) + 3M_1M_2)\frac{\Gamma(2-M_1)\Gamma(2-M_2)\Gamma(1-M_1-M_2)}{\Gamma(4-2M_1)\Gamma(4-2M_2)}\Big]\,.\end{aligned} \tag{4.13}$$

The term proportional to n_c comes from the non-Abelian diagram in fig. 4.1; it contains a line of triple poles at $M_1 + M_2 = 1$, whose origin is the s-channel gluon propagator:

$$h(0, M_1, M_2) \sim \frac{\alpha_s^2 \pi}{n_c^2 - 1}\frac{n_c}{6}\frac{1 - (M_1 - M_2)^2}{(1 - M_1 - M_2)^3}\Big[1 + \mathcal{O}(1 - M_1 - M_2)\Big]\,. \tag{4.14}$$

This singularity is of the same kind as the one discussed in the toy-model, eq. (3.106) and hence it dominates the cross section at high energy. However the degree of this line of singularities changes if the N dependence is kept; in the vicinity of $M_1 = M_2 = 1/2$ one finds the singularity structure [44]:

$$h(0, M_1, M_2) \sim \frac{\alpha_s^2 \pi}{n_c^2 - 1}\frac{n_c}{6}\frac{1}{(1 - M_1 - M_2)}\frac{1}{(1 + N - M_1 - M_2)^2}\,. \tag{4.15}$$

If the resummation is performed at fixed coupling, neglecting the N dependence in the impact factor, it results into a large enhancement of the cross section. As discussed at the end of the previous chapter this effect is smoothed when the resummation is

performed at the running coupling level, and consequently the N dependence is less crucial. Nevertheless the calculation of impact factors with full N and M_i dependence might be phenomenologically relevant. Moreover it has theoretical interest of its own, because it gives access to a class of subleading contributions at high energy.

4.1.2 The N dependence of the impact factor

In this section the impact factor for heavy quark production is computed in the limit

$$M_1 = M\,, \quad M_2 = 0\,,$$

but keeping the N dependence. The limit $M_2 \to 0$ corresponds to setting one of the initial gluon lines on-shell:

$$\begin{aligned}
\lim_{M_2\to 0} h(N,M_1,M_2) &= \lim_{M_2\to 0} M_1 M_2 \int_0^\infty d\xi_1 \int_0^\infty d\xi_2 \xi_1^{M_1-1}\xi_2^{M_2-1}\hat{\Sigma}^{\rm off}_{gg}(N,\xi_1,\xi_2) \\
&= -\lim_{M_2\to 0} M_1 \int_0^\infty d\xi_1 \int_0^\infty d\xi_2 \xi_1^{M_1-1}\xi_2^{M_2}\frac{\partial}{\partial\xi_2}\hat{\Sigma}^{\rm off}_{gg}(N,\xi_1,\xi_2) \\
&= -M_1 \int_0^\infty d\xi_1 \xi_1^{M_1-1}\hat{\Sigma}^{\rm off}_{gg}(N,\xi_1,\xi_2)\Big|_{\xi_2=0}^{\xi_2=\infty} = M_1 \int_0^\infty d\xi_1 \xi_1^{M_1-1}\hat{\Sigma}^{\rm off}_{gg}(N,\xi_1,0)\,,
\end{aligned} \tag{4.16}$$

where the dimensionless variables $\xi_i = \frac{\mathbf{k}_i^2}{m^2}$, with $i = 1,2$ have been introduced. The cross section with only one off-shell gluon can be deduced from eq. (4.5); in this case it is more convenient to perform all the phase space integrals first, so that one is left with

$$\begin{aligned}
h(N,M,0) \;=\; & M\int_0^\infty \frac{d\mathbf{k}^2}{\mathbf{k}^2}\left(\frac{\mathbf{k}^2}{m^2}\right)^M \int_0^1 d\rho\rho^N \\
& \Big[\Sigma_0(\rho,\mathbf{k}^2/m^2)+\Sigma_1(\rho,\mathbf{k}^2/m^2)\Big]\Theta\left(\frac{1}{\rho}-1-\frac{\mathbf{k}^2}{m^2}\right)\,.
\end{aligned} \tag{4.17}$$

The leading and sub-leading colour contributions are obtained from eq. (4.5), taking the on-shell limit $\mathbf{k}_2 \to 0$, and averaging over the azimuthal angle. Their explicit

expressions are:

$$\begin{aligned}\Sigma_0(\rho,\mathbf{k}^2/m^2) &= \frac{\alpha_s^2 n_c}{2(n_c^2-1)}\frac{\pi\beta}{2}\left\{\frac{(1-\beta^2)^2\left(-10-11\rho+6(1+\rho)\mathcal{L}(\beta)\right)}{6\rho^2}\right.\\ &+ \left(\frac{\mathbf{k}^2}{4m^2}\right)\frac{(1-\beta^2)^2\left(76+69\rho-24(1+2\rho)\mathcal{L}(\beta)\right)}{6\rho}\\ &+ \left(\frac{\mathbf{k}^2}{4m^2}\right)^2(1-\beta^2)^2\left(-29-16\rho+(7+13\rho)\mathcal{L}(\beta)\right)\\ &+ \left(\frac{\mathbf{k}^2}{4m^2}\right)^3(1-\beta^2)^2\frac{2}{3}\rho\left(41+10\rho-9(1+\rho)\mathcal{L}(\beta)\right)\\ &+ \left.\left(\frac{\mathbf{k}^2}{4m^2}\right)^4(1-\beta^2)^2\frac{2}{3}\rho^2\left(-14+3\mathcal{L}(\beta)\right)\right\}, \end{aligned} \tag{4.18}$$

$$\begin{aligned}\Sigma_1(\rho,\mathbf{k}^2/m^2) &= -\frac{\alpha_s^2}{2n_c(n_c^2-1)}\frac{\pi\beta}{2}\left\{-1-\rho+\left(1+\rho-\frac{1}{2}\rho^2\right)\mathcal{L}(\beta)\right.\\ &+ \frac{\mathbf{k}^2}{4m^2}\rho\left[8+\rho-(2+3\rho)\mathcal{L}(\beta)\right]\\ &+ \left.\left(\frac{\mathbf{k}^2}{4m^2}\right)^2\rho^2[-8+2\mathcal{L}(\beta)]\right\}. \end{aligned} \tag{4.19}$$

where the following notation has been introduced

$$\mathcal{L}(\beta)=\frac{1}{\beta}\ln\frac{1+\beta}{1-\beta}, \quad \beta=\sqrt{1-\rho\left(1-\frac{\rho\mathbf{k}^2}{4m^2}\right)^{-1}}. \tag{4.20}$$

The two Mellin transforms can be computed by noticing that the off-shell cross section is only a function of β; thus one has to evaluate the following kind of integral

$$\int_0^\infty\frac{d\mathbf{k}^2}{\mathbf{k}^2}\left(\frac{\mathbf{k}^2}{m^2}\right)^M\int_0^1 d\rho\rho^N\Theta\left(\frac{1}{\rho}-1-\frac{\mathbf{k}^2}{m^2}\right)f(\beta). \tag{4.21}$$

This can be achieved by changing the variables of integrations

$$(\rho,\mathbf{k}^2)\to(\eta,\mathbf{k}^2), \tag{4.22}$$

with $\eta=1-\beta^2$ and by performing the the integral with respect to $\mathbf{k}^2$ first:

$$\begin{aligned}&\int_0^\infty\frac{d\mathbf{k}^2}{\mathbf{k}^2}\left(\frac{\mathbf{k}^2}{m^2}\right)^M\frac{1}{\left(1+\frac{\eta\mathbf{k}^2}{4m^2}\right)^{N+2}}\int_0^1 d\eta\,\eta^N f(\sqrt{1-\eta})=\\ &\qquad 4^M\frac{\Gamma(M)\Gamma(2-M+N)}{\Gamma(N+2)}\int_0^1 d\eta\,\eta^{N-M}f(\sqrt{1-\eta}). \end{aligned} \tag{4.23}$$

The only two integrals which have to be computed are:

$$\begin{aligned}\int_0^1 \eta^\alpha \sqrt{1-\eta} &= \frac{\sqrt{\pi}\,\Gamma(1+\alpha)}{2\Gamma\left(\frac{5}{2}+\alpha\right)}\,,\\ \int_0^1 \eta^\alpha \ln\frac{1+\sqrt{1-\eta}}{1-\sqrt{1-\eta}} &= \frac{\sqrt{\pi}\,\Gamma(1+\alpha)}{(\alpha+1)\Gamma\left(\frac{3}{2}+\alpha\right)}\,.\end{aligned} \tag{4.24}$$

After some algebraic manipulations of the Euler Gamma functions one obtains the following expression:

$$\begin{aligned}h(N,M,0) = {} & \frac{\alpha_s^2\pi}{n_c^2-1}\frac{4^N\Gamma(1+N-M)^2\Gamma(1+M)\Gamma(3+N-M)}{\Gamma(N+4)\Gamma(6+2N-2M)}\\ & \Bigg\{ 2n_c\Big(48+79N+48N^2+12N^3+N^4\\ & -M(24+23N+7N^2)-M^2N(N+1)\Big)\\ & -\frac{2}{n_c}\left(14+20N+9N^2+N^3-M(10+7N+N^2)\right)\\ & \times(5+2N-2M)\Bigg\}\,.\end{aligned} \tag{4.25}$$

The colour suppressed contribution, which comes from the Abelian diagrams, is in agreement with the result for photoproduction of heavy quarks in Ref. [45]. The non-Abelian contribution is instead a new and unpublished result.

4.2 Drell-Yan processes

The production of lepton pairs through Drell-Yan mechanism [77] is one of major success of perturbative QCD. The inclusive cross section has been computed at NLO [78] and NNLO [79]. The hard scale of the process is given by the invariant mass of the lepton pair

$$Q^2 = m_{l\bar{l}}^2\,. \tag{4.26}$$

At LHC energies this quantity can be much smaller than the centre-of-mass energy, so the resummation of high energy logarithm is of phenomenological interest, even at the inclusive level. Furthermore the calculation of the Drell-Yan cross section is very similar to the one for vector boson production. The $W^\pm$ and the Z cross sections are meant to be used at LHC as a normalisation for the other cross sections and as a real-time monitor for the luminosity. These tasks require a precision in the computation at the percent level. For this reason the inclusion of the high energy corrections to these processes, even if they are not expected to be dramatic because $x \sim 10^{-3}$ for central rapidities $|y| \lesssim 2$, is important in order to get the sought precision.

4.2.1 The Drell-Yan cross section

In the following the high energy behaviour of the partonic Drell-Yan cross section is computed; for simplicity only one flavour of quarks with electric charge e_q is considered. The $\overline{\text{MS}}$ partonic cross section for the production of a lepton pair via an off-shell photon with squared momentum $q^2 = Q^2$ can be written as:

$$\hat{\sigma}(\tau, Q^2) = \hat{\sigma}_0(Q^2) \sum_{i,j} D_{ij}(\tau, Q^2)\,, \tag{4.27}$$

where $\tau = Q^2/\hat{s}$ and the sum indices run over initial different partons q, $\bar{q}$, g. The LO cross section is

$$\hat{\sigma}_0(Q^2) = \frac{e_q^2 \alpha^2}{Q^4} \frac{4\pi}{3 n_c}\,, \tag{4.28}$$

and the dimensionless coefficient function D_{ij} contains the QCD radiative corrections

$$D_{ij}(\tau, Q^2) = \sum_{k=0}^{\infty} \left(\frac{\alpha_s}{2\pi}\right)^k D_{ij}^{(k)}(\tau, Q^2)\,. \tag{4.29}$$

At LO the only partonic process process is $q\bar{q} \to \gamma^*$ and the coefficient function is simply a delta

$$D_{q\bar{q}}^{(0)}(\tau, Q^2) = \tau \delta(1-\tau)\,. \tag{4.30}$$

At NLO the channel $qg \to q\gamma^*$ opens, while the process with two gluons in the initial state occurs at NNLO.

The Mellin transform of the hadronic coefficient function can be written as

$$D(N, Q^2) = D_{qq}\, q\, q + D_{qg}\, q\, g + D_{gg}\, g\, g\,, \tag{4.31}$$

where $q = q(N, \mu^2)$ and $g = g(N, \mu^2)$ are the Mellin moments of the parton distribution functions. The behaviour of the different partonic coefficient functions in the high energy limit is

$$\begin{aligned} D_{qq} &= 1 + \mathcal{O}\left(\alpha_s \left(\frac{\alpha_s}{N}\right)^k\right)\,, \\ D_{qg} &= \mathcal{O}\left(\alpha_s \left(\frac{\alpha_s}{N}\right)^k\right)\,, \qquad k = 0, 1, 2, \ldots \\ D_{gg} &= \mathcal{O}\left(\alpha_s^2 \left(\frac{\alpha_s}{N}\right)^k\right)\,; \end{aligned} \tag{4.32}$$

hence the quark-gluon contribution is NLL, while the gluon-gluon one is NNLL. The high energy singularities of the D_{qg} coefficient function can be computed to all orders in perturbation theory, using k_T-factorisation. However, the Drell-Yan partonic cross

section has collinear singularities, because of the massless quark line and so the procedure is more complicated than the one described in the previous chapter and used for heavy quark production. More specifically, high energy factorisation in $d = 4 - 2\varepsilon$ dimensions states that

$$D_{qg}(N,Q^2) = \int d^{2-2\varepsilon}\mathbf{k}\,\hat{\Sigma}^{\rm off}_{qg}(N,\frac{\mathbf{k}^2}{Q^2},\varepsilon) f^{\rm bare}(N,\mathbf{k},\alpha_s,\mu^2,\varepsilon) q^{\rm bare}(N,\mu^2,\varepsilon) g^{\rm bare}(N,\mu^2,\varepsilon)\,. \tag{4.33}$$

As opposed to eq. (3.25) the partonic cross section is not free of collinear poles and hence, in principle, has to be evaluated in d-dimensions. The factorisation of collinear singularities has to be treated carefully; the renormalised quark and gluon distributions can be written in terms of the bare ones and of the transition functions Γ_{ab}, analogously to eq. (3.27):

$$\begin{aligned} q &= \Gamma_{qq}\, q^{\rm bare} + \Gamma_{qg}\, g^{\rm bare} \\ g &= \Gamma_{gq}\, q^{\rm bare} + \Gamma_{gg}\, g^{\rm bare}\,, \end{aligned} \tag{4.34}$$

where the explicit arguments of the functions have been omitted for simplicity. Substituting eq. (4.34) into eq. (4.31) one obtains

$$\begin{aligned} D(N,Q^2) &= D_{qq}\left[\Gamma_{qq}\, q^{\rm bare} + \Gamma_{qg}\, g^{\rm bare}\right]\left[\Gamma_{qq}\, q^{\rm bare} + \Gamma_{qg}\, g^{\rm bare}\right] \\ &\quad + D_{qg}\left[\Gamma_{qq}\, q^{\rm bare} + \Gamma_{qg}\, g^{\rm bare}\right]\left[\Gamma_{gq}\, q^{\rm bare} + \Gamma_{gg}\, g^{\rm bare}\right] \\ &\quad + D_{gg}\left[\Gamma_{gq}\, q^{\rm bare} + \Gamma_{gg}\, g^{\rm bare}\right]\left[\Gamma_{gq}\, q^{\rm bare} + \Gamma_{gg}\, g^{\rm bare}\right]. \end{aligned} \tag{4.35}$$

The coefficient of $q^{\rm bare} g^{\rm bare}$ reads as

$$\begin{aligned} D^{\rm bare}_{qg} &= D_{qq}\,\Gamma_{qq}\Gamma_{qg} + D_{qg}\,\Gamma_{qq}\Gamma_{gg} + D_{gg}\,\Gamma_{gq}\Gamma_{gg} \\ &= \Gamma_{qg} + D_{qg}\,\Gamma_{gg} + \mathcal{O}\left(\alpha_s^2\left(\frac{\alpha_s}{N}\right)^k\right), \end{aligned} \tag{4.36}$$

where the high energy behaviour of the different coefficient functions eq. (4.32) have been used. Moreover:

$$\begin{aligned} \Gamma_{qq}(\alpha_s,\varepsilon) &= 1 + \mathcal{O}\left(\alpha_s\left(\frac{\alpha_s}{N}\right)^k\right), \\ \Gamma_{qg}(\alpha_s,\varepsilon) &= \frac{1}{\varepsilon}\int_0^{\alpha_s e^{-\varepsilon(\ln 4\pi - \gamma_E)}} \frac{d\alpha}{\alpha}\gamma_{gg}(N,\alpha)\Gamma_{gg}(\alpha,\varepsilon) + \mathcal{O}\left(\alpha_s\left(\frac{\alpha_s}{N}\right)^k\right). \end{aligned} \tag{4.37}$$

The high energy singularities of D_{qg} are computed using a procedure described in [44] in the case of deep-inelastic scattering. It consists of considering the logarithmic derivative

of the coefficient function with respect Q^2

$$\frac{\partial}{\partial \ln Q^2} D_{qg}^{\rm bare} = \left[\gamma_{qg} + \gamma_{gg} D_{qg} + \varepsilon \alpha_s \frac{\partial}{\partial \alpha_s} D_{qg} \right] \Gamma_{gg} \,. \tag{4.38}$$

This expression has now the same factorisation properties of eq. (3.25), and all the ε poles can be factorised through the transition function. Thus the terms in the square brackets is collinear safe. On the other side, high energy factorisation states that:

$$\frac{\partial}{\partial \ln Q^2} D_{qg}^{\rm bare} = \int d^{2-2\varepsilon}\mathbf{k} \, \frac{\partial}{\partial \ln Q^2} \hat{\Sigma}_{qg}^{\rm off}(N, \frac{\mathbf{k}^2}{Q^2}, \varepsilon) f^{\rm bare}(N, \mathbf{k}, \alpha_s, \mu, \varepsilon) \,. \tag{4.39}$$

Thus, comparing eq. (4.38) and eq. (4.39) taking the $\varepsilon \to 0$ limit, one obtains:

$$\gamma_{gg} D_{qg} + \gamma_{qg} = h(N, M) R(0, M) \,. \tag{4.40}$$

The impact factor in eq. (4.40) is the Mellin transform of the logarithmic derivative of the off-shell cross section $qg^* \to q\gamma^*$ with respect to Q^2:

$$\begin{aligned} h(N, M) &= M \int_0^\infty d\xi \xi^{M-1} \frac{\partial}{\partial \ln Q^2} \hat{\Sigma}_{qg}^{\rm off}(N, \xi) \\ &= -M \int_0^\infty d\xi \xi^{M} \frac{\partial}{\partial \xi} \hat{\Sigma}_{qg}^{\rm off}(N, \xi) \\ &= M^2 \int_0^\infty d\xi \xi^{M-1} \hat{\Sigma}_{qg}^{\rm off}(N, \xi) \,, \end{aligned} \tag{4.41}$$

where $\xi = \mathbf{k}^2/Q^2$. Even though the off-shell cross section $\hat{\Sigma}_{qg}^{\rm off}$ has collinear singularities and a consistent computation in $\overline{\rm MS}$ would require its evaluation in d-dimensions, its logarithmic derivative is collinear safe; hence it can be computed in four dimensions and used to determine the high energy behaviour of the coefficient function D_{qg} through eq. (4.40).

4.2.2 The off-shell calculation

The process which has to be considered is

$$g^*(k) + q(p) \to \gamma^*(q) + q(p') \,;$$

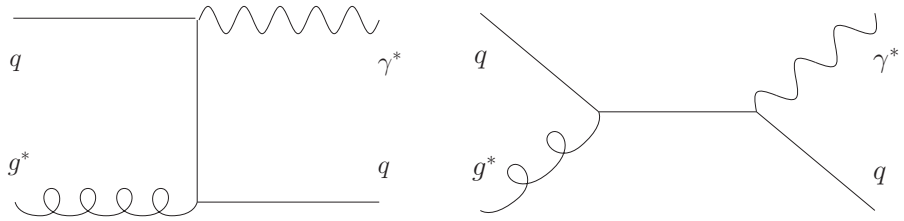

Figure 4.2: Diagrams for the Drell-Yan process with one off-shell gluon $g^*q \to \gamma^* q$.

the relevant Feynman diagrams are shown in fig. 4.2 and the Sudakov decomposition of the four momenta is

$$\begin{aligned} k &= x_1 p_1 + \mathbf{k} \\ p &= x_2 p_2 \\ q &= z_1 x_1 p_1 + (1-z_2) x_2 p_2 + \mathbf{q} \\ p' &= (1-z_1) x_1 p_1 + z_2 x_2 p_2 + \mathbf{k} - \mathbf{q}\,. \end{aligned} \tag{4.42}$$

The two-body phase-space is given in eq. (A.16); with the current convention for the momenta it becomes:

$$\begin{aligned} d\Phi^{(2)} &= \frac{d^4q}{(2\pi)^3}\frac{d^4p'}{(2\pi)^3}\,\delta(q^2-Q^2)\delta(p'^2)(2\pi)^4\delta^{(4)}(k+p-q-p') = \\ &= \frac{d^4q}{(2\pi)^2}\,\delta(q^2-Q^2)\,\delta(p'^2) = \\ &= \frac{\nu}{8\pi^2} dz_1 dz_2 d^2\mathbf{q}\,\delta((1-z_2)z_1\nu - |\mathbf{q}|^2) \\ &\quad \times\delta((1-z_1)z_2\nu - |\mathbf{k}-\mathbf{q}|^2)\,. \end{aligned} \tag{4.43}$$

The squared matrix element is computed using as usual eikonal polarisation for the gluon, while the Lorentz indices coming from the photon-quark coupling are contracted with $g^{\mu\nu}$, because of the conservation of the electro-magnetic current. The result is

$$\begin{aligned} |\mathcal{M}|^2 &= -\tfrac{e_q^2 g_s^2}{n_c}\Big\{ \tfrac{t}{s} + \tfrac{s}{t} + Q^2|\mathbf{k}|^2\left(\tfrac{1}{s^2}+\tfrac{1}{t^2}\right) + 2|\mathbf{k}|^2\left(\tfrac{1}{t}-\tfrac{1}{s}\right) + 4\tfrac{(\mathbf{k}\cdot\mathbf{q})}{s} \\ &\quad -4\tfrac{Q^2(\mathbf{k}\cdot\mathbf{q})}{t^2} + 4\tfrac{Q^2(\mathbf{k}\cdot\mathbf{q})^2}{|\mathbf{k}|^2 t^2} + \tfrac{1}{st}\Big[2|\mathbf{k}|^4 - 4|\mathbf{k}|^2(\mathbf{k}\cdot\mathbf{q}) + 4(\mathbf{k}\cdot\mathbf{q})^2 \\ &\quad -4(\mathbf{k}\cdot\mathbf{q})Q^2 + 2|\mathbf{k}|^2Q^2\Big]\Big\}\,, \end{aligned} \tag{4.44}$$

where the usual Mandelstam invariants have been introduced

$$\begin{aligned} s &= (p+k)^2 = \nu - |\mathbf{k}|^2 \\ t &= (p-q)^2 = Q^2 - z_1\nu \\ s+t+u &= Q^2 - |\mathbf{k}|^2 \,. \end{aligned} \tag{4.45}$$

The matrix element eq. (4.44) in the on-shell limit reduces to

$$\lim_{|\mathbf{k}|\to 0} \langle |\mathcal{M}|^2 \rangle_\vartheta = -\frac{e_q^2 g_s^2}{n_c} \Big\{ \frac{t}{s} + \frac{s}{t} + 2\frac{Q^2 u}{st} \Big\} \,, \tag{4.46}$$

in agreement with the standard NLO calculation [78].

The phase space integration can be easily performed shifting the variable of integration: $\Delta = \mathbf{q} - z_1\mathbf{k}$. One delta function is used to perform the integral over the longitudinal fraction of the momentum z_2

$$d\Phi^{(2)} = \frac{1}{8\pi^2} \frac{dz_1}{(1-z_1)} d^2\Delta \, \delta((1-z_2)z_1\nu - |\mathbf{q}|^2) \,, \tag{4.47}$$

with

$$z_2 = \frac{|(1-z_1)\mathbf{k} - \Delta|^2}{(1-z_1)\nu} \,. \tag{4.48}$$

With the second delta one can compute the integral over $|\Delta|^2$:

$$d\Phi^{(2)} = \frac{1}{16\pi^2} dz_1 d\vartheta \,, \tag{4.49}$$

with

$$|\Delta|^2 = (1-z_1)[z_1(\nu - |\mathbf{k}|^2) - Q^2] \,. \tag{4.50}$$

$$\begin{aligned} 0 < &\quad \vartheta &< 2\pi \\ \frac{Q^2}{\nu - |\mathbf{k}|^2} < &\quad z_1 &< 1 \,. \end{aligned} \tag{4.51}$$

One may introduce the dimensionless variables:

$$\tau = \frac{Q^2}{\nu} \,, \quad \xi = \frac{|\mathbf{k}|^2}{Q^2} \,. \tag{4.52}$$

The reduced cross section, averaged over the azimuth, can be written as follows

$$\Sigma(\tau,\xi) = \frac{e_q^2}{n_c} \frac{\alpha_s}{2\pi} \frac{\tau}{2} \int_{\frac{\tau}{1-\tau\xi}}^1 dz_1 \int_0^{2\pi} \frac{d\vartheta}{2\pi} |\mathcal{M}|^2 \,, \tag{4.53}$$

where, according to eq. (4.28), the factor e_q^2/n_c has been absorbed into the LO cross

section. The explicit result of the integration gives

$$\begin{aligned}\Sigma(\tau,\xi) &= \frac{\alpha_s}{2\pi}T_R\,\tau\Bigg\{\frac{1}{1-\tau\xi}\ln\left(\tfrac{(1-\tau)(1-\xi\tau)}{\tau^2\xi}\right)\Bigg[(\tau^2+(1-\tau)^2)\\ &\quad+\tau^2\xi\left(10+\xi+18\tau^2\xi-6\tau(3+2\xi)\right)\Bigg]\\ &\quad+\frac{1-\tau-\tau\xi}{2(1-\tau)(1-\tau\xi)^3}\Bigg[-1+36\tau^5\xi^3+7\tau(2+\xi)\\ &\quad-6\tau^4\xi^2(15+7\xi)+2\tau^3\xi(35+49\xi+4\xi^2)\\ &\quad-\tau^2(15+71\xi+14\xi^2)\Bigg]\Bigg\}\Theta\left(\frac{1}{\tau}-\xi-1\right). \end{aligned} \tag{4.54}$$

The on-shell limit $\xi \to 0$ is

$$\begin{aligned}\Sigma(\tau,\xi) &= \frac{\alpha_s}{2\pi}\tau\Bigg[-P_{qg}(\tau)\ln\xi+P_{qg}(\tau)\ln\left(\frac{1-\tau}{\tau^2}\right)\\ &\quad+\frac{1}{2}\left(-\frac{1}{2}+7\tau-\frac{15}{2}\tau^2\right)\Bigg]+\mathcal{O}(\xi)\,, \end{aligned} \tag{4.55}$$

where $P_{qg}(\tau)=T_R(\tau^2+(1-\tau)^2)$. The fixed order NLO coefficient function in $\overline{\rm MS}$ is

$$\begin{aligned}D_{qg}^{(1)}(\tau,Q^2) &= \frac{\alpha_s}{2\pi}\tau\Bigg[-P_{qg}(\tau)\left(-\frac{1}{\varepsilon}-\ln 4\pi+\gamma_E+\ln\frac{Q^2}{\mu^2}\right)\\ &\quad+P_{qg}(\tau)\ln\left(\frac{(1-\tau)^2}{\tau}\right)+\frac{1}{2}\left(\frac{1}{2}+3\tau-\frac{7}{2}\tau^2\right)\Bigg]. \end{aligned} \tag{4.56}$$

Only the coefficient of the collinear singularity is the same in the two expressions: it is the DGLAP splitting function. The finite parts instead clearly differ. This is because the virtuality of the gluon acts as a mass regulator and hence the off-shell calculation in four dimensions is performed in a factorisation scheme which is not $\overline{\rm MS}$, as extensively discussed in [81]. However, as already said, the logarithmic derivative of this cross section provides, through eq. (4.40), the $\overline{\rm MS}$ result for the coefficient function D_{qg}.

The impact factor is defined in eq. (4.41) as the double Mellin transform of the logarithmic derivative of the off-shell cross section eq. (4.54). It is useful to change the integration variables according to

$$\begin{aligned}\alpha &= \tau\xi\\ \beta &= \frac{\tau}{1-\tau\xi}\,; \end{aligned} \tag{4.57}$$

the Jacobian determinant is $1/\beta$. In this way the Θ function condition is satisfied for

all $\alpha, \beta \in [0,1]$ and the region of integration becomes simpler:

$$\begin{aligned} h(N,M) &= \frac{\alpha_s}{2\pi} T_R\, M^2 \int_0^1 d\alpha \int_0^1 d\beta\, \alpha^{M-1} (1-\alpha)^{N-M} \beta^{N-M} \\ &\times \left[\ln \frac{1-(1-\alpha)\beta}{\alpha\beta} d_1(\alpha,\beta) - \frac{1}{2} \frac{1}{1-(1-\alpha)\beta} d_2(\alpha,\beta) \right], \end{aligned} \tag{4.58}$$

where the function d_i are

$$\begin{aligned} d_1(\alpha,\beta) &= 1 + \alpha^2 - 2\beta + 12\alpha\beta - 22\alpha^2\beta + 12\alpha^3\beta + 2\beta^2 - 22\alpha\beta^2 \\ &\quad + 56\alpha^2\beta^2 - 54\alpha^3\beta^2 + 18\alpha^4\beta^2\,, \\ d_2(\alpha,\beta) &= (1-\beta)\Big(1 - 6\alpha + 8\alpha^2 - 14\beta + 71\alpha\beta - 98\alpha^2\beta + 42\alpha^3\beta + 15\beta^2 \\ &\quad - 85\alpha\beta^2 + 160\alpha^2\beta^2 - 126\alpha^3\beta^2 + 36\alpha^4\beta^2\Big)\,. \end{aligned} \tag{4.59}$$

Thus only two master integrals are needed in order to compute the Mellin moments of the off-shell cross section. Moreover the integral containing the logarithm can be further simplified, integrating by parts with respect to the variable β:

$$\begin{aligned} &\int_0^1 d\alpha \int_0^1 d\beta\, \alpha^{M-1+p_\alpha} (1-\alpha)^{N-M} \beta^{N-M+p_\beta} \ln \frac{1-(1-\alpha)\beta}{\alpha\beta} = \\ &\frac{1}{1+N-M+p_\beta} \int_0^1 d\alpha \int_0^1 d\beta\, \alpha^{M-1+p_\alpha} (1-\alpha)^{N-M} \beta^{N-M+p_\beta} \frac{1}{1-(1-\alpha)\beta} \end{aligned} \tag{4.60}$$

where p_α and p_β stand for the exponents of α and β in each terms of the functions $d_i(\alpha,\beta)$. Thus only one integral is actually needed:

$$\begin{aligned} &\int_0^1 d\alpha \int_0^1 d\beta\, \alpha^{M-1+p_\alpha} (1-\alpha)^{N-M} \beta^{N-M+p_\beta} \frac{1}{1-(1-\alpha)\beta} = \\ &\qquad \frac{\Gamma(M+p_\alpha)\Gamma(1-M+N)}{\Gamma(1+N+p_\alpha)(1+N-M+p_\beta)} \quad \times \\ &{}_3F_2\Big[\{1, 1+N-M, 1+N-M+p_\beta\}, \{1+N+p_\alpha, 2+N-M+p_\beta\}; 1\Big]\,. \end{aligned} \tag{4.61}$$

It is instructive to rewrite the hypergeometric in the previous expression, in order to show the singularity in $M = 0$. Thomae's theorem [82] states that

$${}_3F_2(\{a,b,c\},\{e,f\};1) = \tfrac{\Gamma(s)\Gamma(e)\Gamma(f)}{\Gamma(s+b)\Gamma(s+c)\Gamma(a)} {}_3F_2(\{s, e-a, e-b\}, \{s+b, s+c\}; 1)\,. \tag{4.62}$$

It is then possible to rearrange the expression in eq. (4.61) as

$$
\begin{aligned}
&{}_3F_2\Big[\{1, 1+N-M, 1+N-M+p_\beta\}, \{1+N+p_\alpha, 2+N-M+p_\beta\}; 1\Big] = \\
&\frac{\Gamma(M+p_\alpha)\Gamma(2+N-M+p_\beta)}{\Gamma(1+N+p_\alpha+p_\beta)} {}_3F_2\Big[\{M+p_\alpha, N+p_\alpha, 1+N-M+p_\beta\}, \\
&\quad \{1+N+p_\alpha, 1+N+p_\alpha+p_\beta\}; 1\Big] \,. \qquad (4.63)
\end{aligned}
$$

Thus the integral in eq. (4.41) has a double pole in $M = 0$ coming from the terms with $p_\alpha = 0$, but the impact factor is regular in the origin because of the prefactor M^2. The expression of impact factor $h(N, M)$ is a fairly complicated sum of terms involving generalised hypergeometric functions ${}_3F_2$:

$$
\begin{aligned}
h(N,M) = \frac{\alpha_s}{2\pi} T_R M^2 \sum_{p_\alpha=0}^{4} \sum_{p_\beta=0}^{3} & \frac{\Gamma(M+p_\alpha)^2 \Gamma(1+N-M)\Gamma(1+N-M+p_\beta)}{\Gamma(1+N+p_\alpha)\Gamma(1+N+p_\alpha+p_\beta)} \\
& {}_3F_2\Big[\{M+p_\alpha, N+p_\alpha, 1+N-M+p_\beta\}, \{1+N+p_\alpha, 1+N+p_\alpha+p_\beta\}; 1\Big] \\
& \left[\frac{\tilde{\Delta}^{(1)}_{1+p_\alpha, 1+p_\beta}}{(1+N-M+p_\beta)} + \tilde{\Delta}^{(2)}_{1+p_\alpha, 1+p_\beta} \right] . \qquad (4.64)
\end{aligned}
$$

The coefficients are deduced from eq. (4.59) and they are collected in the following matrices:

$$
\tilde{\Delta}^{(1)}_{i,j} = \begin{pmatrix} 1 & -2 & 2 & 0 \\ 0 & 12 & -22 & 0 \\ 1 & -22 & 56 & 0 \\ 0 & 12 & -54 & 0 \\ 0 & 0 & 18 & 0 \end{pmatrix} ; \; \tilde{\Delta}^{(2)}_{i,j} = -\frac{1}{2} \begin{pmatrix} 1 & -15 & 29 & -15 \\ -6 & 77 & -156 & 85 \\ 8 & -106 & 258 & -160 \\ 0 & 42 & -168 & 126 \\ 0 & 0 & 36 & -36 \end{pmatrix} , \qquad (4.65)
$$

where $i = 1 + p_\alpha$ and $j = 1 + p_\beta$.

4.2.3 The coefficient function at high energy

The leading high energy behaviour of the coefficient function D_{qg} can be computed through eq. (4.40), using the pole condition $M = \gamma_s\left(\frac{\alpha_s}{N}\right)$

$$
\gamma_s D_{qg} + \gamma_{qg} = h(0, \gamma_s) R(0, \gamma_s) \,, \qquad (4.66)
$$

remembering that $\gamma_{gg} = \gamma_s + \mathcal{O}\left(\alpha_s \left(\frac{\alpha_s}{N}\right)^k\right)$. The explicit N dependence of the impact factor is subleading, so it has been set $N = 0$; in this limit the hypergeometric functions

in eq. (4.64) become

$$ {}_3F_2\Big[\{M+p_\alpha, p_\alpha, 1-M+p_\beta\}, \{1+p_\alpha, 1+p_\alpha+p_\beta\}; 1\Big]\,, \tag{4.67} $$

which for integer values of p_α and p_β can be written as combinations of sine and rational functions. Using the following relation between Euler Gamma function

$$ \Gamma(1+z) = z\Gamma(z)\,, $$

the result remarkably simplifies to:

$$ h(0,M) = \frac{\alpha_s}{2\pi} T_R \frac{4\Gamma(1-M)^2\Gamma(1+M)^2}{(1-M)(2-M)(3-M)}\,. \tag{4.68} $$

The Taylor expansion about $M=0$ gives

$$ \begin{aligned} h(0,M) &= \frac{\alpha_s}{2\pi} T_R \Bigg[\frac{2}{3} + \frac{11}{9}M + \left(\frac{85}{54} + \frac{2\pi^2}{9}\right) M^2 + \left(\frac{575}{324} + \frac{11\pi^2}{27}\right) M^3 \\ &\quad + \left(\frac{3661}{1944} + \frac{85\pi^2}{162} + \frac{2\pi^4}{45}\right) M^4 + \mathcal{O}\left(M^5\right) \Bigg]\,. \end{aligned} \tag{4.69} $$

In order to compute the high energy behaviour of the $\overline{\text{MS}}$ coefficient function, one needs the the BFKL anomalous dimension eq. (3.21) and the scheme change factors between $\overline{\text{MS}}$ and Q_0, given in eq. (3.33). Finally the quark anomalous dimension at high energy was computed in [44] up to $\mathcal{O}\left(\alpha_s \left(\frac{\alpha_s}{N}\right)^5\right)$:

$$ \begin{aligned} \gamma_{qg}\left(\frac{\alpha_s}{N}\right) &= \frac{\alpha_s T_R}{3\pi} \Bigg[1 + \frac{5}{3}\frac{C_A}{\pi}\frac{\alpha_s}{N} + \frac{14}{9}\left(\frac{C_A}{\pi}\frac{\alpha_s}{N}\right)^2 + \left(\frac{82}{81} + 2\zeta_3\right)\left(\frac{C_A}{\pi}\frac{\alpha_s}{N}\right)^3 \\ &+ \left(\frac{122}{243} + \frac{25}{6}\zeta_3\right)\left(\frac{C_A}{\pi}\frac{\alpha_s}{N}\right)^4 + \left(\frac{146}{729} + \frac{14}{3}\zeta_3 + 2\zeta_5\right)\left(\frac{C_A}{\pi}\frac{\alpha_s}{N}\right)^5 + \dots \Bigg]\,. \end{aligned} \tag{4.70} $$

Substituting into eq. (4.40) one obtains

$$ \begin{aligned} D_{qg}\left(\frac{\alpha_s}{N}\right) &= \left(\frac{\alpha_s}{2\pi}\right) T_R \Bigg[\frac{1}{9} + \left(\frac{\alpha_s}{N}\right)\frac{C_A}{2\pi}\left(\frac{29}{27} + \frac{4\pi^2}{9}\right) \\ &+ \left(\frac{\alpha_s}{N}\right)^2 \left(\frac{C_A}{2\pi}\right)^2 \left(\frac{1069}{243} + \frac{44}{27}\pi^2 + \frac{16}{9}\zeta_3\right) \\ &+ \left(\frac{\alpha_s}{N}\right)^3 \left(\frac{C_A}{2\pi}\right)^3 \left(\frac{9031}{729} + \frac{340}{81}\pi^2 + \frac{14}{45}\pi^4 + \frac{584}{27}\zeta_3\right) + \dots \Bigg]\,. \end{aligned} \tag{4.71} $$

The coefficients of $\mathcal{O}(\alpha_s)$ and $\mathcal{O}\left(\alpha_s^2\right)$ are in agreement with the high energy limit of the fixed order NLO and NNLO computations [80]. This is a very non-trivial check of the procedure. The higher order coefficients are instead new results.

The high energy singularities of the quark-quark coefficient function are easily obtained thanks to the colour charge relation between D_{qq} and D_{qg} at high energy

$$D_{qq}\left(\frac{\alpha_s}{N}\right) - 1 - \mathcal{O}(\alpha_s) = \frac{C_F}{C_A}\left[D_{qg}\left(\frac{\alpha_s}{N}\right) - T_R\left(\frac{\alpha_s}{2\pi}\right)\frac{1}{9}\right] + \mathcal{O}\left(\alpha_s^2\left(\frac{\alpha_s}{N}\right)^k\right). \quad (4.72)$$

The explicit result is

$$\begin{aligned} D_{qq}\left(\frac{\alpha_s}{N}\right) - 1 - \mathcal{O}(\alpha_s) \;=\; & \frac{C_F}{C_A}\left(\frac{\alpha_s}{2\pi}\right) T_R\Bigg[\left(\frac{\alpha_s}{N}\right)\frac{C_A}{2\pi}\left(\frac{29}{27}+\frac{4\pi^2}{9}\right) \\ & + \left(\frac{\alpha_s}{N}\right)^2\left(\frac{C_A}{2\pi}\right)^2\left(\frac{1069}{243}+\frac{44}{27}\pi^2+\frac{16}{9}\zeta_3\right) \\ & + \left(\frac{\alpha_s}{N}\right)^3\left(\frac{C_A}{2\pi}\right)^3\left(\frac{9031}{729}+\frac{340}{81}\pi^2+\frac{14}{45}\pi^4+\frac{584}{27}\zeta_3\right) \\ & + \ldots\Bigg]. \end{aligned} \quad (4.73)$$

Again the $\mathcal{O}\left(\alpha_s^2\right)$ term is in agreement with the high energy limit of the fixed order NNLO computation, while the higher order contributions are new results.

4.2.4 Vector boson production

The hadroproduction of vector bosons, either $W^\pm$ or Z, is closely related to the one just discussed. The partonic cross section can be written as

$$\hat{\sigma}^V(\tau, m_V^2) = \hat{\sigma}_0^V(m_V^2)\sum_{i,j} D_{ij}(\tau, m_V^2), \quad V = W^\pm, Z, \quad (4.74)$$

where

$$\hat{\sigma}_0^V = \frac{\pi}{n_c}\sqrt{2}G_F m_V^2, \quad (4.75)$$

$G_F = \frac{1}{\sqrt{2}v^2}$ is the Fermi constant and $n_c = C_A$. The perturbative QCD corrections to vector boson production are the same as the Drell-Yan ones at NLO and they only differ at NNLO because of the diagram with an internal quark triangle, which contributes to the Z boson cross section but it vanishes in the case of a virtual photon or $W^\pm$. The high energy singularities are determined by the off-shell process

$$g^* + q(p) \quad \to \quad W^\pm/Z + q',$$

at $\mathcal{O}(\alpha_s)$; the triangle diagram does not contribute, being $\mathcal{O}\left(\alpha_s^2\right)$ hence the calculation is the same as the one previously described. The gauge bosons couple differently to the various quark flavours, but because there is only one electro-weak vertex for each diagram, such a contribution factorises in the squared matrix element and it results into an over all coefficient:

$$\mathcal{C}_{qq'} = \begin{cases} |V_{qq'}|^2 & \text{for} \quad W^{\pm}\,, \\ \left(v_q^2 + a_q^2\right)\delta_{qq'} & \text{for} \quad Z \end{cases} \tag{4.76}$$

where $V_{qq'}$ is the appropriate CKM matrix element and v_q, a_q denote the vector and axial couplings of the Z bosons to the different quark flavours.

Chapter 5

Higgs boson production via gluon-gluon fusion

In this chapter the inclusive production of a Higgs boson via gluon-gluon fusion is studied in k_T-factorisation. The different high energy limits of the cross section in the case of infinite and finite top mass are analysed in detail. A method to improve the coefficient function obtained in the heavy top limit is proposed.

5.1 Higgs boson at hadron colliders

It is well known that the electro-weak gauge symmetry of the Standard Model Lagrangian forbids explicit mass terms for any particle. Because the weak bosons and the fermions are massive, one should provide a mechanism that allows it. This can be achieved by spontaneous symmetry breaking, which in the Standard Model is realised by the Higgs mechanism. In this framework one introduces a complex scalar $SU(2)$ doublet ϕ, with a potential given by

$$\mathcal{V}(\phi^\dagger\phi) = \lambda(\phi^\dagger\phi)^2 - \mu^2(\phi^\dagger\phi)^4\,; \tag{5.1}$$

this potential has a circle of degenerate minima at

$$|\phi| = \frac{v}{\sqrt{2}} = \sqrt{\frac{\mu^2}{2\lambda}}\,. \tag{5.2}$$

The choice of any of the equivalent vacuum expectation values v breaks the gauge symmetry because it identifies a particular direction in the symmetry group space.

The introduction of a scalar doublet in the theory increases the number of degrees of freedom by four. Three of these provide the longitudinal polarisation for the massive $W^\pm$ and Z bosons; the one that remains, which is a neutral scalar, is a new fundamental

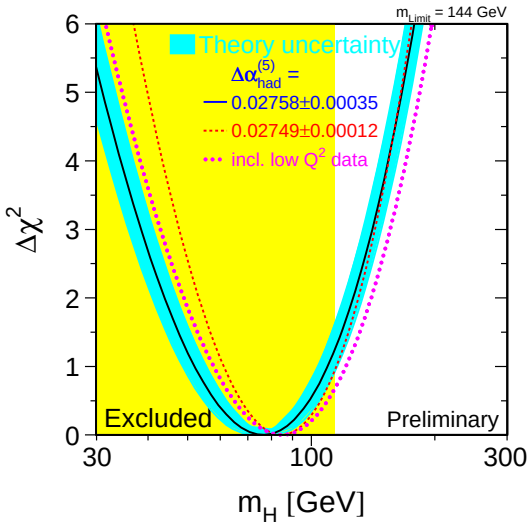

Figure 5.1: This plot shows the limits on the Higgs boson mass coming from electro-weak precision data (blue) and from direct search at LEP (yellow) [83].

particle of the spectrum, the renowned Higgs boson. Thus this mechanism not only gives a solution to the mass problem, but also it provides a way to test it, because it predicts the existence of a new particle. The search for the Higgs is one of the most exciting challenge in modern physics. So far no evidence of its existence has been found at present and past colliders such as Tevatron at Fermilab and LEP at CERN. However, fits to electro-weak precision data constrain the range of values for the Higgs mass [83]. Figure 5.1 shows the result of such fits together with the region excluded by direct searches; Standard Model fits prefer a fairly light Higgs boson, which can be observed at the LHC.

The theoretical and experimental effort which has been put into Higgs studies for LHC phenomenology is remarkable. In the following the attention will be focused on the inclusive Higgs production via gluon-gluon fusion, which is the dominant production channel at the LHC. Because the coupling of the Higgs to any particle is proportional to the mass of the particle itself, the top contribution overwhelms the ones coming from the other quark flavours. The inclusive hadronic cross section can be obtained by the

convolution of the partonic contribution with the parton distribution functions:

$$\begin{aligned}\sigma(\tau_h; y_t, m_H^2) &= \sum_{i,j} \int_{\tau_h}^1 \frac{dx_1}{x_1} \int_{\tau_h}^1 \frac{dx_2}{x_2} \hat{\sigma}_{ij}\left(\alpha_s; \frac{\tau_h}{x_1 x_2}; y_t, m_H^2\right) \\ &\times f_i\left(x_1, m_H^2\right) f_j\left(x_2, m_H^2\right) , \end{aligned} \tag{5.3}$$

where the dimensionless variables τ_h and y_t parametrise the hadronic centre-of-mass energy and the dependence on the top mass, respectively:

$$\tau_h = \frac{m_H^2}{s} , \tag{5.4}$$

$$y_t = \frac{m_t^2}{m_H^2} . \tag{5.5}$$

Even though beyond LO different initial partons contributes to the process, only the gluon channel will be considered in detail. As discussed in Chapter 3, the leading high energy contribution in the different channels can be easily derived from the gluon-gluon one as shown in eq. (3.37). It is convenient to define a dimensionless hard coefficient function $C(\alpha_s(m_H^2); \tau, y_t)$, factoring out the LO cross section σ_0

$$\hat{\sigma}_{gg}\left(\alpha_s; \tau; y_t, m_H^2\right) = \sigma_0(y_t) C(\alpha_s(m_H^2); \tau, y_t) \tag{5.6}$$

$$\begin{aligned} C(\alpha_s(m_H^2); \tau, y_t) &= \delta(1-\tau) + \tfrac{\alpha_s(m_H^2)}{\pi} C^{(1)}(\tau, y_t) \\ &+ \left(\tfrac{\alpha_s(m_H^2)}{\pi}\right)^2 C^{(2)}(\tau, y_t) + \mathcal{O}\left(\alpha_s^3\right) , \end{aligned} \tag{5.7}$$

where $\tau = \frac{\tau_h}{x_1 x_2}$ and hence $0 \leq \tau_h \leq \tau \leq 1$. The leading order cross section was determined long ago [84]:

$$\sigma_0(y_t) = \frac{\alpha_s^2 G_F \sqrt{2}}{256\pi} \left| 4 y_t \left(1 - \frac{1}{4}(1-4y_t) s_0^2(y_t)\right)\right|^2 , \tag{5.8}$$

where

$$s_0(y_t) = \begin{cases} \ln\left(\frac{1-\sqrt{1-4y_t}}{1+\sqrt{1-4y_t}}\right) + \pi\, i & \text{if} \quad y_t < \frac{1}{4} \\ 2\, i \tan^{-1}\left(\sqrt{\frac{1}{4y_t - 1}}\right) = 2\, i \sin^{-1}\left(\sqrt{\frac{1}{4y_t}}\right) & \text{if} \quad y_t \geq \frac{1}{4}. \end{cases} \tag{5.9}$$

Note that if $y_t < \frac{1}{4}$ the intermediate quark-antiquark pair can go on-shell.

The NLO corrections to this processes were computed some times ago [85], [86] and recently confirmed in [87]; they turned out to be very large, about $80\% - 100\%$ of the LO result. The bulk of these corrections comes from the radiation of soft gluons [88], which gives the leading contribution in the soft limit, where the partonic centre-of-mass energy $\hat{s}$ tends to the Higgs mass m_H^2 (or equivalently $\tau \to 1$). In the kinematic region covered by the LHC such regime dominates the hadronic cross section, after convolution with the parton distributions.

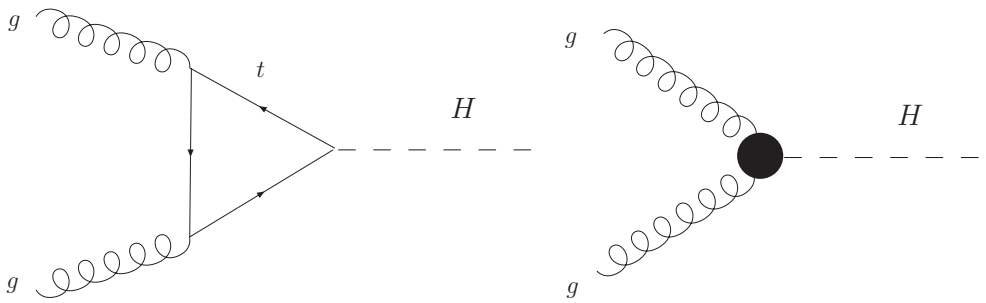

Figure 5.2: The leading order contribution to $gg \to H$ with finite m_t (on the left) and in the heavy top limit (on the right). When $m_t \to \infty$ the top triangle shrinks to a pointlike interaction.

The dominant soft contribution does not resolve the gluon-gluon-Higgs (ggH) coupling induced by the top loop. As a consequence, the QCD corrections can be evaluated quite accurately in the limit $m_t \to \infty$, where the calculation simplifies considerably because the ggH coupling becomes pointlike and the corresponding Feynman diagrams have one less loop. In the heavy top limit the interaction between the Higgs boson and the gluon can be described by an effective Lagrangian:

$$\mathcal{L}_{\text{eff}} = -\frac{\mathcal{W}}{4v} G^a_{\mu\nu} G_{a\mu\nu} H \,, \tag{5.10}$$

where $G^a_{\mu\nu}$ is the gluon strength tensor, H is the Higgs field and $\mathcal{W}$ is a Wilson coefficient, whose $\overline{\text{MS}}$ expression is [90]

$$\mathcal{W} = \frac{-1}{3\pi}\left\{1 + \frac{11}{4}\frac{\alpha_s}{\pi} + \left(\frac{\alpha_s}{\pi}\right)^2\left[\frac{2777}{288} - \frac{19}{16}\ln\frac{m_t^2}{\mu^2} - n_f\left(\frac{67}{96} + \frac{1}{3}\ln\frac{m_t^2}{\mu^2}\right)\right]\right\} . \tag{5.11}$$

In this approximation the NLO corrections were calculated in [89] and [91] and, more recently, the NNLO corrections have been computed by different groups [92]-[94]. The NNLO result appears to be perturbatively quite stable, and this stability is confirmed upon inclusion [95] of terms in the next few perturbative orders, that are logarithmically enhanced as $\tau \to 1$ and that can be determined [96] using soft-gluon resummation methods. This suggests that also at NNLO the large m_t approximation should provide a good approximation to the yet unknown exact result.

The infinite m_t approximation, which becomes exact in the soft limit, fails in the opposite (hard) limit of large partonic centre–of–mass energy $\hat{s} \to \infty$ or equivalently $\tau \to 0$. This is due to the fact that the ggH vertex is pointlike in the heavy top limit, whereas for finite m_t the quark loop provides a form factor, which softens the high energy behaviour. For instance one can compare the NLO contribution to the dimensionless coefficient function eq. (5.7) obtained in the heavy top limit [91] to the

one with finite m_t [86], namely:

$$\begin{aligned} C^{(1)}(\tau,\infty) &= (\pi^2+\frac{11}{2})\delta(1-\tau) - \tau P_{gg}(\tau)\ln\tau - \frac{11}{2}(1-\tau)^3 \\ &+ 12\left[\left(\frac{\ln(1-\tau)}{1-\tau}\right)_+ - \tau[2-\tau(1-\tau)]\ln(1-\tau)\right] \end{aligned} \tag{5.12}$$

and

$$\begin{aligned} C^{(1)}(\tau,y_t) &= (\pi^2+\omega(y_t))\delta(1-\tau) - \tau P_{gg}(\tau)\ln\tau + \mathcal{R}_{gg}(\tau,y_t) \\ &+ 12\left[\left(\frac{\ln(1-\tau)}{1-\tau}\right)_+ - \tau[2-\tau(1-\tau)]\ln(1-\tau)\right]. \end{aligned} \tag{5.13}$$

The second lines of each equation contain the terms which are logarithmically enhanced as $\tau \to 1$. They coincide because, as already stated, the heavy top approximation is exact in the soft limit. It is straightforward to compute the hard limit of eq. (5.12):

$$\lim_{\tau\to 0} C^{(1)}(\tau,\infty) = -2C_A\ln\tau - \frac{11}{2} + \mathcal{O}(\tau)\,. \tag{5.14}$$

More complicated is the calculation of $\tau \to 0$ limit of $\mathcal{R}_{gg}$ in eq. (5.13); it has not been possible to perform it analytically, but looking at the plot shown in figure 5.3 one can convince oneself that the logarithmic growth at small τ cancels and the high energy behaviour is given by

$$\lim_{\tau\to 0} C^{(1)}(\tau,y_t) = C_A\mathcal{C}(y_t) + \mathcal{O}(\tau)\,. \tag{5.15}$$

It was discussed in [44], and it will be explicitly shown in the following sections, that a pointlike interaction at k–th perturbative order has double energy logarithms, while in the resolved case only single logarithms appear. This means that as $\tau \to 0$ the hard coefficient function behaves as

$$C(\alpha_s;\tau,y_t) \underset{\tau\to 0}{\sim} \begin{cases} \sum_{k=1}^{\infty}\alpha_s^k \ln^{2k-1}\left(\frac{1}{\tau}\right) & \text{pointlike: } m_t\to\infty \\ \sum_{k=1}^{\infty}\alpha_s^k \ln^{k-1}\left(\frac{1}{\tau}\right) & \text{resolved: finite } m_t \end{cases} \tag{5.16}$$

Hence, as the centre-of-mass energy grows, eventually $m_t \to \infty$ ceases to be a good approximation to the exact result. Moreover the difference at high energy between the exact and approximate behaviour is stronger at higher orders, so one might expect the relative accuracy of the infinite m_t approximation to the k–th order perturbative contribution to the cross section to become worse as the perturbative order increases.

The computation of the high energy logarithms can be performed thanks to k_T-factorisation. It is then useful to consider Mellin moments of the perturbative

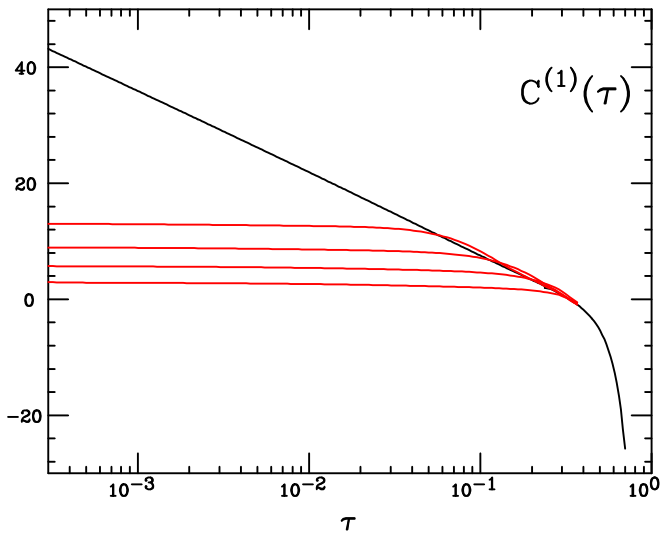

Figure 5.3: The NLO hard coefficient function plotted as a function of τ. The curves from top to bottom correspond to $m_t = \infty$ (black), and to $m_t = 170.9$ GeV (red), with $m_H = 130,\ 180,\ 230,\ 280$ GeV.

coefficient function eq. (5.7):

$$C(\alpha_s(m_H^2), N, y_t) = \int_0^1 d\tau \tau^{N-1} C(\alpha_s(m_H^2), \tau, y_t)\,, \tag{5.17}$$

$$C(\alpha_s(m_H^2), N, y_t) = 1 + \frac{\alpha_s(m_H^2)}{\pi} C^{(1)}(N, y_t) + \left(\frac{\alpha_s(m_H^2)}{\pi}\right)^2 C^{(2)}(N, y_t) + \mathcal{O}\left(\alpha_s^3\right)\,. \tag{5.18}$$

As usual the high energy, or small τ, limit corresponds to $N \to 0$ in Mellin space.

5.2 The $m_t \to \infty$ calculation in k_T-factorisation

In this section the leading high energy behaviour of the $gg \to H$ process is computed to all orders in perturbation theory, in the heavy top limit. In particular the origin of double high energy logarithms is investigated, proving the first line of eq. (5.16). This calculation was firstly performed in [97]; the result obtained in the following differs from the original one, but only for terms which are subleading in the high energy limit. The off-shell matrix element for this process was also computed in [98] but the result was not used to compute high energy corrections to the perturbative coefficient function.

As discussed in section 3.1, the leading logarithmic contribution can be computed

considering the LO process with off-shell gluons:

$$g^*(k_1) + g^*(k_2) \to H(p), \tag{5.19}$$

The kinematics of the process is described by

$$\begin{aligned} k_1 &= z_1 p_1 + \mathbf{k}_1, \\ k_2 &= z_2 p_2 + \mathbf{k}_2, \\ \hat{s} &= (k_1 + k_2)^2 = \nu - |\mathbf{k}_1 + \mathbf{k}_2|^2 , \end{aligned} \tag{5.20}$$

where p_1 and p_2 are, as usual, lightlike vector. The phase space integral is remarkably simple

$$\begin{aligned} d\Phi^{(1)} &= \int \frac{d^4p}{(2\pi)^3}(2\pi)^4\delta^{(4)}(k_1 + k_2 - p)\delta(p^2 - m_H^2) \\ &= \frac{2\pi}{m_H^2}\delta(\frac{1}{\tau} - 1 - \frac{|\mathbf{k}_1 + \mathbf{k}_2|^2}{m_H^2}) , \end{aligned} \tag{5.21}$$

where $\tau = m_H^2/\nu$. The Feynman amplitude obtained from the effective Lagrangian eq. (5.10) is

$$\mathcal{M}^{\mu\nu} = 4\left((k_1 \cdot k_2)g^{\mu\nu} - k_1^\nu k_2^\mu\right). \tag{5.22}$$

The Lorentz indices are contracted with eikonal polarisations eq. (3.6); the colour-averaged squared matrix element is

$$|\mathcal{M}|^2 = \frac{\alpha_s^2}{32}\frac{G_F\sqrt{2}}{9\pi^2}\frac{(\mathbf{k}_1 \cdot \mathbf{k}_2)^2}{|\mathbf{k}_1|^2|\mathbf{k}_2|^2}\nu^2 . \tag{5.23}$$

Thus, the reduced off-shell cross section becomes

$$\hat{\Sigma}_{gg}^{\text{off}} = \frac{\alpha_s^2 m_H^2 G_F\sqrt{2}}{288\pi}\frac{(\mathbf{k}_1 \cdot \mathbf{k}_2)^2}{|\mathbf{k}_1|^2|\mathbf{k}_2|^2}\frac{1}{\tau}\delta(\frac{1}{\tau} - 1 - \frac{(\mathbf{k}_1 + \mathbf{k}_2)^2}{m_H^2}). \tag{5.24}$$

The impact factor is defined by taking Mellin moments of the reduced cross section

$$\begin{aligned} h(N, M_1, M_2) &= M_1 M_2 \int \frac{d^2\mathbf{k}_1}{\pi|\mathbf{k}_1|^2}\left(\frac{|\mathbf{k}_1|^2}{m_H^2}\right)^{M_1} \int \frac{d^2\mathbf{k}_2}{\pi|\mathbf{k}_2|^2}\left(\frac{|\mathbf{k}_2|^2}{m_H^2}\right)^{M_2} \\ &\times \int_0^1 \frac{d\tau}{\tau}\tau^N \hat{\Sigma}_{gg}^{\text{off}} . \end{aligned} \tag{5.25}$$

The N Mellin transformation can be performed using the delta function; the result can

be expressed in terms of dimensionless variables:

$$\xi_i = \frac{|\mathbf{k}_i|^2}{m_H^2} \implies \frac{d^2\mathbf{k}_i}{\pi|\mathbf{k}_1|^2} = \frac{d\vartheta_i}{2\pi}\frac{d\xi_i}{\xi_i}\,, \quad i = 1, 2\,.$$

Thus eq. (5.25) becomes:

$$\begin{aligned} h(N, M_1, M_2) &= \frac{\alpha_s^2 m_H^2 G_F\sqrt{2}}{288\pi} M_1 M_2 \int_0^{+\infty} d\xi_1 (\xi_1)^{M_1-1} \int_0^{+\infty} d\xi_2 (\xi_2)^{M_2-1} \\ &\quad \frac{1}{(1+\xi_1+\xi_2)^N} \int_0^{2\pi} \frac{d\varphi}{2\pi} \frac{\cos^2\varphi}{(1+\sqrt{\alpha}\cos\varphi)^N}\,, \end{aligned} \tag{5.26}$$

where $\alpha = \frac{4\xi_1\xi_2}{(1+\xi_1+\xi_2)^2}$ and φ is the angle between the two transverse momenta, $\varphi = \vartheta_2 - \vartheta_1$. The angular integration can be expressed as the sum of two hypergeometric functions:

$$\begin{aligned} \int_0^{2\pi} \frac{d\varphi}{2\pi} \cos^2\varphi (1+\sqrt{\alpha}\cos\varphi)^{-N} &= \sum_{n=0}^{+\infty} \frac{(-N)!}{(-N-n)!}\frac{\alpha^{n/2}}{n!} \int_0^{2\pi} \frac{d\varphi}{2\pi} \cos^{2+n}\varphi \\ &= \sum_{k=0}^{+\infty} \frac{(-N)!}{(-N-2k)!}\frac{\alpha^k}{(2k)!}\frac{(2k+1)!!}{(2k+2)!!} \\ &= \frac{1}{2}\left[{}_2F_1\left(\frac{N}{2}, \frac{N+1}{2}, 2, \alpha\right) + \frac{\alpha}{4} N(N+1) {}_2F_1\left(\frac{N+2}{2}, \frac{N+3}{2}, 3, \alpha\right)\right]. \end{aligned} \tag{5.27}$$

In order to perform the M Mellin transforms, it is useful to change the variables of integration. Introducing

$$\begin{aligned} u &= \xi_1 + \xi_2\,, \\ t &= \frac{\xi_1}{\xi_1+\xi_2}\,. \end{aligned} \tag{5.28}$$

the impact factor can be expressed as

$$\begin{aligned} h(N, M_1, M_2) = \tfrac{\alpha_s^2 m_H^2 G_F\sqrt{2}}{576\pi} M_1 M_2 \int_0^{+\infty} du\, \tfrac{u^{M_1+M_2-1}}{(1+u)^N} \\ \int_0^1 dt\, t^{M_1-1}(1-t)^{M_2-1}\Bigg[{}_2F_1\left(\tfrac{N}{2}, \tfrac{N+1}{2}, 2, \tfrac{4u^2t(1-t)}{(1+u)^2}\right) + \\ N(N+1)\tfrac{u^2t(1-t)}{(1+u)^2} {}_2F_1\left(\tfrac{N+2}{2}, \tfrac{N+3}{2}, 3, \tfrac{4u^2t(1-t)}{(1+u)^2}\right)\Bigg]. \end{aligned} \tag{5.29}$$

The integration variables only enter the last argument of the hypergeometric functions,

which in turn have the same structure as the prefactor in the integrand. Thus, writing the series representation of the hypergeometric and swapping the integral and the summation, one can integrate the series term by term. The result can be written in terms of generalised hypergeometric functions:

$$\begin{aligned} h(N,M_1,M_2) &= \frac{\alpha_s^2 m_H^2 G_F\sqrt{2}}{576\pi}\Gamma(N-M_1-M_2)\Bigg[\tfrac{\Gamma(1+M_1)\Gamma(1+M_2)}{\Gamma(N)}\times \\ &\quad {}_4F_3\left(\left\{\tfrac{N}{2},\tfrac{N+1}{2},M_1,M_2,\right\},\left\{2,\tfrac{N}{2},\tfrac{N+1}{2}\right\};1\right)+ \\ &\quad N(N+1)M_1M_2\tfrac{\Gamma(1+M_1)\Gamma(1+M_2)}{\Gamma(N+2)}\times \\ &\quad {}_4F_3\left(\left\{\tfrac{N+2}{2},\tfrac{N+3}{2},1+M_1,1+M_2,\right\},\left\{3,\tfrac{N+2}{2},\tfrac{N+3}{2}\right\};1\right)\Bigg] \end{aligned} \tag{5.30}$$

This expression can be simplified and reduced to ratios of Euler Gamma functions thanks to the following identities:

$${}_4F_3(\{a,b,c,d\},\{a,b,e\};z) = {}_2F_1(c,d,e,z)\,, \tag{5.31}$$

$${}_2F_1(a,b,c,1) = \frac{\Gamma(c)\Gamma(c-a-b)}{\Gamma(c-a)\Gamma(c-b)}\,. \tag{5.32}$$

The impact factor can be expressed in a rather compact form:

$$\begin{aligned} h(N,M_1,M_2) &= \frac{\alpha_s^2 m_H^2 G_F\sqrt{2}}{576\pi}\frac{\Gamma(N-M_1-M_2)\Gamma(1+M_1)\Gamma(1+M_2)}{\Gamma(N)}\times \\ &\quad \frac{\Gamma(2-M_1-M_2)}{\Gamma(2-M_1)\Gamma(2-M_2)}\left[1+\frac{2M_1M_2}{1-M_1-M_2}\right]. \end{aligned} \tag{5.33}$$

A crucial point in the resummation of high energy logarithms discussed in Chapter 3 was the observation that all the singularities in $N=0$ and $M_i=0$ are factored into the parton densities, so that the impact factor has a finite radius of convergence in the neighbourhood of the origin. However, this is not the case in the process currently analysed; in particular the Mellin integral eq. (5.26) diverges for all M_1, M_2 when $N=0$, and it has only a finite radius of convergence when $N>0$. As a consequence eq. (5.33) has singularities in the (M_1,M_2) plane, whose location depends on the value of N:

$$\begin{aligned} h(N,M_1,M_2) &= \frac{\alpha_s^2 m_H^2 G_F\sqrt{2}}{576\pi}\frac{\Gamma(N-M_1-M_2)}{\Gamma(N)}\Big[1+\mathcal{O}\left(M_1,M_2\right)\Big] \\ &= \frac{\alpha_s^2 m_H^2 G_F\sqrt{2}}{576\pi}\frac{N}{N-M_1-M_2}+\ldots \end{aligned} \tag{5.34}$$

Thus the expansion in powers of M_1+M_2 converges for $M_1+M_2 < N$, resulting into an expansion if powers of $\frac{M_1+M_2}{N}$. The leading high energy singularities are found setting $M_1 = M_2 = \gamma(\alpha_s, N)$, with $\gamma(\alpha_s, N) \simeq \frac{\alpha_s C_A}{\pi N}$

$$\begin{aligned} h(N, M_1, M_2) &= \frac{\alpha_s^2 m_H^2 G_F \sqrt{2}}{576\pi} \left[1 + \frac{M_1+M_2}{N} + \left(\frac{M_1+M_2}{N} \right)^2 + \dots \right] \\ &= \frac{\alpha_s^2 m_H^2 G_F \sqrt{2}}{576\pi} \left[1 + \frac{\alpha_s}{\pi} \frac{2C_A}{N^2} + \left(\frac{\alpha_s}{\pi} \right)^2 \left(\frac{2C_A}{N^2} \right)^2 + \dots \right], \end{aligned} \tag{5.35}$$

which exhibits double N poles at every perturbative order. The Mellin inversion of this result is readily computed by noticing that

$$\mathbb{M}^{-1} \left[\frac{1}{N^p} \right] = \frac{1}{(p-1)!} \ln^{p-1} \frac{1}{\tau}, \quad p \geq 1. \tag{5.36}$$

For instance the leading high energy behaviours of the NLO and NNLO coefficient functions are

$$\begin{aligned} \lim_{\tau \to 0} C^{(1)}(\tau, \infty) &= -6 \ln \tau + \mathcal{O}(\tau^0), \\ \lim_{\tau \to 0} C^{(2)}(\tau, \infty) &= -6 \ln^3 \tau + \mathcal{O}(\ln^2 \tau), \end{aligned} \tag{5.37}$$

in agreement with the high energy limit of the fixed order calculations.

5.3 The finite top mass case

In this section the calculation of the leading high energy singularity of the coefficient function is performed keeping the full top mass dependence. The results of this computation have been published in [102].

5.3.1 The off-shell cross section

The LO amplitude for the production of a Higgs boson from two off-shell gluons, through a top loop is equal to

$$\begin{aligned} \mathcal{M}_{ab}^{\mu\nu} &= 4i\,\delta^{ab} \frac{g_s^2 m_t^2}{v} \left[\frac{k_2^\mu k_1^\nu}{m_H^2} A_1(\xi_1, \xi_2; y_t) - g^{\mu\nu} A_2(\xi_1, \xi_2; y_t) \right. \\ &\quad + \left(\frac{k_1 \cdot k_2}{m_H^2} A_1(\xi_1, \xi_2; y_t) - A_2(\xi_1, \xi_2; y_t) \right) \\ &\quad \left. \frac{k_1 \cdot k_2 k_1^\mu k_2^\nu - k_1^2 k_2^\mu k_2^\nu - k_2^2 k_1^\mu k_1^\nu}{k_1^2 k_2^2} \right], \end{aligned} \tag{5.38}$$

where a, b are the colour indices and the dimensionless kinematical variables are the same as in the previous section. The dimensionless form factors $A_1(\xi_1, \xi_2; y_t)$ and $A_2(\xi_1, \xi_2; y_t)$ have been computed in [99] and subsequently re-derived in [100], where an expression for the Higgs production cross section from the fusion of two off-shell gluons was also determined; there it was used in a numerical study and not to obtain high energy corrections to perturbative coefficient function. Explicit expressions for form factors in eq. (5.38) are collected in Appendix B. The spin- and colour-averaged dimensionless cross section is

$$\begin{aligned}\hat{\Sigma}^{\rm off}_{gg}(\tau, \xi_1, \xi_2, \varphi) &= 8\sqrt{2}\pi^3\alpha_s^2 G_F m_H^2 \frac{y_t^2}{\xi_1\xi_2}\left|\frac{1}{2\tau}A_1 - A_2\right|^2 \\ &\quad \delta\left(\frac{1}{\tau} - 1 - \xi_1 - \xi_2 - \sqrt{\xi_1\xi_2}\cos\varphi\right). \end{aligned} \tag{5.39}$$

As in the infinite top mass case the delta function is used to perform the N Mellin transformation. Because the form factors A_i are independent of φ, all the angular integrals can be performed in terms of hypergeometric functions, with the result

$$\begin{aligned}&\hat{\Sigma}^{\rm off}_{gg}(N, \xi_1, \xi_2) = 8\sqrt{2}\pi^3\alpha_s^2 G_F m_H^2 y_t^2 \frac{1}{(1+\xi_1+\xi_2)^N} \\ &\left\{\frac{|A_1|^2}{2}\Big({}_2F_1(\frac{N}{2}, \frac{N+1}{2}, 2, \alpha) + \frac{\alpha}{4}N(N+1){}_2F_1(\frac{N+2}{2}, \frac{N+3}{2}, 3, \alpha)\Big)\right. \\ &\qquad +\xi_1\xi_2|A_3|^2{}_2F_1(\frac{N}{2}, \frac{N+1}{2}, 1, \alpha) - N\Big[|A_1|^2(1+\xi_1+\xi_2) \\ &\qquad \left.-(A_1^* A_2 + A_1 A_2^*)\Big]\frac{1}{1+\xi_1+\xi_2}{}_2F_1(\frac{N+1}{2}, \frac{N+2}{2}, 2, \alpha)\right\}. \end{aligned} \tag{5.40}$$

where α is the same as in eq. (5.26), and the new impact factor A_3 is defined as:

$$A_3(\xi_1, \xi_2, y_t) \equiv \frac{1}{\xi_1\xi_2}\left[\frac{1+\xi_1+\xi_2}{2}A_1 - A_2\right]. \tag{5.41}$$

The $m_t \to \infty$ of the form factors can be computed using eq. (B.9)

$$\begin{aligned}\lim_{m_t\to\infty} m_t^2 A_1 &= m_H^2 \frac{1}{48\pi^2}, \\ \lim_{m_t\to\infty} 4m_t^2 A_2 &= m_H^2 \frac{1}{48\pi^2}\frac{1+\xi_1+\xi_2}{2}, \\ \lim_{m_t\to\infty} m_t^2 A_3 &= 0. \end{aligned} \tag{5.42}$$

Thus the last two lines of eq. (5.40) vanish in the heavy top limit and the remaining terms, proportional to $|A_1|^2$, give the result in the pointlike limit.

The spurious high energy growth in the pointlike approximation is due to the fact that the Mellin integral eq. (5.26) had an N-dependent radius of convergence, vanishing for $N = 0$. In order to prove that the result obtained with finite m_t has the correct high energy behaviour, one should study the radius of convergence of the integral:

$$h(0, M_1, M_2) = 8\sqrt{2}\pi^3 \alpha_s^2 G_F m_H^2 y_t^2 \times M_1 M_2 \int_0^{+\infty} d\xi_1 \xi_1^{M_1-1} \int_0^{+\infty} d\xi_2 \xi_2^{M_2-1} \left[\frac{1}{2}|A_1|^2 + \xi_1\xi_2|A_3|^2 \right] . \tag{5.43}$$

The analytic computation of the full impact factor is hampered by the complicated structure of the scalar integrals B_0 and C_0 eq. (B.4), (B.5). However, their expressions greatly simplify in particular limits; for instance the form factors are regular for ξ_1, $\xi_2 \to 0$. Furthermore defining

$$C_0 = \frac{\bar{C}_0(\xi_1, \xi_2, y_t)}{\sqrt{\Delta_3}} , \tag{5.44}$$

one can notice that the functions $\bar{C}_0$ and B_0 are complicated combination of logarithms and dilogarithms [101], which in the limit of large virtualities behave at most as powers of logarithms. Because logarithmic factors in the integrand cannot change the position of the poles of its Mellin transformed, one can study the Mellin transform of the rational factors and look for the singularities in the (M_1, M_2) plane. The position of these singularities determines the radius of convergence of the integral. If the logarithmic dependence is ignored the structure of the integrals that one has to compute is similar to the one found in the heavy top case, but with an extra factor in the denominator, which softens the behaviour at large virtualities:

$$\int_0^{+\infty} d\xi_1 (\xi_1)^{M_1-1} \int_0^{+\infty} d\xi_2 (\xi_2)^{M_2-1} \frac{1}{(1+\xi_1+\xi_2)^N} \frac{1}{\Delta_3^p} = \frac{\Gamma(M_1)\Gamma(M_2)\Gamma(N-M_1-M_2+2p)}{\Gamma(N+2p)} {}_3F_2(\{p, M_1, M_2\}, \left\{ \tfrac{N+2p}{2}, \tfrac{N+1+2p}{2} \right\}; 1) , \tag{5.45}$$

where

$$\Delta_3 = 1 + \xi_1^2 + \xi_2^2 - 2\xi_1\xi_2 + 2(\xi_1 + \xi_2) = (1 + \xi_1 + \xi_2)^2 - 4\xi_1\xi_2 . \tag{5.46}$$

One can use Thomae's theorem [82] to rearrange the hypergeometric function in eq. (5.45) in a more instructive way; setting $N = 0$ wherever is safe, one can rewrite the r.h.s. of eq. (5.45) as

$$\frac{\Gamma(M_1)\Gamma(M_2)\Gamma(\frac{2p+1}{2})\Gamma(N+2p-M_1-M_2)\Gamma(N+p+\frac{1}{2}-M_1-M_2)}{\Gamma(2p)\Gamma(p+\frac{1}{2}-M_1)\Gamma(p+\frac{1}{2}-M_2)} . \tag{5.47}$$

The form factor $|A_1|^2$ contains, for instance, a contribution like $\frac{(\xi_1\xi_2)^2}{\Delta_3^2}$, which upon Mellin transform becomes

$$\int_0^{+\infty} d\xi_1 (\xi_1)^{M_1-1} \int_0^{+\infty} d\xi_2 (\xi_2)^{M_2-1} \frac{(\xi_1\xi_2)^2}{\Delta_3^3} \propto \Gamma(N+2-M_1-M_2)\Gamma(N-\frac{1}{2}-M_1-M_2)\,. \tag{5.48}$$

The first Gamma function in eq. (5.48) is safe but not the second one, because when $N=0$, the line of singularities is at $M_1+M_2=-\frac{1}{2}$ and hence the radius of convergence is zero. The origin of this problem can be traced down to the behaviour of the integrand along $\xi_1=\xi_2=\xi$. In this direction because of a cancellation, the denominator eq. (5.46) is linear in ξ, rather than quadratic:

$$\Delta_3\Big|_{\xi_1=\xi_2=\xi} = 1+4\xi\,; \tag{5.49}$$

if one sets $M_1=M_2=0$, then the integral in eq. (5.48) is ultra-violet divergent. In order to prove that there are no double logarithms, one has to show that all these problematic contributions cancel out and the integrand is well behaved at large virtualities. In particular when $\xi_1\to\infty$, $\xi_2\to\infty$ with $\xi_1\neq\xi_2$ one has

$$\begin{aligned}
\lim_{\xi_1\to\infty,\,\xi_2\to\infty} A_1(\xi_1,\xi_2,y_t) &= 0\,,\\
\lim_{\xi_1\to\infty,\,\xi_2\to\infty} A_3(\xi_1,\xi_2,y_t) &= 0\,,\\
\lim_{\xi_1\to\infty,\,\xi_2\to\infty} A_2(\xi_1,\xi_2,y_t) &= \frac{1}{(4\pi)^2}\,.
\end{aligned} \tag{5.50}$$

If $\xi_1\to\infty$, $\xi_2\to\infty$ with $\xi_1=\xi_2$ the limit is more subtle. For instance, in the case of A_1 one obtains

$$\begin{aligned}
\lim_{\xi\to\infty} A_1(\xi,\xi,y_t) &= \lim_{\xi\to\infty} \frac{\bar{C}_0(\xi,\xi,y_t)}{4}\sqrt{\xi}\\
&\quad -\frac{1}{16\pi^2}\left[\frac{1}{2}\ln\frac{y_t}{\xi}-1+\sqrt{4y_t-1}\tan^{-1}\sqrt{\frac{1}{4y_t-1}}\right]\\
&\quad +O\left(\frac{1}{\sqrt{\xi}}\right).
\end{aligned} \tag{5.51}$$

However, it turns out that

$$\begin{aligned}
\lim_{\xi\to\infty} \bar{C}_0(\xi,\xi,y_t) &= \frac{1}{16\pi^2\sqrt{\xi}}\left[2\ln\frac{y_t}{\xi}-4+4\sqrt{4y_t-1}\tan^{-1}\sqrt{\frac{1}{4y_t-1}}\right]\\
&\quad +O\left(\frac{1}{\xi}\right),
\end{aligned} \tag{5.52}$$

similar relations hold for the other form factors. Hence eq. (5.50) holds also when $\xi_1 = \xi_2$. These conditions ensure that one can safely set $N = 0$ in the computation of the impact factor and the Mellin integrals in eq. (5.43) have finite radius of convergence. Therefore the coefficient function contains only single high energy logarithms to all orders in perturbation theory.

5.3.2 The high energy behaviour

The impact factor eq. (5.43) resums the high energy logarithms to all orders, once the identification $M_i = \gamma_s$ has been made. On the other hand one can take this result, expand it in powers of the strong coupling and determine the leading high energy behaviour of the coefficient function order by order in perturbation theory. Because of the complexity of the scalar integrals which appear in the form factors, one cannot perform the Mellin transformations analytically. Alternatively, one can first Taylor expand eq. (5.43) in powers of M_i and then compute the coefficients numerically. Because powers of M_i correspond to powers of the strong coupling, this method provides the leading high energy behaviour of the coefficient function to any desired order in α_s.

The first term in the expansion $h(0,0,0)$ is determined by the on-shell limit of the form factor A_1

$$\begin{aligned} h(0,0,0) &= 8\sqrt{2}\pi^3\alpha_s^2 G_F m_H^2 y_t^2 \left[\frac{1}{2}|A_1|^2 + \xi_1\xi_2|A_3|^2\right]_{\xi_1=\xi_2=0} \\ &= 8\sqrt{2}\pi^3\alpha_s^2 G_F m_H^2 y_t^2 \frac{1}{2}|A_1(0,0)|^2\,; \end{aligned} \tag{5.53}$$

using the on-shell limit of the scalar integrals eq. (B.11), one obtains

$$A_1(0,0) = \frac{1}{8\pi^2} + \frac{1}{32\pi^2}\left(\ln^2\frac{-z_-}{z_+}\right)(4y_t - 1)\,. \tag{5.54}$$

Substituting this expression into eq. (5.53) one recovers the leading order cross section eq. (5.8):

$$h(0,0,0) = m_H^2\sigma_0\,. \tag{5.55}$$

In order to be consistent with the definition of the coefficient function in eq. (5.6), the LO contribution is factored out from the Taylor expansion of the impact factor:

$$\begin{aligned} &h(0,M_1,M_2) = \\ &\quad \sigma_0 m_H^2\left[1 + s_1^2(M_1+M_2) + s_2^2(M_1^2+M_2^2) + s_{1,1}^2 M_1 M_2 + \dots\right], \end{aligned} \tag{5.56}$$

where the coefficients are

$$s_k^2(y_t) = \frac{(8\pi^2)^2}{\left|\left(1-\frac{1}{4}(1-4y_t)s_0(y_t)^2\right)\right|^2}\int_0^{+\infty} d\xi \frac{\ln^k \xi}{k!}\left(-\frac{d|A_1(\xi,0)|^2}{d\xi}\right), \tag{5.57}$$

$$\begin{aligned} s_{1,1}^2(y_t) = {} & \frac{(8\pi^2)^2}{\left|\left(1-\frac{1}{4}(1-4y_t)s_0(y_t)^2\right)\right|^2}\int_0^{+\infty} d\xi_1 \int_0^{+\infty} d\xi_2 \\ & \left[\ln\xi_1 \ln\xi_2 \frac{\partial^2|A_1(\xi_1,\xi_2)|^2}{\partial\xi_1\partial\xi_2} + 2|A_3(\xi_1,\xi_2)|^2 \right]. \end{aligned} \tag{5.58}$$

A rather compact expression for the form factor with one on-shell gluon can be derived:

$$\begin{aligned} A_1(\xi,0) = {} & \frac{1}{32\pi^2}\frac{1}{(1+\xi)^2}\left\{(4y_t-1-\xi)\left(s_0(y_t)^2 - \ln^2\left(-\frac{1-\beta}{1+\beta}\right)\right)\right. \\ & \left. + \; 4\xi\left(i\sqrt{4y_t-1}\, s_0(y_t) + \beta\ln\left(-\frac{1-\beta}{1+\beta}\right)\right) + 4(1+\xi)\right\}, \end{aligned} \tag{5.59}$$

with $\beta = \sqrt{1+\frac{4y_t}{\xi}}$. The $N \to 0$ limit of the NLO coefficient function is obtained from the $\mathcal{O}(M_i)$ terms in eq. (5.56), after the identification of M_1 and M_2 with the anomalous dimension. One obtains:

$$\begin{aligned} C^{(1)}(N,y_t) &= \mathcal{C}^{(1)}(y_t)\frac{C_A}{N}\left[1+O(N)\right], \\ \mathcal{C}^{(1)}(y_t) &= 2\, s_1^2(y_t). \end{aligned} \tag{5.60}$$

The value of the coefficient $\mathcal{C}^{(1)}$ is determined from a numerical evaluation of the integral in eq. (5.57) with $k=1$, using the `Fortran` routine `DGAUSS`. The result is tabulated in the second column of table 5.1, for different values of the Higgs mass. Upon inverse Mellin transformation, one finds that

$$\lim_{\tau\to 0} C^{(1)}(\tau,y_t) = C_A \mathcal{C}^{(1)}(y_t). \tag{5.61}$$

The values of the coefficient are indeed found to be in perfect agreement with a numerical evaluation of the small τ limit of the full NLO coefficient function $C^{(1)}(\tau,y_t)$ eq. (5.13); this is a very non-trivial test of the computation.

The determination of the hitherto unknown NNLO leading singularity proceeds in a very similar way. At this order the Mellin transformed of the coefficient function behaves like

$$C^{(2)}(N,y_t) = \mathcal{C}^{(2)}(y_t)\frac{C_A^2}{N^2}\left[1+O(N)\right]; \tag{5.62}$$

m_H	$\mathcal{C}_1$	$\mathcal{C}_2$	$\mathcal{C}_3$	$\mathcal{C}_4$
110	5.0447	16.2570	38.4552	79.6844
120	4.6873	14.5133	32.8727	66.6218
130	4.3568	13.0155	28.2489	56.2102
140	4.0490	11.7196	24.3760	47.8068
150	3.7607	10.5919	21.0998	40.9517
160	3.4890	9.6058	18.3040	35.3079
170	3.2318	8.7406	15.8989	30.6251
180	2.9872	7.9794	13.8145	26.7138
190	2.7536	7.3085	11.9953	23.4288
200	2.5297	6.7166	10.3969	20.6571
210	2.3140	6.1946	8.9833	18.3108
220	2.1057	5.7346	7.7247	16.3197
230	1.9037	5.3303	6.5965	14.6285
240	1.7072	4.9761	5.5780	13.1921
250	1.5151	4.6677	4.6517	11.9753
260	1.3267	4.4012	3.8021	10.9492
270	1.1409	4.1738	3.0159	10.0907
280	0.9568	3.9828	2.2807	9.3818
290	0.7731	3.8269	1.5849	8.8095
300	0.5884	3.7049	0.9168	8.3643
310	0.4006	3.6171	0.2631	8.0421
320	0.2063	3.5655	-0.3928	7.8457
330	-0.0008	3.5556	-1.0783	7.7914
340	-0.2400	3.6074	-1.8669	7.9446
350	-0.5321	3.7511	-2.8444	8.4097
360	-0.7258	3.8390	-3.4840	8.6865

Table 5.1: Numerical results for the coefficients $\mathcal{C}^{(i)}$

the coefficient is given by the sum of two terms:

$$\mathcal{C}^{(2)}(N, y_t) = 2\, s_2^2(y_t) + s_{1,1}^2(y_t)\,. \tag{5.63}$$

The first term is given by a numerical evaluation of the integral in eq. (5.57) with $k = 2$ using the `Fortran` routine `DGAUSS`; the second term comes from the two-dimensional integral in eq. (5.58), which has been computed with the `Fortran` routine `DGMLT` (from `CERNLIB`). The results are shown in the third column of table 5.1. Upon Mellin inversion, one finds that the behaviour of the NNLO coefficient function at small τ is logarithmic

$$\lim_{\tau\to 0} C^{(2)}(\tau, y_t) = -C_A^2 \mathcal{C}^{(2)}(y_t) \ln\tau + \mathcal{O}(\tau^0)\,, \tag{5.64}$$

while in the heavy top case it exhibits a spurious $\ln^3\tau$ growth as in eq. (5.37).

The computation of higher-order terms in the expansion of the impact factor in

powers of M_i is a straightforward generalisation of the procedure just described.

$$h = \sigma_0 m_H^2 \left[1 + \left(\frac{\alpha_s}{\pi} \frac{C_A}{N} \right) \mathcal{C}^{(1)} + \left(\frac{\alpha_s}{\pi} \frac{C_A}{N} \right)^2 \mathcal{C}^{(2)} + \left(\frac{\alpha_s}{\pi} \frac{C_A}{N} \right)^3 \mathcal{C}^{(3)} + \left(\frac{\alpha_s}{\pi} \frac{C_A}{N} \right)^4 \mathcal{C}^{(4)} + O\left(\alpha_s^5\right) \right]. \tag{5.65}$$

The new coefficients are:

$$\begin{aligned} \mathcal{C}^{(3)} &= \frac{2s_3^2 + 2s_{1,2}^2}{\left|\left(1 - \frac{1}{4}(1-4y_t)s_0(y_t)^2\right)\right|^2}, \\ \mathcal{C}^{(4)} &= \frac{2s_4^2 + s_{2,2}^2 + 2s_{1,4}^2}{\left|\left(1 - \frac{1}{4}(1-4y_t)s_0(y_t)^2\right)\right|^2}, \end{aligned} \tag{5.66}$$

where s_k^2 is defined as in eq. (5.57) and $s_{i,j}^2$ are the numerical results of the following integrals:

$$s_{1,2}(y_t)^2 = (8\pi^2)^2 \int_0^{+\infty} d\xi_1 \int_0^{+\infty} d\xi_2 \left[\frac{1}{2} \ln^2 \xi_1 \ln \xi_2 \frac{\partial^2 |A_1(\xi_1,\xi_2)|^2}{\partial\xi_1 \partial\xi_2} + 2 \ln \xi_1 |A_3(\xi_1,\xi_2)|^2 \right], \tag{5.67}$$

$$s_{2,2}(y_t)^2 = (8\pi^2)^2 \int_0^{+\infty} d\xi_1 \int_0^{+\infty} d\xi_2 \left[\frac{1}{4} \ln^2 \xi_1 \ln^2 \xi_2 \frac{\partial^2 |A_1(\xi_1,\xi_2)|^2}{\partial\xi_1 \partial\xi_2} + 2 \ln \xi_1 \ln \xi_2 |A_3(\xi_1,\xi_2)|^2 \right], \tag{5.68}$$

$$s_{1,3}(y_t)^2 = (8\pi^2)^2 \int_0^{+\infty} d\xi_1 \int_0^{+\infty} d\xi_2 \left[\frac{1}{6} \ln^3 \xi_1 \ln \xi_2 \frac{\partial^2 |A_1(\xi_1,\xi_2)|^2}{\partial\xi_1 \partial\xi_2} + \ln^2 \xi_1 |A_3(\xi_1,\xi_2)|^2 \right]. \tag{5.69}$$

Explicit results are collected in table 5.1.

5.4 Improvement of the NNLO coefficient function

The knowledge of the leading small τ behaviour of the exact coefficient function $C(\alpha_s;\tau,y_t)$ can be used to improve its determination. This is particularly interesting at NNLO, where the fixed order computation has been performed only in the heavy top limit, so it is affected by the wrong high energy behaviour. More specifically, having determined the exact small τ limit, one can improve the approximate pointlike determination of the coefficient function by subtracting its spurious small τ growth and replacing it with the exact behaviour.

The NLO is known both for infinite and finite m_t, so it can be used as a testing ground. In the pointlike approximation, the high energy behaviour is dominated by a double pole in N, whereas it is given by the simple pole eq. (5.60) in the exact case. As already discussed, this corresponds to a NLO contribution which grows logarithmically at small τ in the heavy top case, and which tends to a constant when the top mass is kept finite:

$$C^{(1)}(\tau,\infty) = d^{(1)}_{\rm point}(\tau) + O(\tau)\,; \quad d^{(1)}_{\rm point}(\tau) = c^1{}_2 \ln\tau + c^1{}_1 \tag{5.70}$$

$$C^{(1)}(\tau,y_t) = d^{(1)}_{\rm ex}(\tau,y_t) + O(\tau)\,; \quad d^{(1)}_{\rm ex}(\tau,y_t) = 3\mathcal{C}^{(1)}(y_t)\,, \tag{5.71}$$

where

$$c^1{}_2 = -6; \quad c^1{}_1 = -\frac{11}{2}. \tag{5.72}$$

The NLO term $C^{(1)}(\tau,y_t)$ has already been plotted in fig. 5.3, both in the pointlike approximation, and in its exact form, computed for increasing values of the Higgs mass, i.e. decreasing values of y_t. It is clear from that plot that the pointlike approximation is very accurate, up to the point where the spurious logarithmic growth eq. (5.70) sets in. Therefore, one can construct an approximation to $C^{(1)}(\tau,y_t)$ by combining the pointlike curve with the exact small τ behaviour:

$$C^{(1),\rm app.}(\tau,y_t) = C^{(1)}(\tau,\infty) + \left[d^{(1)}_{\rm ex}(\tau,y_t) - d^{(1)}_{\rm point}(\tau)\right] T(\tau,\tau_0)\,, \tag{5.73}$$

where $d^{(1)}_{\rm point}(\tau)$ and $d^{(1)}_{\rm ex}(\tau,y_t)$ are defined as in eq. (5.70) and eq. (5.71) respectively, while $T(\tau,\tau_0)$ is a matching function, which may be introduced in order to tune the point τ_0 where the small τ behaviour given by $d^{(1)}_{\rm ex}(\tau,y_t)$ sets in. As $\tau\to 0$ the approximation eq. (5.73) reproduces the small τ behaviour of the exact coefficient function eq. (5.71), provided only that the interpolating function satisfies

$$\lim_{\tau\to 0} T(\tau,\tau_0) = 1\,,$$

Furthermore, the pointlike approximation is exact for $\tau\to 1$ because the behaviour of

the coefficient function in such a limit is to all orders controlled by soft logarithms, which do not depend on y_t. Because the functions $d^{(1)}_{\rm ex}(\tau, y_t)$ and $d^{(1)}_{\rm point}(\tau)$ are regular as $\tau \to 1$, the exact soft behaviour is also reproduced by the approximation eq. (5.73), provided only $\lim_{\tau\to 1} T(\tau, \tau_0)$ is finite. In the following the function $T(\tau, \tau_0)$ is chosen in such a way that $T(1, \tau_0) = 0$, so that $C^{(1)}(\tau, y_t)$ agrees with the pointlike approximation $C^{(1)}(\tau, \infty)$ in a neighbourhood of $\tau = 1$. For instance, fig. 5.3 suggests to choose

$$T(\tau, \tau_0) = \Theta(\tau_0 - \tau)\,, \tag{5.74}$$

where $\Theta(\tau)$ is the Heaviside function, so that $C^{(1),\rm app.}(\tau, y_t)$ only differs from the pointlike approximation when $\tau < \tau_0$. The plot in fig. 5.3 suggests to choose, for each y_t, the matching point τ_0 as the value of τ where the pointlike approximation equals the exact asymptotic small τ constant. However, the choice of the matching function eq. (5.74) leads to a form of $C^{(1),\rm app.}(\tau, y_t)$ whose first derivative is discontinuous at $\tau = \tau_0$. A smoother behaviour can be obtained using instead an hyperbolic tangent as matching function

$$T(\tau, \tau_0) = \frac{1}{2}\left[1 + \tanh\left(\frac{\tau_0 - \tau}{w}\right)\right]. \tag{5.75}$$

In fig. 5.4 and 5.5 the approximate NLO term eq. (5.73) is compared to the exact and pointlike results, for two different values of the Higgs mass, namely $m_H = 130, 280$ GeV. The values of the matching points are found to be $\tau_0 = 0.057$ and $\tau_0 = 0.315$, respectively. The approximate NLO coefficient function is very close to the exact one in the all region $0 < \tau < 1$.

At NNLO, the pointlike approximation to the coefficient function exhibits a $\ln^3 \tau$ growth, while the exact result only rises linearly with $\ln \tau$:

$$\begin{aligned} C^{(2)}(\tau, \infty) &= d^{(2)}_{\rm point}(\tau) + O(\tau)\,, \\ d^{(2)}_{\rm point}(\tau) &= c^2{}_4 \ln^3 \tau + c^2{}_3 \ln^2 \tau + c^2{}_2 \ln \tau + c^2{}_1 \qquad (5.76) \\ C^{(2)}(\tau, y_t) &= d^{(2)}_{\rm ex}(\tau, y_t) + O(\tau)\,, \\ d^{(2)}_{\rm ex}(\tau, y_t) &= -9\,\mathcal{C}^{(2)}(y_t) \ln \tau + \mathcal{C}^{(2)}_0(y_t), \qquad (5.77) \end{aligned}$$

where from Ref. [92] one gets

$$\begin{aligned} c^2{}_4 &= -6\,, \quad c^2{}_3 = -\frac{231}{4} + n_f \frac{17}{18}\,, \\ c^2{}_2 &= \left(-\frac{2333}{8} + 3\pi^2\right) + n_f \frac{641}{108}\,, \\ c^2{}_1 &= \frac{27\zeta_3 + 15\pi^2}{2} - \frac{6591}{16} + n_f\left(\frac{14939}{1296} - \frac{17}{54}\pi^2 - \frac{\zeta_3}{3}\right). \end{aligned} \tag{5.78}$$

Analogously to the NLO case, one can construct an approximation to the unknown

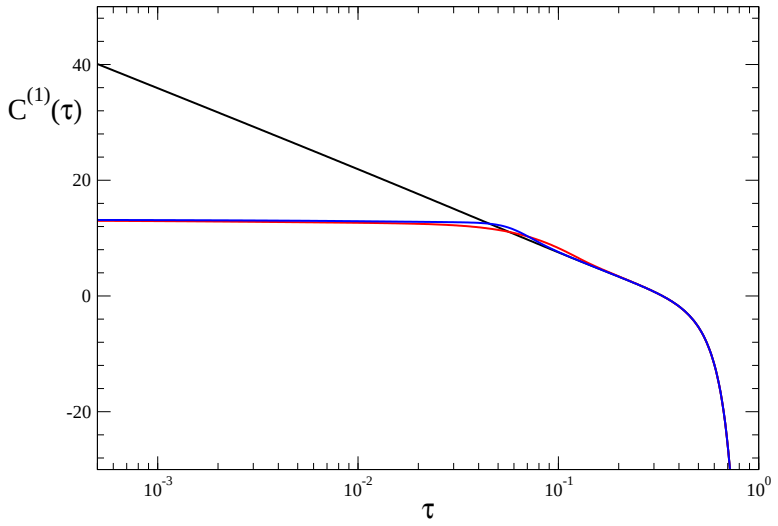

Figure 5.4: The hard coefficient function $C^{(1)}(\tau, y_t)$ with $m_H = 130$ GeV. The black curve corresponds to $m_t = \infty$ and the red one to the exact case with $m_t = 170.9$ GeV (same as fig. 5.3). The blue curve corresponds to the approximation eq. (5.73), with interpolating function as in (5.75), $\tau_0 = 0.057$ and $w = 1/50$.

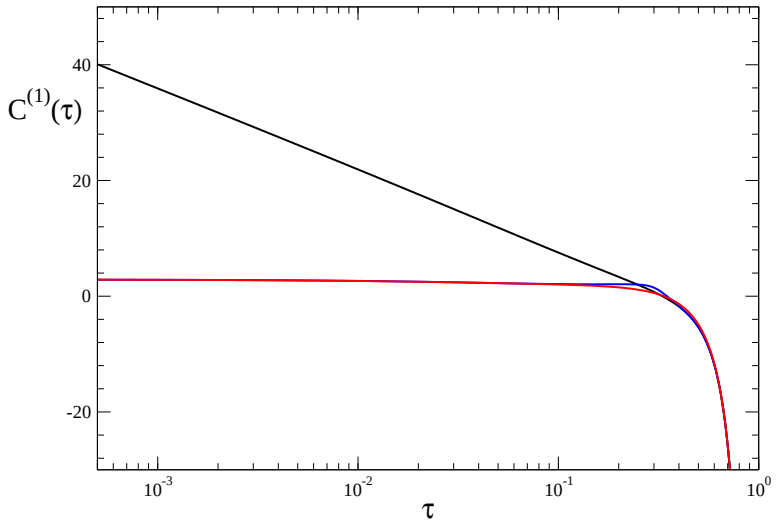

Figure 5.5: Same as fig. 5.4 for $m_H = 130$ GeV. In this case $\tau_0 = 0.315$ and $w = 1/20$.

coefficient function using the pointlike limit, combined with the exact small τ behaviour eq. (5.62):

$$C^{(2),\text{app.}}(\tau, y_t) = C^{(2)}(\tau, \infty) + \left[d^{(2)}_{\text{ex}}(\tau, y_t) - d^{(2)}_{\text{point}}(\tau) \right] T(\tau, \tau_0) \,. \tag{5.79}$$

Note that k_T-factorisation only provides the leading behaviour at small τ. This implies that in the NLO case the approximation eq. (5.73) reproduces the exact result up to terms which vanish at least as $O(\tau)$. At NNLO the high energy calculation with finite m_t only reproduces the slope $\mathcal{C}^{(2)}(y_t)$ of the logarithmic growth in eq. (5.77), while the asymptotic constant $\mathcal{C}^{(2)}_0(y_t)$ remains undetermined. The plot in fig. 5.6 shows the NNLO coefficient function in the $m_t \to \infty$, together with correct asymptotic limit at small τ for $m_H = 130$ GeV; it is clear that different choices of the subleading constant would lead to fairly different results. Thus, at NNLO the approximate coefficient function eq. (5.79) suffers from a twofold ambiguity: the choice of the matching point τ_0 and the value of the subleading constant $\mathcal{C}^{(2)}_0(y_t)$. The dependence of the result on either of these choices contributes to the uncertainty related to the matching procedure.

As far as the matching point is concerned, two different choices have been studied. In the first procedure one takes the same matching point as in the NLO case:

$$\begin{aligned} \tau_0 &= 0.057 \,, \qquad \text{for} \qquad m_H = 130\,\text{GeV} \,, \\ \tau_0 &= 0.315 \,, \qquad \text{for} \qquad m_H = 280\,\text{GeV} \,. \end{aligned} \tag{5.80}$$

Alternatively one can choose τ_0 as the point where the difference between the derivative of the $m_t \to \infty$ curve and the asymptotic slope is at its minimum, so that

$$\frac{d}{d\ln\tau} C^{(2)}(\tau, \infty)\Big|_{\tau=\tau_0} \simeq -9\,\mathcal{C}^{(2)}(y_t) \,. \tag{5.81}$$

This second choice is motivated by the expectation that the coefficient function should have a fairly steady behaviour. The values for the matching point obtained with this second procedure for the two cases previously analysed are

$$\begin{aligned} \tau_0 &= 0.011 \,, \qquad \text{for} \qquad m_H = 130\,\text{GeV} \,, \\ \tau_0 &= 0.317 \,, \qquad \text{for} \qquad m_H = 280\,\text{GeV} \,. \end{aligned} \tag{5.82}$$

Thus, for a light Higgs one obtains a value of the matching point sensibly lower than the NLO case, while for a heavier Higgs the result is the same.

Once the value of the matching point has been chosen, one can turn one's attention to the subleading constant $\mathcal{C}^{(2)}_0(y_t)$. A sensible criterion to adjust it appears to be the continuity of approximate coefficient function $C^{(2),\text{app.}}(\tau, y_t)$ at $\tau = \tau_0$, when the

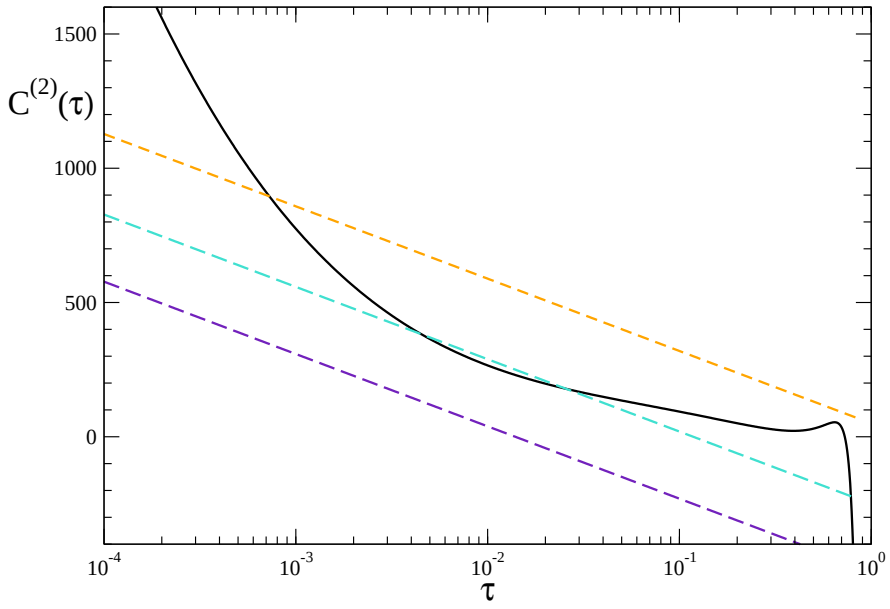

Figure 5.6: The NNLO hard coefficient function plotted as a function of τ. The solid black curve is to $m_t = \infty$. The dashed lines correspond to the asymptotic slope for $m_t = 170.9$ GeV and $m_H = 130$ GeV, with different choices of the subleading constant.

matching is performed with the Heavyside function:

$$C^{(2)}(\tau_0,\infty) = C^{(2)}(\tau_0,\infty) + \left[d^{(2)}_{\rm ex}(\tau_0,y_t) - d^{(2)}_{\rm point}(\tau_0)\right] , \tag{5.83}$$

which gives

$$\mathcal{C}^{(2)}_0(y_t) = {c^2}_4 \ln^3\tau_0 + {c^2}_3 \ln^2\tau_0 + {c^2}_2 \ln\tau_0 + {c^2}_1 - 9C^{(2)}(y_t)\ln\tau_0 . \tag{5.84}$$

In fig. (5.7) the approximate coefficient function is plotted in the case of a light Higgs, for the two different choices of the matching point τ_0. As already noticed the two methods give fairly different results for τ_0 . However, in the region about $\tau = 0.02$ the $m_t \to \infty$ curve exhibits a linear behaviour in $\ln\tau$, with slope very close to $\mathcal{C}^{(2)}(y_t)$ for $m_H = 130$ GeV. Hence the approximate coefficient functions obtained with the two matching procedure are actually very close. The impact of this difference on a physical observable will be discussed in the following. For the heavier Higgs boson, the two matching procedures provide almost the same value for τ_0. However, in this case the approximate coefficient function does not look as smooth as the previous case. The dip in the right-hand plot, in fig. 5.8, suggests that in such a region positive powers of τ play a non-negligible role.

It is well known that the pointlike approximation to the NLO inclusive cross section is very good, and thus the impact of the improvement eq. (5.73) is moderate. Also at NNLO one would not expect large deviations from the heavy top approximation, mainly for kinematical reasons. In order to give a quantitative assessment, one can define a K factor by letting:

$$\sigma_{gg}(\tau_h; y_t, m_H^2) = \sigma^0_{gg}(\tau_h; y_t, m_H^2) K(\tau_h; y_t, m_H^2) , \tag{5.85}$$

where σ^0_{gg} is the LO contribution eq. (5.3) to the gluon–gluon cross section, computed with LO parton distributions and LO coupling constant. The value of the NLO and NNLO K factors, determined using the MRST2002 [103] gluon distribution in eq. (5.3) are given in table 5.2 at the LHC centre-of-mass energy $s = 14$ TeV. In the table the pointlike, exact and approximate (eq. (5.73) and eq. (5.79)) cases are shown. At NLO the discrepancy between the infinite top mass approximation and the exact result is tiny, less than 1% even for a fairly heavy Higgs. Finite top mass effects at small τ are not very large, but as table 5.2 shows, once they are included the deviation from the exact result is considerably reduced. At NNLO the exact result is not known. The inclusion of the correct small τ dependence of the partonic coefficient function changes the K factor by 0.3% for $m_H = 130$ GeV. For $m_H = 280$ GeV, the effect is at the percent level.

Less inclusive quantities can be more sensitive to the small τ tail of the partonic

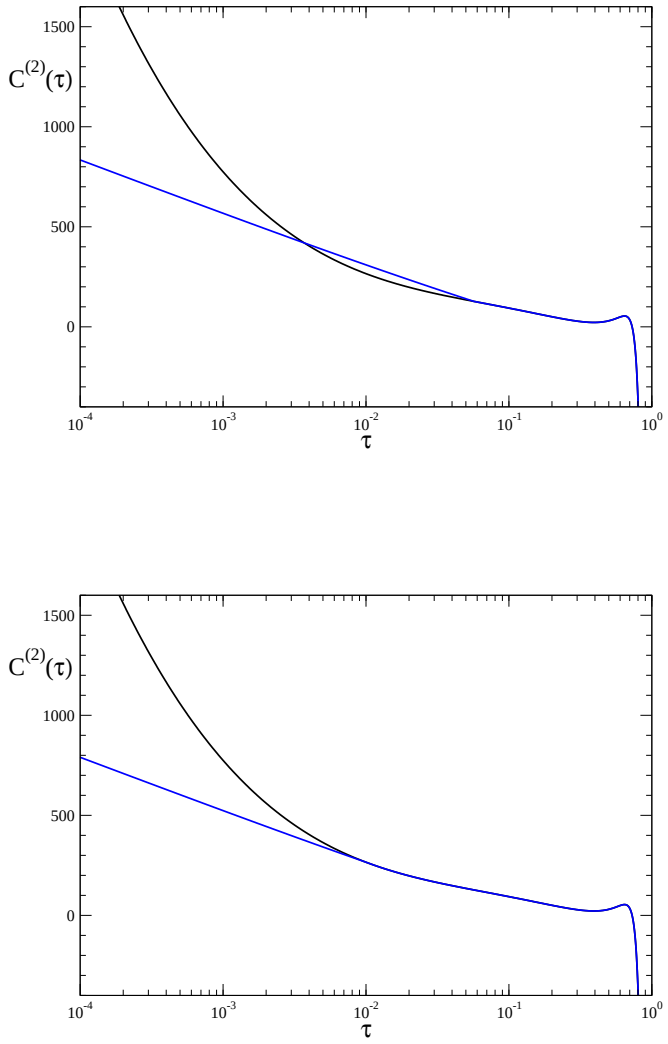

Figure 5.7: The NNLO coefficient function for $m_H = 130$ GeV. In the plot on the top the matching point τ_0 is the same as in the NLO case, while in the bottom one, it is chosen according to eq. (5.81).

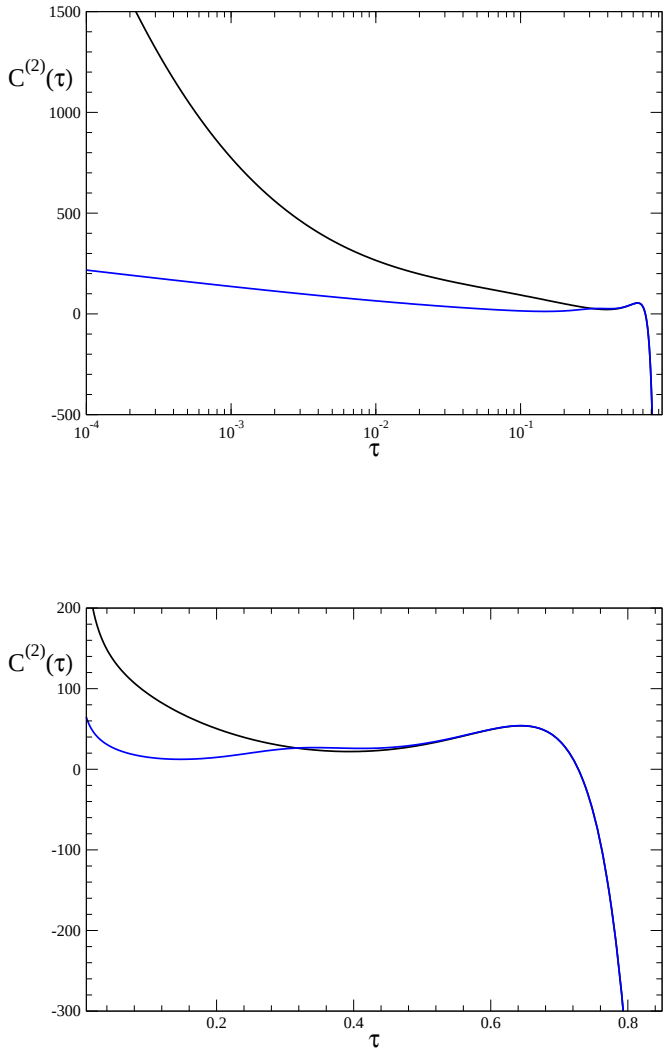

Figure 5.8: The NNLO coefficient function $m_H = 280$ GeV on a logarithmic (top) and linear scale (bottom). The curves determined with the two different matching procedures coincide.

	K^{NLO}	K^{NNLO}
$m_H = 130$ GeV		
pointlike	1.800	2.140
exact	1.797	n.a.
appr.	1.796	2.136
$m_H = 280$ GeV		
pointlike	1.976	2.420
exact	1.958	n.a.
appr.	1.959	2.395

Table 5.2: The NLO and NNLO K factors eq. (5.85), computed with centre-of-mass energy $s = 14$ TeV, and $m_t \to \infty$, denoted with pointlike, or $m_t = 170.9$ GeV, denoted with exact or approximate. The approximate result uses eqs. (5.73),(5.79). The NNLO matching point has been determined according to eq. (5.81). The two different choices for τ_0 lead to very similar values for the K factors. The MRST2002 [103] gluon distribution has been used.

coefficient functions. For instance rapidity distribution has been computed both at NLO [104] and NNLO [105] only in the $m_t \to \infty$ limit. This quantity can show more pronounced finite top mass effects at large rapidities.

Chapter 6

BFKL from DGLAP at next-to-next-to-leading order

In this chapter an approximation to the BFKL kernel at $\mathcal{O}\left(\alpha_s^3\right)$ is computed. This result includes all collinear and anticollinear contributions and it is derived using duality relations between the DGLAP and BFKL evolution kernels.

At the end of section 2.2.3 was pointed out that the calculation of the NNLO contribution to the BFKL kernel is hampered by various issues. In particular the framework in which the NLO corrections were computed does not seem to be valid at the next perturbative order. Nevertheless collinear factorisation and all-order duality relations, presented in section 3.2, guarantee the existence of a universal and factorised leading twist kernel for high energy evolution. It was shown in section 3.2.1 how duality relations eq. (3.39) are modified by running coupling corrections; an operator method to compute these corrections order by order in perturbation theory was also presented. Such an approach was used to derive the running–coupling corrections to the small x resummation of the DGLAP kernel eq. (3.70).

Conversely, because at fixed-coupling duality maps the expansion of $\gamma(N, \alpha_s)$ in powers of α_s at fixed N onto the expansion of $\chi(M, \alpha_s)$ in powers of α_s at fixed α_s/M, it is possible to use it to determine the collinear behaviour ($M \to 0$) of the BFKL kernel. This remains true also when the coupling runs, because running–coupling corrections to duality are given as a series in α_s of terms each of which is a function of the fixed-coupling dual expressions. Specifically, if one considers the expansion

$$\chi(M, \hat{\alpha}_s) = \hat{\alpha}_s \chi_0(M) + \hat{\alpha}_s^2 \chi_1(M) + \dots \tag{6.1}$$

then

$$\chi_i(M) = \frac{c_{i,-i-1}}{M^{i+1}} + \frac{c_{i,-i}}{M^i} + \dots \tag{6.2}$$

for some coefficients $c_{i,j}$. Through duality it is possible to determine from the NNLO

DGLAP anomalous dimension, the first three orders of the expansion eq. (6.1) of $\chi_i(M)$ for all i, i.e. $c_{i,j}$ for all i and $j = -i-1, -i, -i+1$. This means that knowledge of the anomalous dimension γ at NNLO allows one to determine all the collinear singular contributions to the NNLO BFKL kernel χ_2. Furthermore, the symmetry properties of χ allow one to determine its expansion about $M = 1$ from the knowledge of the coefficients of the expansion about $M = 0$. This procedure requires some care in the treatment of the running of the coupling, which affects the way the symmetry is realised.

6.1 Factorisation schemes

Beyond leading order, both the DGLAP and BFKL kernels are only defined up to a choice of factorisation scheme. Namely, if the normalisation of the parton density G is redefined by a subleading function $R(N, \alpha_s) = 1 + O(\alpha_s)$, then the evolution kernel beyond leading order changes, as shown for instance in eq. (3.77). Thus, before the computation of the collinear approximation to the kernel is performed, a full understanding of this issue has to be achieved. This is particularly important in this calculation because the BFKL kernel has different symmetry properties in different schemes.

The normalisation of the parton distribution which appears in the DGLAP equation is fixed by the standard factorisation of collinear singularities, and a choice of subtraction prescription such as dimensional regularisation and the $\overline{\text{MS}}$ prescription. This defines the anomalous dimension in the $\overline{\text{MS}}$ factorisation scheme. Duality then implicitly defines a corresponding factorisation scheme for the BFKL equation. However, the gluon density which enters the k_T-factorisation formula is normalised differently. Even though the gluon Green's function itself is computed in the $\overline{\text{MS}}$ scheme, the evolution kernel extracted from it corresponds to a scheme which is not $\overline{\text{MS}}$, because it describes the evolution of a quantity which differs from the $\overline{\text{MS}}$ parton distribution by a normalisation factor, i.e. it can be obtained from the $\overline{\text{MS}}$ parton distribution by the scheme-change function R, eq. (3.30). This scheme change function defines the so-called Q_0 factorisation scheme. Furthermore, the quantity which naturally enters k_T-factorisation formulae is the unintegrated parton distribution $\mathcal{G}$, so Q_0 scheme results are usually given for this quantity.

The normalisation mismatch between k_T-factorisation and collinear factorisation, and thus the precise definition of the Q_0 scheme, has been determined in [46] at the leading nontrivial order, which affects the definition of χ_1 in the expansion of the BFKL kernel χ, and therefore its dual DGLAP anomalous dimension at NLO in the expansion of $\gamma(N, \alpha_s)$ in powers of α_s at fixed α_s/N. It is important to notice that while in the literature a leading-order redefinition of the gluon normalisation is usually called a leading-log scheme change, here it is called a next-to-leading scheme change, because

it affects the next-to-leading kernel.

The normalisation mismatch between collinear and high energy factorisation, beyond the leading accuracy, was investigated in [106]. The main result of that study is an expression, proven up to NNLO, but conjectured to hold in general, which relates the t dependence of the integrated parton distributions $G(N,t)$ (as defined in standard collinear factorisation) in the $\overline{\text{MS}}$ and Q_0 scheme. This relation is expressed in terms of the BFKL kernel for the unintegrated distribution. Specifically, the t dependence can be written in terms of a saddle-point evolution factor $E(t,t_0)$, a running–coupling duality correction $\mathcal{N}(N,t)$, and a normalisation factor $\mathcal{R}(t_0)$ which is characteristic of the way minimal subtraction with dimensional regularisation is defined:

$$G^{Q_0}(N,t) = \mathcal{N}(N,t)E(t,t_0)\mathcal{R}(N,t_0)G^{\overline{\text{MS}}}(N,t_0)\,. \tag{6.3}$$

The saddle-point evolution factor is obtained by solving the running–coupling BFKL equation for the unintegrated distribution in the saddle-point approximation. This leads to evolution driven by the anomalous dimension $\tilde{\gamma}_u(N,\alpha_s(t))$, obtained from the BFKL kernel using fixed-coupling duality, but with $\alpha_s = \alpha_s(t)$:

$$E(t,t_0) = \exp\left[\int_{t_0}^{t} \tilde{\gamma}_u(N,\alpha_s(t'))\,dt'\right]\,, \tag{6.4}$$

where the index u indicates a DGLAP kernel which describes the evolution of an unintegrated parton distribution; similarly an index i denotes an integrated BFKL kernel, as in eq. (3.75). Henceforth the tilde indicates a kernel obtained through fixed-coupling duality. The running–coupling correction to duality eq. (3.70) can be combined with the contribution eq. (3.75), which relates the integrated and unintegrated parton distributions into the factor $\mathcal{N}$. This gives

$$\begin{aligned}\frac{\mathcal{N}(N,t)}{\mathcal{N}(N,t_0)} &= \frac{\gamma(N,\alpha_s(t_0))}{\gamma(N,\alpha_s(t))}\exp\left\{\int_{t_0}^{t}\left[\gamma_u(N,\alpha_s(t')) - \tilde{\gamma}_u(N,\alpha_s(t'))\right]dt'\right\} \\ &= \exp\left\{\int_{t_0}^{t}\left[\gamma(N,\alpha_s(t')) - \tilde{\gamma}_u(N,\alpha_s(t'))\right]dt'\right\}\,.\end{aligned} \tag{6.5}$$

Finally, the normalisation factor $\mathcal{R}$ is related to the definition of anomalous dimension in $\overline{\text{MS}}$ and it can be computed considering the analytic continuation of the evolution kernels in $d = 4 - 2\varepsilon$ dimensions. The explicit calculation of the $\mathcal{R}$ factor is described in section 6.2.1.

Equation (6.3) gives the scale dependence of the parton distribution in either scheme in terms of a boundary condition determined in the other scheme: therefore, it fully specifies both the relation between the two schemes, and the scale dependence in either of them. Letting $t = t_0$ in eq. (6.3) immediately gives the relation between $G^{Q_0}(N,t)$

and $G^{\overline{\rm MS}}(N,t)$, through the function

$$R(N,t) \equiv \mathcal{N}(N,t)\mathcal{R}(N,t)\,. \tag{6.6}$$

The scale dependence of the parton distribution in the Q_0 scheme is found by keeping t_0 fixed in eq. (6.3) and varying t: thus

$$\begin{aligned} G^{Q_0}(N,t) &= \frac{\mathcal{N}(N,t)}{\mathcal{N}(N,t_0)} E(t,t_0) G^{Q_0}(N,t_0) \\ &= \exp\left[\int_{t_0}^{t} \gamma(N,\alpha_s(t'))\,dt'\right] G^{Q_0}(N,t_0),\,. \end{aligned} \tag{6.7}$$

So the integrated parton distribution in the Q_0 scheme evolves with the anomalous dimension $\gamma(N,\alpha_s(t))$ which is related to the starting unintegrated BFKL kernel by running–coupling duality combined with the transformation to the integrated level. The scale dependence in the $\overline{\rm MS}$ scheme is instead given by

$$\begin{aligned} G^{\overline{\rm MS}}(N,t) &= \frac{\mathcal{R}(N,t_0)}{\mathcal{R}(N,t)} E(t,t_0) G^{\overline{\rm MS}}(N,t_0) \\ &= \frac{\mathcal{R}(N,t_0)}{\mathcal{R}(N,t)} \exp\left[\int_{t_0}^{t} \tilde{\gamma}_u(N,\alpha_s(t'))\,dt'\right] G^{\overline{\rm MS}}(N,t_0)\,, \end{aligned} \tag{6.8}$$

namely, the integrated parton distribution in the $\overline{\rm MS}$ scheme evolves with an anomalous dimension which is closely related to the fixed-coupling dual $\tilde{\gamma}_u(N,\alpha_s(t))$ of the starting BFKL kernel, and only differs from it through the scale dependence of the $\mathcal{R}$ factor. It is possible, and useful, to define an auxiliary scheme, $\overline{\rm MS}^*$, which differs from $\overline{\rm MS}$ by a factor $\mathcal{R}(N,t)$: namely

$$G^{\overline{\rm MS}^*}(N,t) = \mathcal{R}(N,t) G^{\overline{\rm MS}}(N,t) \tag{6.9}$$

In this $\overline{\rm MS}^*$ scheme the parton distribution evolves with the naive dual anomalous dimension:

$$G^{\overline{\rm MS}^*}(N,t_1) = \exp\left[\int_{t_0}^{t_1} \tilde{\gamma}_u(N,\alpha_s(t))\,dt\right] G^{\overline{\rm MS}^*}(N,t_0)\,. \tag{6.10}$$

The relations between different quantities in various schemes, which will be computed in the following, are summarised in figure 6.1. In the figure, horizontal lines denote duality: either at the running–coupling level, relating χ to γ, or at the fixed-coupling, relating γ to $\tilde{\chi}$. Vertical lines denote relations between schemes, specifically the Q_0, $\overline{\rm MS}^*$ and $\overline{\rm MS}$ schemes. Eq. (6.10) means that the anomalous dimension in the $\overline{\rm MS}^*$ scheme coincides with the naive dual of the Q_0 scheme BFKL kernel (at the unintegrated level):

$$\tilde{\gamma}_u^{Q_0}(N,\alpha_s) = \gamma^{\overline{\rm MS}^*}(N,\alpha_s)\,, \tag{6.11}$$

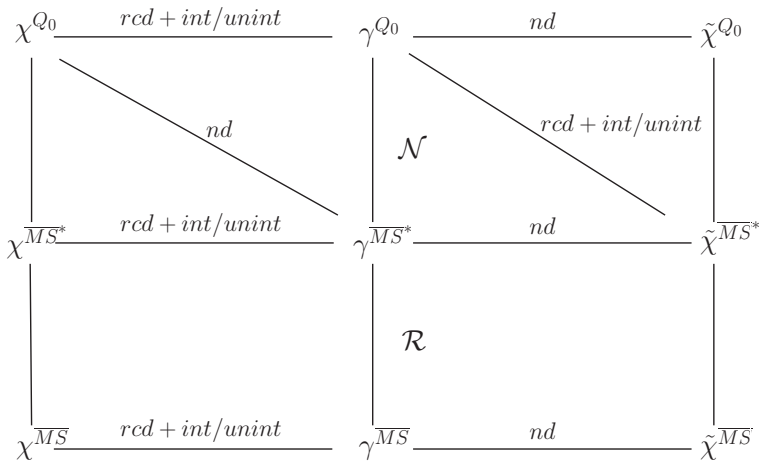

Figure 6.1: Schematic relation between BFKL kernels χ and DGLAP anomalous dimensions γ in various schemes. Horizontal lines denote running coupling and naive duality relations (*rcd* and *nd*, respectively), together with the relation between integrated and unintegrated parton densities (*int / unint*). Vertical lines denote scheme transformations. The diagonal lines express the identities eq. (6.11), (6.12).

and thus, by duality, also that

$$\tilde{\chi}_i^{\overline{\rm MS}^*}(M,\alpha_s) = \chi^{Q_0}(M,\alpha_s)\,, \tag{6.12}$$

where $\tilde{\chi}_i^{\overline{\rm MS}^*}(M,\alpha_s)$ is the naive dual of the standard DGLAP anomalous dimension in the $\overline{\rm MS}^*$ scheme, while $\chi^{Q_0}(M,\alpha_s)$ is the kernel for the BFKL equation satisfied by the unintegrated parton distribution in the Q_0 scheme. This further implies that if $\tilde{\chi}_i^{\overline{\rm MS}^*}(M,\alpha_s)$ is interpreted as an operator by letting $\alpha_s \to \hat{\alpha}_s$ (ordered in the same way as $\chi^{Q_0}(M,\hat{\alpha}_s)$), then it is related by running–coupling duality to $\gamma^{Q_0}(N,\alpha_s)$. These relations are denoted by diagonal lines in the figure.

6.2 The collinear approximation

The starting point for the computation of the collinear approximation of the BFKL kernel is the DGLAP anomalous dimension, which, as already said, has been computed at $\mathcal{O}(\alpha_s^3)$ in [16]. The largest eigenvalue of the anomalous dimension matrix in the singlet sector eq. (2.57) admits the following expansion

$$\begin{aligned}
\gamma_0(N) &= \frac{g_{0,-1}}{N} + g_{0,0} + g_{0,1}N + O(N^2)\,,\\
\gamma_1(N) &= \frac{g_{1,-1}}{N} + g_{1,0} + O(N)\,,\\
\gamma_2(N) &= \frac{g_{2,-2}}{N^2} + \frac{g_{2,-1}}{N} + O(N^0)\,;
\end{aligned} \tag{6.13}$$

the explicit $\overline{\rm MS}$ coefficients can be found in Appendix C. One can compute the running coupling dual to this object exploiting the operator formalism presented in section 3.2. In this case the starting equation is the DGLAP one in the double Mellin space (N, M):

$$MG(N,M) = \gamma(N, \hat{\alpha}_s) G(N,M)\,; \tag{6.14}$$

thus the operators which enters eq. (3.65) are

$$\begin{aligned} \hat{p} &= \gamma(N\hat{\alpha}_s^{-1}, \hat{\alpha}_s)\,, \\ \hat{q} &= M\,, \end{aligned}$$

and the function f is chosen to be the naive dual to the anomalous dimension. The relevant commutators are computed considering the running coupling operator at two loops, as given in eq. (3.72); they can be easily calculated if one considers the expansion of the anomalous dimension in powers of α_s at fixed α_s/N:

$$\gamma(N\hat{\alpha}_s^{-1}, \hat{\alpha}_s) = \gamma_s(N\hat{\alpha}_s^{-1}) + \hat{\alpha}_s \gamma_{ss}(N\hat{\alpha}_s^{-1}) + \mathcal{O}\left(\hat{\alpha}_s^2\right)\,. \tag{6.15}$$

The commutators which are needed are

$$\begin{aligned} [\hat{p}, \hat{q}] &= -(N\beta_0 + N\beta_0 \hat{\alpha}_s \beta_1) \frac{\partial \gamma(N\hat{\alpha}_s^{-1}, \hat{\alpha}_s)}{\partial N \hat{\alpha}_s^{-1}} \\ &\quad + \beta_0 \hat{\alpha}_s^2 \frac{\partial \gamma(N\hat{\alpha}_s^{-1}, \hat{\alpha}_s)}{\partial \hat{\alpha}_s} + O(\hat{\alpha}_s^3)\,, \end{aligned} \tag{6.16}$$

$$[\hat{p}, [\hat{p}, \hat{q}]] = O(\hat{\alpha}_s^3)\,, \tag{6.17}$$

$$[\hat{q}, [\hat{q}, \hat{p}]] = (N\beta_0)^2 \frac{\partial^2 \gamma(N\hat{\alpha}_s^{-1}, \hat{\alpha}_s)}{\partial (N\hat{\alpha}_s^{-1})^2} + O(\hat{\alpha}_s^3)\,, \tag{6.18}$$

$$([\hat{p}, \hat{q}])^2 = (N\beta_0)^2 \left(\frac{\partial \gamma(N\hat{\alpha}_s^{-1}, \hat{\alpha}_s)}{\partial N \hat{\alpha}_s^{-1}} \right)^2 + O(\hat{\alpha}_s^3)\,. \tag{6.19}$$

Substituting these commutators into eq. (3.65) and back-substituting lower order expressions to remove the explicit N dependence in the evolution kernel, one recovers a BFKL-type equation

$$\begin{aligned} N\hat{\alpha}_s^{-1} G &= \left\{ \chi_0^i(M) + \hat{\alpha}_s \chi_1^i(M) + \hat{\alpha}_s^2 \chi_2^i(M) \right\} G \\ &= \left\{ \tilde{\chi}_0(M) + \hat{\alpha}_s \left(\tilde{\chi}_1(M) + \Delta^{\rm rc} \chi_1(M) \right) \right. \\ &\quad \left. + \hat{\alpha}_s^2 \left(\tilde{\chi}_2(M) + \Delta^{\rm rc} \chi_2(M) \right) \right\} G\,. \end{aligned} \tag{6.20}$$

The index i reminds that the kernel describes the evolution of the integrated parton distribution G. The running-coupling dual is written in terms of the function obtained

from the anomalous dimension through naive duality ($\tilde{\chi}$) plus running coupling-corrections:

$$\begin{aligned}
\Delta^{\rm rc}\chi_1(M) &= -\frac{1}{2}\beta_0\frac{\tilde{\chi}_0\tilde{\chi}_0''}{\tilde{\chi}_0'}\,,\\
\Delta^{\rm rc}\chi_2(M) &= -\frac{1}{2}\beta_0\beta_1\frac{\tilde{\chi}_0\tilde{\chi}_0''}{\tilde{\chi}_0'}+\frac{1}{4}\beta_0^2\frac{\tilde{\chi}_0}{(\tilde{\chi}_0')^2}\left(2\tilde{\chi}_0'\tilde{\chi}_0'''-\left(\tilde{\chi}_0''\right)^2\right)\\
&\quad+\frac{1}{24}\beta_0^2\frac{(\tilde{\chi}_0)^2}{(\tilde{\chi}_0')^4}\left(12\left(\tilde{\chi}_0''\right)^3-14\tilde{\chi}_0'\tilde{\chi}_0''\tilde{\chi}_0'''+3\left(\tilde{\chi}_0'\right)^2\tilde{\chi}_0^{IV}\right)\\
&\quad-\frac{1}{2}\beta_0\frac{\tilde{\chi}_0\tilde{\chi}_1''}{\tilde{\chi}_0'}-\beta_0\frac{\tilde{\chi}_1\tilde{\chi}_0''}{\tilde{\chi}_0'}+\frac{1}{2}\beta_0\frac{\tilde{\chi}_0\tilde{\chi}_0''\tilde{\chi}_1'}{(\tilde{\chi}_0')^2}\,.
\end{aligned}\tag{6.21}$$

In order to obtain the evolution kernel at the unintegrated level, one has to consider

$$\begin{aligned}
\chi(M,\hat{\alpha}_s) &= M\chi^i(M,\hat{\alpha}_s)M^{-1}=M\left(\hat{\alpha}_s\chi_0^i+\hat{\alpha}_s^2\chi_1^i+\hat{\alpha}_s^3\chi_2^i\right)M^{-1}\\
&= \hat{\alpha}_s\chi_0^i+\hat{\alpha}_s^2\chi_1^i+\hat{\alpha}_s^3\chi_2^i+[M,\hat{\alpha}_s]\,\frac{\chi_0^i}{M}+\left[M,\hat{\alpha}_s^2\right]\frac{\chi_1^i}{M}+\mathcal{O}\left(\hat{\alpha}_s^4\right)\,.
\end{aligned}\tag{6.22}$$

The computation of the commutators is straightforward and it leads to the following relations

$$\begin{aligned}
\chi_0 &= \chi_0^i\,,\\
\chi_1 &= \chi_1^i-\beta_0\frac{\chi_0^i}{M}\,,\\
\chi_2 &= \chi_2^i-\beta_0\beta_1\frac{\chi_0^i}{M}-2\beta_0\frac{\chi_1^i}{M}\,.
\end{aligned}\tag{6.23}$$

Collecting the contributions from eq. (6.21) and eq. (6.23) it is possible to write an expression for the BFKL kernel in the $\overline{\rm MS}$ scheme to NNLO, in terms of the naive duals of the DGLAP anomalous dimension

$$\begin{aligned}
\chi_0^{\overline{\rm MS}} &= \tilde{\chi}_0\,,\\
\chi_1^{\overline{\rm MS}} &= \tilde{\chi}_1+\Delta^{\rm rc}\chi_1-\beta_0\frac{\tilde{\chi}_0}{M}\,,\\
\chi_2^{\overline{\rm MS}} &= \tilde{\chi}_2+\Delta^{\rm rc}\chi_2-\beta_0\beta_1\frac{\tilde{\chi}_0}{M}-2\beta_0\frac{\tilde{\chi}_1+\Delta^{\rm rc}\chi_1}{M}\,.
\end{aligned}\tag{6.24}$$

In order to obtain an explicit result, the naive duals to eq. (6.13) have to be computed. Using perturbative duality eq. (3.85), one obtains

$$\begin{aligned}
\tilde{\chi}_0(M) &= \frac{g_{0,-1}}{M} + \mathcal{O}\left(M^2\right) \\
\tilde{\chi}_1(M) &= \frac{g_{0,-1}g_{0,0}}{M^2} + \frac{g_{1,-1}}{M} + \frac{g_{2,-2}}{g_{0-1}} + \mathcal{O}\left(M\right) \\
\tilde{\chi}_2(M) &= \frac{(g_{0,-1})^2 g_{0,1} + g_{0,-1}(g_{0,0})^2}{M^3} + \frac{g_{1,0}g_{0,-1} + g_{0,0}g_{1,-1}}{M^2} + \frac{g_{2,-1}}{M} + \mathcal{O}\left(M^0\right) .
\end{aligned} \tag{6.25}$$

Substituting the previous expressions into eq. (6.24), one obtains the collinear approximation to the BFKL kernel at $\mathcal{O}(\hat{\alpha}_s^3)$. The factorisation scheme is the same as the anomalous dimension's one, namely $\overline{\text{MS}}$. However, as already discussed, a direct diagrammatic computation would lead to the kernel in the Q_0 scheme rather than $\overline{\text{MS}}$. Moreover, it is only in Q_0 that one can exploits the symmetry of the underlying Feynman diagrams eq. (2.101) and extend the results into the anticollinear region $M \sim 1$. Thus, before the symmetrisation, one should compute the scheme change function which relates the BFKL kernel in $\overline{\text{MS}}$ and Q_0. The diagram in fig. 6.1 suggests that one may achieve the same result transforming the initial anomalous dimension from $\overline{\text{MS}}$ to the auxiliary scheme $\overline{\text{MS}}^*$ (vertical line in the middle) and then simply use fixed-coupling duality to obtain χ^{Q_0}, going along the diagonal line. The scheme change function $\mathcal{R}$ has been studied beyond the leading logarithmic accuracy in [106], where an expression for the NNLLx scheme change was written in terms of an unknown function, which basically comes from the analytic continuation of the NLO BFKL kernel χ_1 in d-dimensions. In the next section it is shown how it is possible to go about this problem and compute the collinear approximation to the scheme change $\mathcal{R}$ to $\mathcal{O}(\alpha_s^3)$.

6.2.1 The $\mathcal{R}$ factor

The factorisation of collinear singularities in dimensional regularisation was discussed in Chapter 2. A generic partonic cross section $\hat{\sigma}$ which depends on a single dimensional variable Q^2 can be written in $d = 4 - 2\varepsilon$ dimensions as

$$\sigma\left(\frac{Q^2}{\mu^2}, \alpha_s(\mu^2), N, \varepsilon\right) = \sigma^{(0)}(Q^2, \alpha_0, N, \varepsilon) \exp\left[\int_0^{\alpha_s(\mu^2)} d\alpha \frac{\gamma(N, \alpha, \varepsilon)}{\beta(\alpha, \varepsilon)}\right] , \tag{6.26}$$

where $\alpha_s(\mu^2)$ is the dimensionless renormalised coupling, α_0 is the bare coupling, $\sigma^{(0)}(Q^2, \alpha_0, N, \varepsilon)$ is the regularised cross section and $\sigma(\frac{Q^2}{\mu^2}, \alpha_s(\mu^2), N, \varepsilon)$ is free of collinear singularities. The d–dimensional DGLAP kernel $\gamma(N, \alpha_s, \varepsilon)$ is defined as the Mellin transform of the d–dimensional Altarelli–Parisi splitting function. The β-

function in d-dimension is given by

$$\beta(\alpha_s, \varepsilon) = \alpha_s \varepsilon + \beta(\alpha_s)\,, \tag{6.27}$$

where $\beta(\alpha_s)$ is the four dimensional β-function eq. (3.71).

In $\overline{\rm MS}$ the anomalous dimension is the residue of the simple pole in ε in the integrand of the exponential in eq. (6.26), namely

$$\begin{aligned}\gamma^{\overline{\rm MS}}(N, \alpha_s) &= {\rm Res}_\varepsilon \left[\frac{\alpha_s \gamma(N, \alpha_s, \varepsilon)}{\beta(\alpha_s, \varepsilon)} \right] \\ &= \gamma(N, \alpha_s) - \frac{\beta(\alpha_s)}{\alpha_s} \dot{\gamma}(N, \alpha_s) + \left(\frac{\beta(\alpha_s)}{\alpha_s} \right)^2 \ddot{\gamma}(N, \alpha_s) + \dots \end{aligned} \tag{6.28}$$

where the various coefficients are defined through the Taylor expansion

$$\gamma(N, \alpha_s, \varepsilon) \equiv \gamma(N, \alpha_s) + \varepsilon \dot{\gamma}(N, \alpha_s) + \varepsilon^2 \ddot{\gamma}(N, \alpha_s) + \dots . \tag{6.29}$$

Thus the $\overline{\rm MS}$ anomalous dimension receives two different classes of contributions: pure collinear singularities and interference terms between the ε-dependent anomalous dimension and the poles arising from the expansion of the d-dimensional β-function. In particular up to next-to-next-to leading order one obtains

$$\begin{aligned}\gamma_0^{\overline{\rm MS}} &= \gamma_0\,, \\ \gamma_1^{\overline{\rm MS}} &= \gamma_1 + \beta_0 \dot{\gamma}_0\,, \\ \gamma_2^{\overline{\rm MS}} &= \gamma_2 + \beta_0 \beta_1 \dot{\gamma}_0 + \beta_0^2 \ddot{\gamma}_0 + \beta_0 \dot{\gamma}_1\,. \end{aligned} \tag{6.30}$$

The $\mathcal{R}$ factor defines the auxiliary scheme $\overline{\rm MS}^*$ eq. (6.9), where the anomalous dimension is simply given by $\gamma(N, \alpha_s, 0)$, i.e. $\gamma_0(N)$, $\gamma_1(N)$, etc. Hence in order to compute $\gamma^{\overline{\rm MS}^*}$ one has to subtract from the $\overline{\rm MS}$ anomalous dimension the contributions coming from the interference between the d-dimensional kernel and the β function, i.e. the dotted terms in eq. (6.30). The $\mathcal{O}(\varepsilon)$ and $\mathcal{O}(\varepsilon^2)$ contribution to the LO anomalous dimension, $\dot{\gamma}_0$ and $\ddot{\gamma}_0$ respectively, are obtained from the Mellin transform of the d-dimensional leading order splitting kernel. Such objects have been known for

a long time [108], at least for $x < 1$:

$$\begin{aligned}
P_{qq}(x,\varepsilon) &= C_F \frac{1}{(1-x)^\varepsilon}\left[\frac{1+x^2}{1-x} - \varepsilon(1-x)\right] + a_{qq}(x,\varepsilon)\delta(1-x)\,,\\
P_{qg}(x,\varepsilon) &= C_F \frac{1}{(1-x)^\varepsilon}\left[\frac{1+(1-x)^2}{x} - \varepsilon x\right]\,,\\
P_{gq}(x,\varepsilon) &= T_R \frac{1}{(1-x)^\varepsilon}\left[1 - 2x\frac{1-x}{1-\varepsilon}\right]\,,\\
P_{gg}(x,\varepsilon) &= 2C_A \frac{1}{(1-x)^\varepsilon}\left[\frac{x}{1-x} + \frac{1-x}{x} + x(1-x)\right] + a_{gg}(x,\varepsilon)\delta(1-x)\,.
\end{aligned} \tag{6.31}$$

The end–point contribution a_{qq} (a_{gg}) can be extracted from any process with collinear radiation from incoming quarks, such as Drell-Yan [78], or gluons, such as Higgs production from gluon-gluon fusion [91]: the $O(\alpha_s)$ coefficient of the $\delta(1-x)$ provides a determination of the end–point term in the splitting function after factoring a simple ε pole and the Born cross section (and a factor of two when there are two incoming partons). One obtains:

$$\begin{aligned}
a_{qq}(\varepsilon) &= C_F\left[\frac{2}{\varepsilon} + \frac{3}{2} + \varepsilon\left(4 - \frac{\pi^2}{3}\right)\right] + O(\varepsilon^2)\,,\\
a_{gg}(\varepsilon) &= \frac{2C_A}{\varepsilon} + \frac{11C_A - 4n_f T_R}{6} - \varepsilon\pi^2 + O(\varepsilon^2)\,.
\end{aligned} \tag{6.32}$$

The simple ε pole cancels against the one coming from the expansion of $(1-x)^{-(1+\varepsilon)} = \frac{1}{\varepsilon}\delta(1-x) + \ldots$ in the splitting functions P_{qq} and P_{gg}, thereby providing a check of the result.

The coefficients of the expansion in powers of N of the relevant contributions to the analytic continuation of the LO anomalous dimension in d-dimensions are

$$\begin{aligned}
\dot\gamma_0(N) &= \frac{\dot g_{0,-2}}{N^2} + \frac{\dot g_{0,-1}}{N} + \dot g_{0,0} + O(N)\,,\\
\ddot\gamma_0(N) &= \frac{\ddot g_{0,-1}}{N} + O(N^0)\,,
\end{aligned} \tag{6.33}$$

with

$$\begin{aligned}
\dot g_{0,-2} &= 0\,, \qquad \dot g_{0,-1} = 0\,,\\
\dot g_{0,0} &= -\frac{67}{12\pi} - \frac{7}{81}\frac{n_f}{\pi}\,, \qquad \ddot g_{0,-1} = -\frac{\pi^2}{12}\,.
\end{aligned} \tag{6.34}$$

The only missing quantity in eq. (6.9) is $\dot\gamma_1$; the next-to-leading order d-dimensional splitting function is not available, though in principle it could be extracted from d–dimensional splitting amplitudes [109]. The relevant terms in this discussion are

given by the Laurent expansion about $N = 0$

$$\dot{\gamma}_1 = \frac{\dot{g}_{1,-3}}{N^3} + \frac{\dot{g}_{1,-2}}{N^2} + \frac{\dot{g}_{1,-1}}{N} + O(N^0)\,. \tag{6.35}$$

On the other hand, some of the remaining coefficients can be computed, remembering that the $\mathcal{R}$ scheme change has been originally determined as a NLLx [46] or NNLLx [106] scheme change:

$$\begin{aligned}
\gamma_s^{\overline{\rm MS}} &= \gamma_s\,, \\
\gamma_{ss}^{\overline{\rm MS}} &= \gamma_{ss} + \beta_0\dot{\gamma}_s\,, \\
\gamma_{sss}^{\overline{\rm MS}} &= \gamma_{sss} + \beta_0\beta_1\dot{\gamma}_s + \beta_0^2\ddot{\gamma}_s + \beta_0\dot{\gamma}_{ss}\,,
\end{aligned} \tag{6.36}$$

where in this framework the dotted γ_{s^n} are determined through duality from the d-dimensional BFKL kernel:

$$\chi(M,\alpha_s,\varepsilon) = \chi(M,\alpha_s) + \varepsilon\dot{\chi}(M,\alpha_s) + \varepsilon^2\ddot{\chi}(M,\alpha_s) + \ldots \tag{6.37}$$

The explicit expressions are

$$\begin{aligned}
\dot{\gamma}_s &= -\frac{\dot{\chi}_0}{\chi_0'}\bigg|_{M=\gamma_s}\,, \\
\ddot{\gamma}_s &= -\frac{\ddot{\chi}_0}{\chi_0'} + \frac{\dot{\chi}_0\dot{\chi}_0'}{(\chi_0')^2} - \frac{1}{2}\frac{(\dot{\chi}_0)^2\chi_0''}{(\chi_0')^3}\bigg|_{M=\gamma_s}\,, \\
\dot{\gamma}_{ss} &= -\frac{\dot{\chi}_1}{\chi_0'} - \frac{\chi_1\dot{\chi}_0\dot{\chi}_0''}{(\chi_0')^3} + \frac{(\dot{\chi}_0)\chi_1' + \chi_1\dot{\chi}_0'}{(\chi_0')^2}\bigg|_{M=\gamma_s}\,.
\end{aligned} \tag{6.38}$$

Eq. (6.36) shows that γ_s is left unaffected by the scheme change, as one would expect because the LLx singularities are not scheme dependent. It follows that the coefficients of the $\left(\frac{\alpha_s}{N}\right)^k$ contributions are the same in the two schemes. This confirms that $\dot{g}_{0,-2} = 0$ and sets $\dot{g}_{1,-3} = 0$. Moreover the NLLx scheme change starts at $O\left(\alpha_s\left(\frac{\alpha_s}{N}\right)^3\right)$

$$\dot{\gamma}_s\left(\frac{\alpha_s}{N}\right) = 2\zeta(3)\left(\frac{\alpha_s}{N}\right)^3 + O\left(\left(\frac{\alpha_s}{N}\right)^4\right)\,. \tag{6.39}$$

Again this confirms the result $\dot{g}_{0,-1} = 0$ and sets $\dot{g}_{1,-2} = 0$. The sub–subleading coefficient $\dot{g}_{1,-1}$ remains undetermined: it would require knowledge of the $O(\varepsilon)$ correction to the NLO kernel $\dot{\chi}_1$.

Collecting these results together one can write the $\overline{\rm MS}^*$ anomalous dimension in terms of the coefficients of the expansion of the $\overline{\rm MS}$ anomalous dimension and of the

scheme change coefficients:

$$\begin{aligned}\gamma_0^{\overline{\rm MS}^*} &= \frac{g_{0,-1}}{N} + g_{00} + g_{0,1}N + O(N^2)\,,\\ \gamma_1^{\overline{\rm MS}^*} &= \frac{g_{1,-1}}{N} + \bar{g}_{1,0} + O(N)\,,\\ \gamma_2^{\overline{\rm MS}^*} &= \frac{g_{2,-2}}{N^2} + \frac{\bar{g}_{2,-1}}{N} + O(N^0)\,,\end{aligned} \tag{6.40}$$

where

$$\begin{aligned}\bar{g}_{1,0} &= g_{1,0} - \beta_0 \dot{g}_{0,0}\,,\\ \bar{g}_{2,-1} &= g_{2,-1} - \beta_0 \dot{g}_{1,-1} - \beta_0^2 \ddot{g}_{0,-1}\,.\end{aligned} \tag{6.41}$$

6.2.2 Symmetrisation and results

Once that an expression for the anomalous dimension in $\overline{\rm MS}^*$ has been determined, it is straightforward to compute, through fixed-coupling duality, the first three coefficients of the Laurent expansion about $M = 0$ of the BFKL in the Q_0 scheme

$$\begin{aligned}\chi_0^{Q_0}(M) &= \frac{g_{0,-1}}{M} + \mathcal{O}\left(M^2\right)\\ \chi_1^{Q_0}(M) &= \frac{g_{0,-1}g_{0,0}}{M^2} + \frac{g_{1,-1}}{M} + \frac{g_{2,-2}}{g_{0-1}} + \mathcal{O}\left(M\right)\\ \chi_2^{Q_0}(M) &= \frac{(g_{0,-1})^2 g_{0,1} + g_{0,-1}(g_{0,0})^2}{M^3} + \frac{\bar{g}_{1,0}g_{0,-1} + g_{0,0}g_{1,-1}}{M^2} + \frac{\bar{g}_{2,-1}}{M} + \mathcal{O}\left(M^0\right)\,.\end{aligned} \tag{6.42}$$

Note that the dependence on the factorisation scheme is not strong; the LO and NLO kernels in Q_0 are the same as in eq. (6.25). The scheme-dependent coefficients eq. (6.41) affect only χ_2.

So far the information from the DGLAP anomalous dimension has been used to determine the first few terms in the expansion of the BFKL kernel about $M = 0$. Exploiting the underlying symmetry of the BFKL kernel $M \leftrightarrow 1 - M$, it is possible to determine the corresponding terms of the expansion about $M = 1$. However, it has already been noticed that this symmetry is realised only if one chooses a symmetric definition of the dimensionless variable x, as in eq. (3.43). Moreover, an asymmetric choice for the argument of the running coupling breaks the symmetry of the kernel, as shown in eq. (2.110) and eq. (2.113). The relation between the BFKL kernel in symmetric and asymmetric variables was given in eq. (3.45). Indicating with the indices σ and Σ, the kernel in symmetric and asymmetric variables respectively, the implicit relation becomes

$$\chi^\sigma(M, \hat{\alpha}_s) = \chi^\Sigma(M + \tfrac{1}{2}\chi^\sigma(M, \hat{\alpha}_s), \hat{\alpha}_s)\,, \tag{6.43}$$

where $\alpha_s \to \hat{\alpha}_s$ because at $\mathcal{O}(\hat{\alpha}_s^3)$ the running of the coupling can no longer be neglected. The result obtained from duality eq. (6.42) is clearly in asymmetric variables; it can be converted into symmetric ones by expanding out eq. (6.43)

$$\begin{aligned}
\chi^\sigma(M,\hat{\alpha}_s) &= \hat{\alpha}_s\chi_0\left(M+\tfrac{1}{2}\hat{\alpha}_s\chi_0^\sigma(M)+\tfrac{1}{2}\hat{\alpha}_s^2\chi_1^\sigma(M)\right)\\
&\quad +\hat{\alpha}_s^2\chi_1\left(M+\tfrac{1}{2}\hat{\alpha}_s\chi_0^\sigma(M)\right)+\hat{\alpha}_s^3\chi_2(M)+O(\hat{\alpha}_s^4)\\
&= \hat{\alpha}_s\chi_0\left(M+\tfrac{1}{2}\hat{\alpha}_s\chi_0^\sigma(M)\right)+\hat{\alpha}_s^3\chi_0'\left(M+\tfrac{1}{2}\hat{\alpha}_s\chi_0^\sigma(M)\right)\tfrac{1}{2}\chi_1^\sigma(M)\\
&\quad +\hat{\alpha}_s^2\chi_1(M)+\hat{\alpha}_s^3\chi_1'(M)\tfrac{1}{2}\chi_0^\sigma(M)+\hat{\alpha}_s^3\chi_2(M)+O(\hat{\alpha}_s^4)\,, \qquad (6.44)
\end{aligned}$$

where on the right-hand side the Σ index has been dropped for simplicity. The first term in the previous equation must be computed by carefully keeping operator ordering into account. This can be done by using the operator technique previously described

$$\begin{aligned}
&\chi_0(M+\tfrac{1}{2}\hat{\alpha}_s\chi_0^\sigma(M)) = e^{\frac{1}{2}\hat{\alpha}_s\chi_0^\sigma(M)\frac{d}{d\lambda}+\frac{1}{2}\left[M,\frac{1}{2}\hat{\alpha}_s\chi_0^\sigma(M)\right]\frac{d^2}{d\lambda^2}+\ldots}\chi_0(M+\lambda)|_{\lambda=0}\\
&=\chi_0(M)+\tfrac{1}{2}\hat{\alpha}_s\chi_0^\sigma(M)\chi_0'(M)+\tfrac{1}{4}\left[M,\hat{\alpha}_s\chi_0^\sigma(M)\right]\chi_0''(M)+\tfrac{1}{8}\hat{\alpha}_s^2{\chi_0^\sigma}^2(M)\chi_0''(M)+O(\hat{\alpha}_s^3)\\
&=\chi_0(M)+\tfrac{1}{2}\hat{\alpha}_s\chi_0^\sigma(M)\chi_0'(M)-\tfrac{1}{4}\beta_0\hat{\alpha}_s^2\chi_0^\sigma(M)\chi_0''(M)+\tfrac{1}{8}\hat{\alpha}_s^2{\chi_0^\sigma}^2(M)\chi_0''(M)+O(\hat{\alpha}_s^3)\,.
\end{aligned} \qquad (6.45)$$

The contributions to the kernel in symmetric variables are

$$\begin{aligned}
\chi_0^\sigma(M) &= \chi_0(M)\,,\\
\chi_1^\sigma(M) &= \chi_1(M)+\tfrac{1}{2}\chi_0'(M)\chi_0(M)\,,\\
\chi_2^\sigma(M) &= \chi_2(M)+\tfrac{1}{2}\chi_1'(M)\chi_0(M)+\tfrac{1}{2}\chi_0'(M)\chi_1(M)\,,\\
&\quad +\tfrac{1}{2}\chi_0'(M)^2\chi_0(M)+\tfrac{1}{8}\chi_0''(M){\chi_0}^2(M)-\tfrac{1}{4}\beta_0\chi_0''(M)\chi_0(M)\,.
\end{aligned} \qquad (6.46)$$

In order to determine the constant term of χ_1 and the simple pole of χ_2 in symmetric variables, one has to substitute the expansion of χ_0 up to $O(M^2)$. In principle the linear term of χ_1 is needed too, but its dependence cancels out in the expression for χ_2. Using the expressions eq. (6.42) for the unintegrated Q_0 scheme kernels $\chi_i^{Q_0}$ one

finally obtains

$$\begin{aligned}
\chi_0^\sigma(M) &= \frac{g_{0,-1}}{M} + O(M^2)\,, \\
\chi_1^\sigma(M) &= -\frac{(g_{0,-1})^2}{2M^3} + \frac{g_{0,0}g_{0,-1}}{M^2} + \frac{g_{1,-1}}{M} + \frac{g_{2,-2}}{g_{0,-1}} + g_{0,-1}^2\zeta(3) + O(M)\,, \\
\chi_2^\sigma(M) &= \frac{(g_{0,-1})^3}{2M^5} - \frac{3g_{0,0}(g_{0,-1})^2 + \beta_0(g_{0,-1})^2}{2M^4} + \frac{(g_{0,0})^2 g_{0,-1} + g_{0,1}(g_{0,-1})^2 - g_{0,-1}g_{1,-1}}{M^3} \\
&\quad + \frac{-\frac{1}{2}g_{2,-2} + g_{0,0}g_{1,-1} + g_{0,-1}\bar{g}_{1,0}}{M^2} + \frac{\bar{g}_{2,-1} - 2\beta_0(g_{0,-1})^2\zeta(3)}{M} + O(M^0)\,.
\end{aligned} \tag{6.47}$$

The previous equation explicitly shows that the BFKL kernel in symmetric variables has collinear poles of higher order, than one would expect from duality. The NLO kernel behaves as $\chi_1^\sigma \sim -1/M^3$, and the NNLO one as $\chi_2^\sigma \sim 1/M^5$. Clearly this is the main source of instability of the perturbative expansion: the order of the leading pole increases with alternating sign. This feature also ensures that the NNLO has the same qualitative behaviour of the LO.

The symmetry of the kernel implies that $\chi(M, \hat{\alpha}_s)$ must admit an expansion of the form

$$\begin{aligned}
\chi(M, \hat{\alpha}_s) &= \hat{\alpha}_s\chi_0^\sigma(M) + \hat{\alpha}_s^2\chi_1^\sigma(M) + \hat{\alpha}_s^3\chi_2^\sigma(M) + O(\hat{\alpha}_s^3) \\
&= \chi_0^{sym}(M, \hat{\alpha}_s) + \chi_1^{sym}(M, \hat{\alpha}_s) + \chi_2^{sym}(M, \hat{\alpha}_s) + O(\hat{\alpha}_s^3)\,,
\end{aligned} \tag{6.48}$$

where $\chi_i^{sym}(M, \hat{\alpha}_s)$ are symmetrised functions, obtained exploiting the $M \leftrightarrow 1 - M$, with a symmetric choice for the running coupling:

$$\begin{aligned}
\chi_0^{sym}(M, \hat{\alpha}_s) &= c_{0,-1}\left[\hat{\alpha}_s\frac{1}{M} + \frac{1}{1-M}\hat{\alpha}_s\right] + \hat{\alpha}_s c_{0,0} + c_{0,1}\left[\hat{\alpha}_s M + (1-M)\hat{\alpha}_s\right] \\
&\quad + c_{0,2}\left[\hat{\alpha}_s M^2 + (1-M)^2\hat{\alpha}_s\right] + O(M^3)\,, \\
\chi_1^{sym}(M, \hat{\alpha}_s) &= c_{1,-3}\left[\hat{\alpha}_s^2\frac{1}{M^3} + \frac{1}{(1-M)^3}\hat{\alpha}_s^2\right] + c_{1,-2}\left[\hat{\alpha}_s^2\frac{1}{M^2} + \frac{1}{(1-M)^2}\hat{\alpha}_s^2\right] \\
&\quad + c_{1,-1}\left[\hat{\alpha}_s^2\frac{1}{M} + \frac{1}{1-M}\hat{\alpha}_s^2\right] + \hat{\alpha}_s c_{1,0} + c_{1,1}\left[\hat{\alpha}_s^2 M + (1-M)\hat{\alpha}_s^2\right] \\
&\quad + O(M^2)\,, \\
\chi_2^{sym}(M, \hat{\alpha}_s) &= \sum_{j=1,5} c_{2,-j}\left[\hat{\alpha}_s^3\frac{1}{M^j} + \frac{1}{(1-M)^j}\hat{\alpha}_s^3\right] + O(M^0)\,.
\end{aligned} \tag{6.49}$$

It is then possible to determine the symmetrised kernel with the running coupling operator canonically ordered on the left, which corresponds to the choice $\alpha_s = \alpha_s(Q^2)$. This choice modifies the residues of the anticollinear poles, thereby breaking the

symmetry, as already observed in eq. (2.113) for the NLO kernel. One obtains

$$\begin{aligned}
\hat{\alpha}_s\bar{\chi}_0^{sym}(M) &= \chi_0^{sym}(M,\hat{\alpha}_s)\,,\\
\hat{\alpha}_s^2\bar{\chi}_1^{sym}(M) &= \chi_1^{sym}(M,\hat{\alpha}_s) - \hat{\alpha}_s^2\beta_0\frac{c_{0,-1}}{(1-M)^2} + \beta_0\hat{\alpha}_s^2(c_{0,1}+2c_{0,2}) + O(M)\,,\\
\hat{\alpha}_s^3\bar{\chi}_2^{sym}(M) &= \chi_2^{sym}(M,\hat{\alpha}_s) - \hat{\alpha}_s^3\beta_0\beta_1\frac{c_{0,-1}}{(1-M)^2} + 2\hat{\alpha}_s^3\beta_0^2\frac{c_{0,-1}}{(1-M)^3}\\
&- 2\hat{\alpha}_s^3\beta_0\frac{c_{1,-1}}{(1-M)^2} - 4\hat{\alpha}_s^3\beta_0\frac{c_{1-2}}{(1-M)^3} - 8\hat{\alpha}_s^3\beta_0\frac{c_{1-3}}{(1-M)^4} + O(M^0)\,.
\end{aligned} \tag{6.50}$$

In order to compute the coefficients c_{ij} in eq. (6.49) one can equate the Laurent series about $M = 0$ of the symmetrised kernel eq. (6.50) to the expansion of the unsymmetrised kernels χ_i^σ eq. (6.47), which is accurate to the stated power of M. Because the anticollinear terms with poles at $M = 1$ are regular in $M = 0$, the symmetrised χ_i^{sym} have the same $M = 0$ poles as their unsymmetrised counterparts and their residues can be read off eq. (6.47). However, the anticollinear terms do contribute to all regular terms in the expansion of χ_i^σ about $M = 0$. This is why higher–order regular terms must be included in the right-hand side of eq. (6.49): specifically, symmetric terms up to $O(M^2)$ must be included in $\chi_0^{sym}(M)$ in order for its expansion to coincide with that of $\chi_0^\sigma(M)$ up to and including $O(M)$; one finds:

$$c_{0,0} = -\tfrac{3}{2}g_{0,-1}, \qquad c_{0,1} = 0, \qquad c_{0,2} = \tfrac{1}{2}g_{0,-1}\,; \tag{6.51}$$

terms up to $O(M)$ must be considered in $\chi_1^{sym}(M)$ in order for its expansion to coincide with that of $\chi_1^\sigma(M)$ up to and including $O(M^0)$:

$$c_{1,0} = \tfrac{g_{2,-2}}{g_{0,-1}} + (g_{0,-1})^2\zeta(3), \qquad c_{1,1} = \tfrac{1}{2}(g_{0,-1})^2 - g_{0,-1}g_{0,0} - g_{1,-1}\,. \tag{6.52}$$

No addition is necessary for χ_2 because the known coefficients in its expansion about $M = 0$ are all singular.

Substituting the explicit values for the coefficients c_{ij} into eq. (6.50), one determines the approximate expression for the BFKL kernel up to NNLO, at the unintegrated level in the Q_0 scheme, in symmetric variables, with $\alpha_s = \alpha_s(Q^2)$. The LO kernel of course does not depend on either the scheme, the choice of variables, or the running of the coupling:

$$\chi_0(M) = \tfrac{C_A}{\pi}\left(\tfrac{1}{M} + \tfrac{1}{(1-M)} - 1 - M(1-M)\right)\,; \tag{6.53}$$

the NLO kernel corresponds to the widely used form of the kernel as given in [34]:

$$\begin{aligned}\chi_1(M) &= -\frac{C_A^2}{2\pi^2}\Big(\frac{1}{M^3}+\frac{1}{(1-M)^3}\Big)+\frac{C_A}{\pi}\Big(-\frac{11C_A}{12\pi}-\frac{n_f}{6\pi}+\frac{C_F n_f}{3\pi C_A}\Big)\Big(\frac{1}{M^2}+\frac{1}{(1-M)^2}\Big)\\ &-\frac{C_A}{\pi}\beta_0\frac{1}{(1-M)^2}+\Big(\frac{13C_F n_f}{18\pi^2}-\frac{23C_A n_f}{36\pi^2}\Big)\Big(\frac{1}{M}+\frac{1}{1-M}\Big)\\ &+\Big(\frac{C_A^2\zeta(3)}{\pi^2}-\frac{\zeta(3)C_A^2}{2\pi^2}+\frac{11C_A^2}{72}-\frac{395C_A^2}{108\pi^2}+\frac{C_A n_f}{36}-\frac{71C_A n_f}{108\pi^2}-\frac{C_F n_f}{18}\\ &+\frac{71C_F n_f}{54\pi^2}+\beta_0\frac{C_A}{\pi}\Big)+\frac{C_A^2}{2\pi^2}-\frac{C_A}{\pi}\Big(-\frac{11C_A}{12\pi}-\frac{n_f}{6\pi}+\frac{C_F n_f}{3\pi C_A}\Big)\\ &-\Big(\frac{13C_F n_f}{18\pi^2}-\frac{23C_A n_f}{36\pi^2}\Big)-\frac{C_A}{\pi}\beta_0 M\,; \end{aligned} \tag{6.54}$$

it has been checked that the Laurent expansions of eq. (6.54) about $M=0$ and $M=1$ coincides with the expansions of the complete result up to and including $\mathcal{O}(1)$ terms. The NNLO kernel is a new result:

$$\begin{aligned}\chi_2(M) &= \frac{C_A^3}{2\pi^3}\Big(\frac{1}{M^5}+\frac{1}{(1-M)^5}\Big)-\frac{C_A^2}{2\pi^2}\Big(-\frac{11C_A}{4\pi}-\frac{n_f}{2\pi}+\frac{C_F n_f}{\pi C_A}+\beta_0\Big)\Big(\frac{1}{M^4}+\frac{1}{(1-M)^4}\Big)\\ &+4\beta_0\frac{C_A^2}{\pi^2}\frac{1}{(1-M)^4}+\frac{C_A}{\pi}\Big[\Big(-\frac{11C_A}{12\pi}-\frac{n_f}{6\pi}+\frac{C_F n_f}{3\pi C_A}\Big)^2\\ &+\frac{C_A}{\pi}\Big(-\frac{C_F^2 n_f^2}{9C_A^3\pi}+\frac{C_F n_f^2}{18C_A^2\pi}-\frac{11C_F n_f}{36C_A\pi}-\frac{C_A\pi}{6}+\frac{67C_A}{36\pi}\Big)-\Big(\frac{13C_F n_f}{18\pi^2}-\frac{23C_A n_f}{36\pi^2}\Big)\Big]\\ &\cdot\Big(\frac{1}{M^3}+\frac{1}{(1-M)^3}\Big)+2\frac{C_A}{\pi}\beta_0\Big(\beta_0+\frac{11C_A}{6\pi}+\frac{n_f}{3\pi}-\frac{2C_F n_f}{3\pi C_A}\Big)\frac{1}{(1-M)^3}\\ &+\Big[-\frac{1}{2}\Big(\frac{C_A^3\zeta(3)}{2\pi^3}+\frac{11C_A^3}{72\pi}-\frac{395C_A^3}{108\pi^3}+\frac{C_A^2 n_f}{36\pi}-\frac{71C_A^2 n_f}{108\pi^3}-\frac{C_A C_F n_f}{18\pi}+\frac{71C_A C_F n_f}{54\pi^3}\Big)\\ &+\Big(-\frac{11C_A}{12\pi}-\frac{n_f}{6\pi}+\frac{C_F n_f}{3\pi C_A}\Big)\Big(\frac{13C_F n_f}{18\pi^2}-\frac{23C_A n_f}{36\pi^2}\Big)\\ &+\frac{C_A}{\pi}\Big(-\frac{2\zeta(3)C_A^2}{\pi^2}+\frac{1643C_A^2}{216\pi^2}-\frac{11C_A^2}{36}+\frac{43C_A n_f}{54\pi^2}+\frac{C_F n_f}{18}-\frac{547C_F n_f}{216\pi^2}+\frac{13C_F n_f^2}{108\pi^2 C_A}\\ &+\frac{C_F^2 n_f}{4\pi^2 C_A}-\frac{13C_F^2 n_f^2}{54\pi^2 C_A^2}+\beta_0\Big(\frac{67}{12\pi}+\frac{7n_f}{81\pi}\Big)\Big)+\frac{3\zeta(3)C_A^3}{2\pi^3}\Big]\Big(\frac{1}{M^2}+\frac{1}{(1-M)^2}\Big)\\ &-\beta_0\Big(\frac{C_A}{\pi}\beta_1+2\Big(\frac{13C_F n_f}{18\pi^2}-\frac{23C_A n_f}{36\pi^2}\Big)\Big)\frac{1}{(1-M)^2}\\ &+\Big[-\frac{143\zeta(3)C_A^3}{24\pi^3}-\frac{29\pi C_A^3}{720}-\frac{389C_A^3}{432\pi}+\frac{73091C_A^3}{2592\pi^3}-\frac{11C_A^2\zeta(3)n_f}{12\pi^3}-\frac{C_A^2 n_f}{9\pi}\\ &+\frac{301C_A^2 n_f}{81\pi^3}+\frac{8\zeta(3)C_A C_F n_f}{3\pi^3}+\frac{35C_A C_F n_f}{108\pi}+\frac{59C_A n_f^2}{648\pi^3}-\frac{28853C_A C_F n_f}{2592\pi^3}\\ &-\frac{2\zeta(3)C_F^2 n_f}{3\pi^3}-\frac{65C_F n_f^2}{324\pi^3}+\frac{11C_F^2 n_f}{12\pi^3}-\beta_0\dot{g}_{1-1}+\beta_0^2\frac{\pi^2}{12}-2\beta_0\frac{\zeta(3)C_A^2}{\pi^2}\Big]\Big(\frac{1}{M}+\frac{1}{1-M}\Big)\,. \end{aligned} \tag{6.55}$$

The BFKL kernel is plotted as a function of M in fig. 6.2. The LO and NLO are exact while the NNLO contains the approximate expression for χ_2 eq. (6.55). Because of the positive sign of the residue of the dominant singularity both in $M=0$ and $M=1$, the NNLO kernel has a minimum for every value of the strong coupling. This minimum determines the high energy asymptotic behaviour; thus, the NNLO kernel has better stability properties than the NLO one. The expression of the collinear approximation of the kernel in asymmetric variables can be computed inverting eq. (6.46); the kernel at the integrated level is found using eq. (6.23). Explicit results are collected in

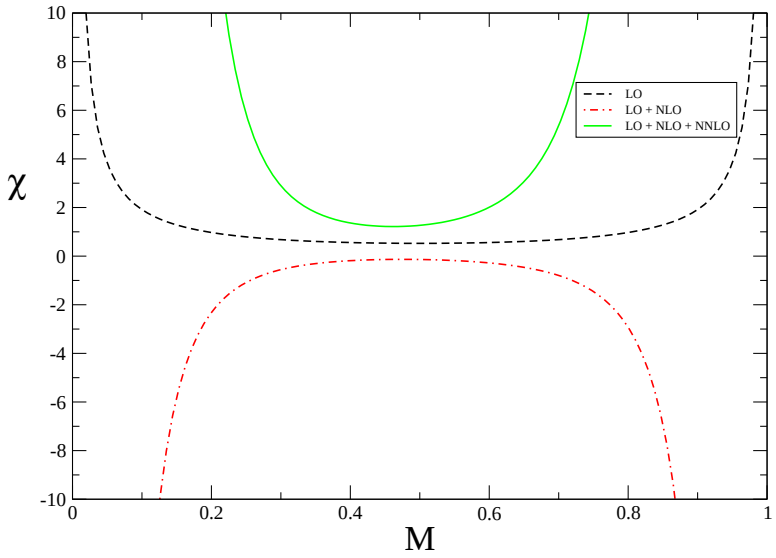

Figure 6.2: The full BFKL kernel at leading, next-to-leading, and next-to-next-to leading order obtained combining the known expressions for the LO and NLO contributions and the approximate expression (with $\dot{g}_{1,-1} = 0$) for NNLO eq. (6.55), with $\hat{\alpha}_s \to 0.2$, $n_f = 4$. The kernel is in the Q_0 scheme, at the unintegrated level with symmetric variables, and $\alpha_s = \alpha_s(Q^2)$. The symmetry about $M = \frac{1}{2}$ is only broken by the argument of the running coupling. The LO and NLO kernels are the same as in fig. 2.6.

Appendix C. In figure 6.3 the Pomeron intercept $c(\alpha_s) = \chi(\frac{1}{2}, \alpha_s)$ is plotted as a function of the coupling constant. The inclusion of the NNLO contribution improves the convergence of the perturbative expansion; however, for values of the coupling constant relevant for phenomenology (say $\alpha_s \gtrsim 0.1$) the series has yet to converge.

The Laurent series of the BFKL kernel in $M = 0$ and $M = 1$ have radius of convergence one. Thus one expects the approximate calculations to do well over the central region $0 \leq M \leq 1$, but to break down as $M \to -1$, $M \to 2$. In figure 6.4 the collinear approximations of χ_0, eq. (6.53) and χ_1, eq. (6.54), are plotted together with the full LO and NLO results. In both cases the curves are almost indistinguishable in the all region $0 < M < 1$. This analysis can be quantified by plotting the relative difference between the exact and approximate results $\Delta =$ (exact-approximate)/exact, as in figure 6.5. The agreement is excellent close to $M = 0$ and $M = 1$, and even in the central region the difference between the collinear approximation and the full result is at the percent level; the approximation breaks down as $M \to -1$, $M \to 2$. Hence it is possible to conclude that, at leading twist, the collinear kernel is a very good approximation to the full LO and NLO ones. For this reason one would expect the result for χ_2 to be a good approximation, within a few per cent, of the complete

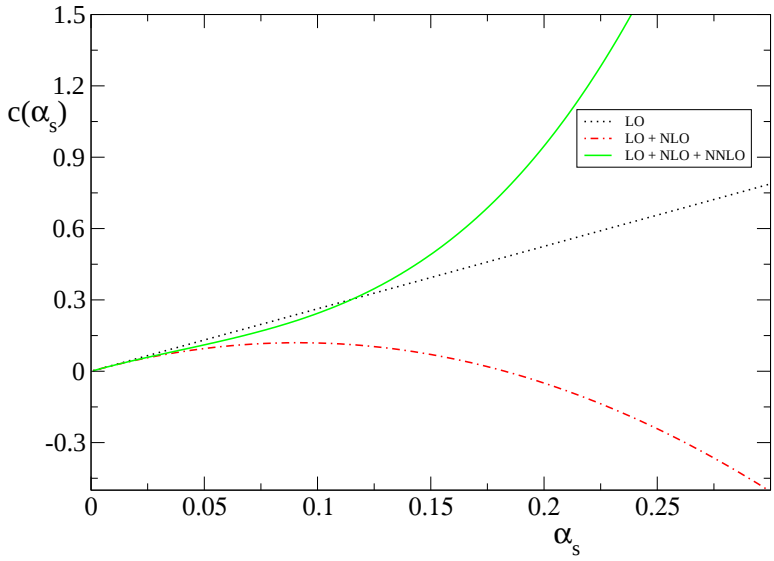

Figure 6.3: The BFKL intercept $c(\alpha_s) = \chi(\frac{1}{2}, \alpha_s)$ at leading, next-to-leading, and next-to-next-to-leading order, obtained with χ in symmetric variables and with a symmetric argument for the running coupling as in eq. (6.49). The LO and NLO results are the same as in fig. 2.7.

result in the region $0 < M < 1$.

Finally, the uncertainty due to the the unknown coefficient $\dot{g}_{1,-1}$ in the scheme change $\mathcal{R}$ is estimated in figure 6.6. This coefficient affects the simple (sub-subleading) poles, and has therefore a moderate impact. Noting that all the scheme-change coefficients are of order one, it is possible to estimate the uncertainty by varying $-5 \leq \dot{g}_{1,-1} \leq 5$. It is seen to be similar to the uncertainty of a few percent that one might expect to affect the approximate form of χ_2, on the basis of the LO and NLO results.

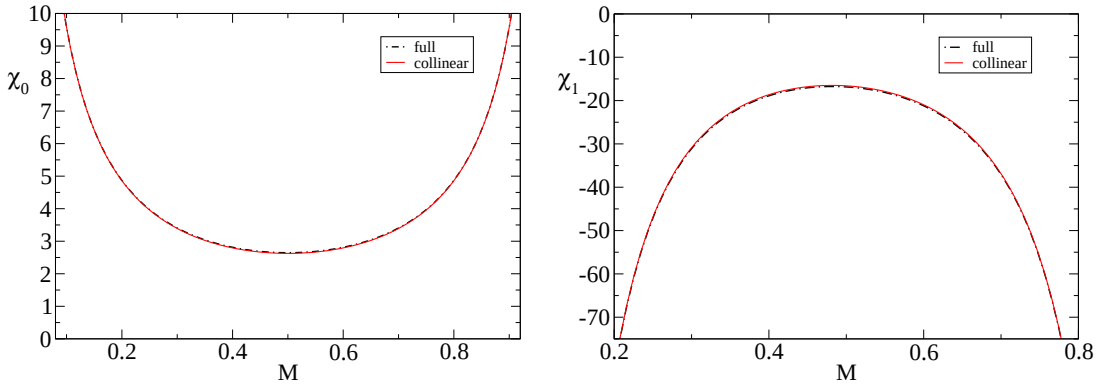

Figure 6.4: Comparison of the exact (dot-dash) and approximate expressions (solid red) of the LO and NLO contributions to the BFKL kernels $\chi_0(M)$ on the left and $\chi_1(M)$ on the right.

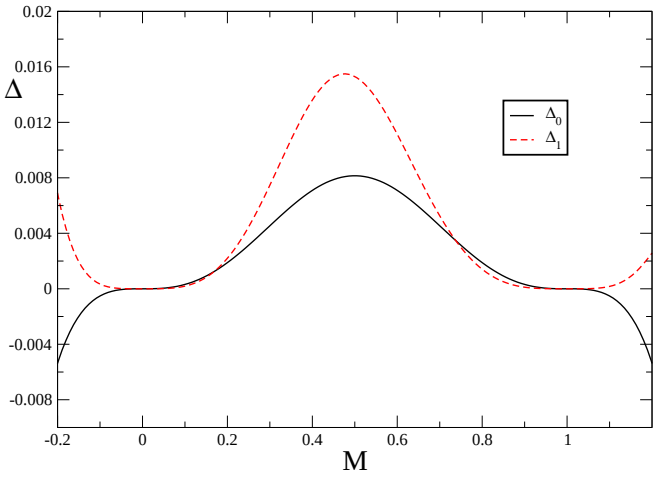

Figure 6.5: The relative differences Δ = (exact-approximate)/exact for the leading order kernel (Δ_0, solid black) and the next-to-leading kernel (Δ_1, dashed red), plotted as a function of M. The discrepancy in the region $0 < M < 1$ is at the percent level in both cases.

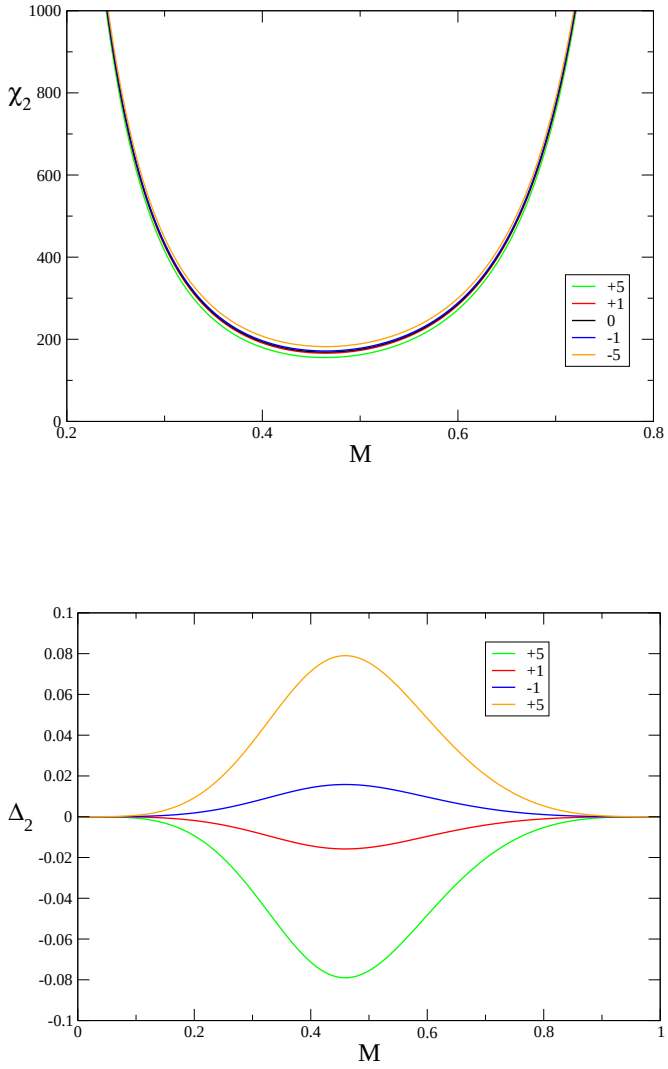

Figure 6.6: These plots assess the uncertainty on the approximate NNLO kernel in the Q_0 scheme due to the unknown coefficient in the $\mathcal{R}$ scheme change. On the top the NNLO contribution χ_2 is plotted as a function of M, varying the coefficient $\dot{g}_{1,-1}$ between 5 and -5. On the bottom the relative uncertainty with respect to the choice $\dot{g}_{1,-1} = 0$.

Chapter 7

Conclusions and Outlook

As pointed out several times in this thesis, the search for new physics at hadron colliders requires precise results in QCD phenomenology. The theoretical uncertainties in cross sections for hadron-hadron collisions can be reduced by computing higher order contributions in perturbative QCD, both at fixed order and at the resummed level. Particularly at high energy colliders such as the LHC, it is important to control both the collinear and high energy logarithms. In the past years different groups have intensively studied the evolution of parton distribution functions at high energy. In this thesis the ABF approach has been discussed in some detail. Thanks to these results evolution kernels which resum both collinear and high energy logarithms are now available. However a resummed evolution is not enough to produce resummed hadronic cross sections because high energy effects on the partonic cross section have to be considered too. This can be achieved by considering processes in the framework of k_T-factorisation and matching these results to standard fixed order calculations, obtained in collinear factorisation. Before the work carried out in this thesis, resummed results existed for deep inelastic scattering [46], heavy quark production [44], [48] and Higgs production via gluon gluon fusion in the heavy top limit [97]. However, this last result suffers of a spurious double logarithmic growth at high energy. In this thesis the partonic coefficient functions for Drell-Yan processes and Higgs boson production with finite top mass have been computed.

7.1 Drell-Yan and vector boson production

The leading singularities of the D_{qg} and D_{qq} coefficient functions have been computed to all orders for Drell-Yan cross sections and vector boson production. The production of a lepton pair via the Drell-Yan mechanism can, in principle, receive significant contributions from high energy resummation, because the invariant mass of the final state can be fairly low and hence logarithms of the ratio $m^2_{l\bar{l}}/s$ can be large. Furthermore

the $W^{\pm}$ and the Z cross sections are meant to be used as normalisation for the other cross sections and as a real-time monitor for the luminosity. These tasks require a precision in the computation at the percent level and high energy corrections play a relevant role [51]. In order to make these statements quantitative one has to compute the hadronic cross sections for these quantities, using parton distribution functions with high energy evolution.

It has been shown that the logarithms in the gluon-gluon channels are formally subleading because of the extra power of the coupling constant. Nevertheless it would be important to compute such contributions because the singlet distribution is relatively suppressed compared to the gluon density in the high energy limit. This implies that the contributions from D_{gg} might be effectively as important as the ones which have been computed in this thesis.

7.2 Higgs production

The leading behaviour at high energy of the partonic coefficient function for Higgs production via gluon gluon fusion has been computed to all orders in the strong coupling. It has been shown that the high energy behaviour obtained keeping the top mass finite is the one expected from k_T-factorisation and BFKL arguments. This is in contrast to the infinite top mass approximation, where the coefficient function exhibits double high energy logarithms. The result which has been obtained is expressed in form of an impact factor eq. (5.43), whose Taylor expansion provides the high energy singularities order by order in perturbation theory. The coefficients can be expressed in terms of double integrals, which have been numerically evaluated up to $\mathrm{N}^4\mathrm{LO}$.

An approximation to the exact and as yet unknown NNLO coefficient function has been constructed by combining the pointlike approximation at large τ with the exact small τ behaviour. Some care must be taken in the matching procedure and in the treatment of the subleading contributions. The effect of high energy terms on the total inclusive hadronic cross section remains moderate, because the latter is dominated by the region of low partonic centre–of–mass energy, partly due to shape of the gluon parton distributions, which are peaked in the region where the gluons carry a small fraction of the incoming nucleon's energy, and partly because the partonic cross section is peaked in the threshold $\tau \sim 1$ region. Even so, one can claim that hard effects on the inclusive cross section are now under control.

The approximation to the coefficient function presented in this thesis can be used to study less inclusive objects such as the rapidity distribution, which presently has been computed only in the $m_t \to \infty$ limit [104], [105]. An interesting idea would be to use resummed results to estimate unknown higher-order contributions. Specifically one can combine, order by order in perturbation theory, the high energy tail of the partonic

coefficient function to the $\tau \to 1$ behaviour obtained with soft resummation techniques, constraining the result also for values of τ away from the asymptotic regions.

7.3 Approximate BFKL kernel

The idea of constructing approximate fixed-order results from resummed ones can be also applied to the evolution kernels. In this thesis an approximate expression for the NNLO BFKL kernel has been obtained. In principle the DGLAP anomalous dimension determines, through duality, the collinear singularities of the BFKL kernel to all orders in perturbation theory. However the calculation is not straightforward because, beyond leading order, various issues which affect the determination of the BFKL kernel arise. Specifically it has been necessary to study the relation between the $\overline{\rm MS}$ and Q_0 factorisation schemes, the running-coupling corrections to duality, the choice of kinematic variables in the definition of the BFKL kernel, the relation between the form of the BFKL kernel and the argument of the running coupling and, finally, the relation between BFKL kernels for integrated and unintegrated parton distributions. All these issues become rather nontrivial at next-to-next-to leading order. Because the perturbative expansion of the BFKL kernel in both the collinear and anticollinear regions is alternating in sign, a knowledge of NNLO corrections is necessary for an accurate assessment of the uncertainty involved in a fixed–order determination of the kernel: indeed, whereas the qualitative features of the NLO kernel are completely different from those of the LO, the NNLO result is qualitatively similar, though it is quantitatively not so reliable because of the slow convergence of the perturbative expansion, even in the central region away from the singularities. As a final remark the approximate form of the LO and NLO kernels given in eq. (6.53) and eq. (6.54) are extremely accurate while having a very simple analytic form, and they can be easily used in numerical and phenomenological implementations.

7.4 Outlook

In this thesis the high energy resummation of partonic coefficient functions of processes, relevant for LHC phenomenology, has been presented. Now one can use use these expressions, together with resummed parton distributions, to compute hadronic cross sections. In order to achieve this, it is important to include running coupling effects into the resummation, with the techniques explained in section 3.3. Finally, high energy resummation has been discussed in this thesis for inclusive cross sections. It would be important to extend this formalism to differential quantities, such as, for instance, rapidity and transverse momentum distributions.

Appendix A

Kinematics of $2 \to 2$ processes

A.1 d-dimensional two-body phase space

The d-dimensional two-body phase space for a process like

$$a(p_1) + b(p_2) \to c(p_3) + d(p_4)$$

can be written as

$$\begin{aligned} d\Phi^{(2)} &= \frac{d^{d-1}p_3}{(2\pi)^{d-1}\,2E_3}\frac{d^{d-1}p_4}{(2\pi)^{d-1}\,2E_4}(2\pi)^d\delta^{(d)}(p_1+p_2-p_3-p_4) \\ &= 2^{-d}\pi^{2-d}\frac{d^{d-1}p_1}{E_3E_4}\delta(E_1+E_2-E_3-E_4). \end{aligned} \tag{A.1}$$

In the centre-of-mass frame, the delta function can be expressed in the following form:

$$\begin{aligned} \delta(E-E_3+E_4) &= \delta\left(E-\sqrt{|\vec{p}_3|^2+m_3^2}-\sqrt{|\vec{p}_4|^2+m_4^2}\right) \\ &= \frac{E_3E_4}{|\vec{p}_1|\,E}\delta\left(|\vec{p}_3|-\frac{\sqrt{\omega}}{2E}\right), \end{aligned} \tag{A.2}$$

where

$$E = E_1 + E_2\,, \tag{A.3}$$

and

$$\omega = E^4 + m_3^4 + m_4^4 - 2E^2m_3^2 - 2E^2m_4^2 - 2m_3^2m_4^2. \tag{A.4}$$

Using d-dimensional polar coordinates for $\vec{p}_3$, one obtains

$$\begin{aligned} d\Phi^{(2)} &= 2^{-d}\pi^{2-d}\,\frac{|\vec{p}_3|^{d-2}\,d\,|\vec{p}_3|\,d\Omega_{d-1}}{|\vec{p}_3|\,E}\,\delta\left(|\vec{p}_3|-\frac{\sqrt{\omega}}{2E}\right) \\ &= 2^{-d}\pi^{2-d}\,\left[\frac{\sqrt{\omega}}{2E}\right]^{d-3}\frac{1}{E}\,d\Omega_{d-1}\,. \end{aligned} \tag{A.5}$$

Since the invariant two-body squared amplitude only depends on one scattering angle, one can integrate over $d\Omega_{d-2}$, using the result

$$\Omega_p = \int d\Omega_p = \frac{2\pi^{p/2}}{\Gamma(p/2)}\,. \tag{A.6}$$

Thus the angular integration in $d = 4 - 2\varepsilon$ dimensions can be written as

$$d\Omega_{d-1} \to \Omega_{d-2}\, d\vartheta_{d-2} \sin^{d-3}\vartheta_{d-1} = \frac{2\pi^{1-\varepsilon}}{\Gamma(1-\varepsilon)}\, 2^{1-2\varepsilon}\, y^{-\varepsilon}(1-y)^{-\varepsilon}\, dy, \tag{A.7}$$

where the dimensionless variable y has been defined

$$y = \frac{1+\cos\vartheta_{d-2}}{2}; \qquad 0 \le y \le 1\,. \tag{A.8}$$

Finally the two body phase space takes the form

$$d\Phi^{(2)} = \frac{1}{8\pi}\,\frac{(4\pi)^{\varepsilon}}{\Gamma(1-\varepsilon)}\,\frac{\sqrt{\omega}}{E^2}\,\left[\frac{\omega}{E^2}\right]^{-\varepsilon}\, y^{-\varepsilon}(1-y)^{-\varepsilon}\, dy. \tag{A.9}$$

In the case of one-gluon emission in deep-inelastic scattering, analysed in Chapter 2, one has $m_3 = m_4 = 0$, and therefore

$$\omega_{\rm DIS} = E^4; \qquad E = \sqrt{\frac{Q^2(1-x)}{x}}. \tag{A.10}$$

So, in this case, the phase space is given by

$$d\Phi^{(2)} = \frac{1}{8\pi}\,\frac{(4\pi)^{\varepsilon}}{\Gamma(1-\varepsilon)}\left[\frac{Q^2(1-x)}{x}\right]^{-\varepsilon}\, y^{-\varepsilon}(1-y)^{-\varepsilon}\, dy. \tag{A.11}$$

In the case of Drell-Yan at NLO, one has $m_3 = 0$, $m_4^2 = Q^2$:

$$\omega_{\rm DY} = s^2 + Q^4 - 2sQ^2 = \frac{Q^4(1-x)^2}{x^2}; \qquad E = \sqrt{s} = \frac{Q}{\sqrt{x}}, \tag{A.12}$$

which gives

$$d\Phi^{(2)} = \frac{1}{8\pi}\,\frac{(4\pi)^{\varepsilon}}{\Gamma(1-\varepsilon)}\,(1-x)\,\left[\frac{Q^2(1-x)^2}{x}\right]^{-\varepsilon}\, y^{-\varepsilon}(1-y)^{-\varepsilon}\, dy. \tag{A.13}$$

A.2 Kinematics of off-shell processes

For calculations in k_T-factorisation one has to consider processes with initial off-shell gluons

$$g^*(k_1) + g^*(k_2) \to c(p_3) + d(p_4)\,.$$

It is useful to introduce Sudakov parametrisation of the four-momenta

$$\begin{aligned} k_1 &= x_1 p_1 + \mathbf{k}_1 \\ k_2 &= x_2 p_2 + \mathbf{k}_2 \\ p_3 &= z_1 x_1 p_1 + (1-z_2) x_2 p_2 + \mathbf{p} \\ p_4 &= (1-z_1) x_1 p_1 + z_2 x_2 p_2 + \mathbf{k}_1 + \mathbf{k}_2 - \mathbf{p}\,, \end{aligned} \tag{A.14}$$

where p_1 and p_2 are lightlike momenta and $\mathbf{k}_i$ and $\mathbf{p}$ are transverse. The centre-of-mass energy is given by the Mandelstam variable

$$\hat{s} = (k_1 + k_2)^2 = \nu - |\mathbf{k}_1 + \mathbf{k}_2|^2\,, \tag{A.15}$$

where $\nu = 2 x_1 x_2 p_1 \cdot p_2$. The phase-space becomes

$$\begin{aligned} d\Phi^{(2)} &= \frac{d^4 p_3}{(2\pi)^3} \frac{d^4 p_4}{(2\pi)^3}\, \delta(p_3^2 - m_3^2)\delta(p_4^2 - m_4^2)(2\pi)^4 \delta^{(4)}(k_1 + k_2 - p_3 - p_4) = \\ &= \frac{d^4 p_3}{(2\pi)^2}\, \delta(p_3^2 - m_3^2)\, \delta(p_4^2 - m_4^2) = \\ &= \frac{1}{4\pi^2} \frac{\nu}{2} dz_1 dz_2 d^2\mathbf{p}\, \delta((1-z_2) z_1 \nu - |\mathbf{p}|^2) \\ &\quad \times \delta((1-z_1) z_2 \nu - |\mathbf{k}_1 + \mathbf{k}_2 - \mathbf{p}|^2)\,, \end{aligned} \tag{A.16}$$

where the factor $\nu/2$ is the Jacobian for the transformation from Cartesian to Sudakov coordinates.

Appendix B

Form factors for $g^*g^* \to H$

In this appendix the explicit expressions for the form factors, which appear in the Higgs production cross section, are collected:

$$\begin{aligned}
A_1(\xi_1,\xi_2,y_t) &= C_0(\xi_1,\xi_2,y_t)\Big[\frac{4y_t}{\Delta_3}(1+\xi_1+\xi_2)-1-\frac{4\xi_1\xi_2}{\Delta_3} \\
&\quad +12\frac{\xi_1\xi_2}{\Delta_3^2}(1+\xi_1+\xi_2)\Big] \\
&- [B_0(-\xi_2)-B_0(1)]\left[-\frac{2\xi_2}{\Delta_3}+12\frac{\xi_1\xi_2}{\Delta_3^2}(1+\xi_1-\xi_2)\right] \\
&- [B_0(-\xi_1)-B_0(1)]\left[-\frac{2\xi_1}{\Delta_3}+12\frac{\xi_1\xi_2}{\Delta_3^2}(1-\xi_1+\xi_2)\right] \\
&+ \frac{2}{\Delta_3}\frac{1}{(4\pi)^2}(1+\xi_1+\xi_2)\,, \qquad \text{(B.1)} \\
A_2(\xi_1,\xi_2,y_t) &= C_0(\xi_1,\xi_2,y_t)\left[2y_t-\frac{1}{2}(1+\xi_1+\xi_2)+\frac{2\xi_1\xi_2}{\Delta_3}\right] \\
&+ [B_0(-\xi_2)-B_0(1)]\left[\frac{\xi_2}{\Delta_3}(1-\xi_1+\xi_2)\right] \\
&+ [B_0(-\xi_1)-B_0(1)]\left[\frac{\xi_1}{\Delta_3}(1+\xi_1-\xi_2)\right]+\frac{1}{(4\pi)^2}\,, \qquad \text{(B.2)}
\end{aligned}$$

with

$$\Delta_3 = 1+\xi_1^2+\xi_2^2-2\xi_1\xi_2+2(\xi_1+\xi_2) = (1+\xi_1+\xi_2)^2-4\xi_1\xi_2\,. \qquad \text{(B.3)}$$

The scalar integrals B_0 and C_0 are

$$\begin{aligned} B_0(\rho) &= -\frac{1}{8\pi^2}\sqrt{\frac{4y_t-\rho}{\rho}}\,\tan^{-1}\sqrt{\frac{\rho}{4y_t-\rho}}\,, \quad \text{if} \quad 0<\rho<4y_t\,; \\ B_0(\rho) &= -\frac{1}{16\pi^2}\sqrt{\frac{\rho-4y_t}{\rho}}\,\ln\frac{1+\sqrt{\frac{\rho}{\rho-4y_t}}}{1-\sqrt{\frac{\rho}{\rho-4y_t}}}\,, \quad \text{if} \quad \rho<0 \text{ or } \rho>4y_t\,; \end{aligned} \tag{B.4}$$

$$\begin{aligned} C_0(\xi_1,\xi_2) \equiv\ & \frac{1}{16\pi^2}\frac{1}{\sqrt{\Delta_3}}\Big\{ \ln(1-y_-)\ln\left(\frac{1-y_-\delta_1^+}{1-y_-\delta_1^-}\right) \\ & +\ln(1-x_-)\ln\left(\frac{1-x_-\delta_2^+}{1-x_-\delta_2^-}\right)+\ln(1-z_-)\ln\left(\frac{1-z_-\delta_3^+}{1-z_-\delta_3^-}\right) \\ & +\mathrm{Li}_2(y_+\delta_1^+)+\mathrm{Li}_2(y_-\delta_1^+)-\mathrm{Li}_2(y_+\delta_1^-)-\mathrm{Li}_2(y_-\delta_1^-) \\ & +\mathrm{Li}_2(x_+\delta_2^+)+\mathrm{Li}_2(x_-\delta_2^+)-\mathrm{Li}_2(x_+\delta_2^-)-\mathrm{Li}_2(x_-\delta_2^-) \\ & +\mathrm{Li}_2(z_+\delta_3^+)+\mathrm{Li}_2(z_-\delta_3^+)-\mathrm{Li}_2(z_+\delta_3^-)-\mathrm{Li}_2(z_-\delta_3^-) \quad \Big\}\,, \end{aligned} \tag{B.5}$$

where

$$\delta_1 \equiv \frac{-\xi_1+\xi_2-1}{\sqrt{\Delta_3}}\,, \quad \delta_2 \equiv \frac{\xi_1-\xi_2-1}{\sqrt{\Delta_3}}\,, \quad \delta_3 \equiv \frac{\xi_1+\xi_2+1}{\sqrt{\Delta_3}}\,, \tag{B.6}$$

$$\delta_i^\pm \equiv \frac{1\pm\delta_i}{2}\,, \tag{B.7}$$

and

$$\begin{aligned} x_\pm &\equiv -\frac{\xi_2}{2y_t}\left(1\pm\sqrt{1+\frac{4y_t}{\xi_2}}\right)\,, \\ y_\pm &\equiv -\frac{\xi_1}{2y_t}\left(1\pm\sqrt{1+\frac{4y_t}{\xi_1}}\right)\,, \\ z_\pm &\equiv \frac{1}{2y_t}\left(1\pm i\sqrt{4y_t-1}\right)\,. \end{aligned} \tag{B.8}$$

In the infinite top mass limit the scalar integrals become

$$\lim_{y_t\to\infty} B_0(\rho) = \frac{1}{16\pi^2}\left(-2+\frac{\rho}{6y_t}\right)+O\left(\frac{1}{y_t^2}\right)\,, \tag{B.9}$$

$$\lim_{y_t\to\infty} C_0(\xi_1,\xi_2) = -\frac{1}{32\pi^2 y_t}\left(1+\frac{1-\xi_1-\xi_2}{12y_t}\right)+O\left(\frac{1}{y_t^3}\right)\,. \tag{B.10}$$

In the on-shell limit the scalar integrals are

$$\begin{aligned}
\lim_{\xi_i \to 0} B_0(\xi_i) &= -\frac{1}{8\pi^2}\,, \\
\lim_{\xi_1 \to 0} C_0(\xi_1, \xi_2, y_t) &= \frac{1}{32\pi^2}\frac{1}{1+\xi_2}\left(\ln^2\frac{-z_-}{z_+} - \ln^2\frac{-x_-}{x_+}\right)\,, \\
\lim_{\xi_1, \xi_2 \to 0} C_0(\xi_1, \xi_2, y_t) &= \frac{1}{32\pi^2}\left(\ln^2\frac{-z_-}{z_+}\right)\,.
\end{aligned} \tag{B.11}$$

Appendix C

Explicit results for $\chi 2$

The coefficients of the expansion of the leading, next-to-leading and next-to-next-to-leading DGLAP anomalous dimensions in powers of N are easily determined by recalling that γ is the larger eigenvalue of the 2×2 anomalous dimension matrix, given by

$$\gamma = \frac{1}{2}\left[\gamma_{gg} + \gamma_{qq} + \sqrt{(\gamma_{gg} - \gamma_{qq})^2 + 8 n_f \gamma_{gq}\gamma_{qg}}\right], \tag{C.1}$$

and by using the expressions of γ_{ij} given in Refs. [14] and [16]. In the $\overline{\rm MS}$ scheme one obtains

$$\begin{aligned}
g_{0,-1} &= \frac{C_A}{\pi} \\
g_{0,0} &= -\frac{11C_A}{12\pi} + \left(-\frac{1}{6\pi} + \frac{C_F}{3\pi C_A}\right) n_f \\
g_{0,1} &= -\frac{C_A\pi}{6} + \frac{67C_A}{36\pi} - \frac{11C_F n_f}{36\pi C_A} + \left(-\frac{C_F^2}{9\pi C_A^3} + \frac{C_F}{18\pi C_A^2}\right) n_f^2 \\
g_{1,-1} &= \left(\frac{13C_F}{18\pi^2} - \frac{23C_A}{36\pi^2}\right) n_f \\
g_{1,0} &= -\frac{2\zeta(3)C_A^2}{\pi^2} + \frac{1643C_A^2}{216\pi^2} - \frac{11C_A^2}{36} + \left(\frac{43C_A}{54\pi^2} + \frac{C_F}{18} - \frac{547C_F}{216\pi^2} + \frac{C_F^2}{4\pi^2 C_A}\right) n_f \\
&\quad + \left(\frac{13C_F}{108\pi^2 C_A} - \frac{13C_F^2}{54\pi^2 C_A^2}\right) n_f^2 \\
g_{2,-2} &= \frac{\zeta(3)C_A^3}{2\pi^3} + \frac{11C_A^3}{72\pi} - \frac{395C_A^3}{108\pi^3} + \left(\frac{C_A^2}{36\pi} - \frac{71C_A^2}{108\pi^3} - \frac{C_F C_A}{18\pi} + \frac{71C_F C_A}{54\pi^3}\right) n_f \\
g_{2,-1} &= -\frac{143\zeta(3)C_A^3}{24\pi^3} - \frac{29\pi C_A^3}{720} - \frac{389C_A^3}{432\pi} + \frac{73091C_A^3}{2592\pi^3} + \left(-\frac{11\zeta(3)C_A^2}{12\pi^3} - \frac{C_A^2}{9\pi}\right. \\
&\quad \left. + \frac{301C_A^2}{81\pi^3} + \frac{8\zeta(3)C_F C_A}{3\pi^3} + \frac{35C_F C_A}{108\pi} - \frac{28853C_F C_A}{2592\pi^3} - \frac{2C_F^2\zeta(3)}{3\pi^3} + \frac{11C_F^2}{12\pi^3}\right) n_f \\
&\quad + \left(\frac{59C_A}{648\pi^3} - \frac{65C_F}{324\pi^3}\right) n_f^2 .
\end{aligned} \tag{C.2}$$

The explicit numerical expression for the approximate contributions to the kernel in symmetric variables can be found substituting the values of the Casimirs $C_A = 3$,

$C_F = \frac{4}{3}$ in eq. (6.55)–(6.55). One obtains:

$$\chi_0(M) = \tfrac{3}{\pi}\big(\tfrac{1}{M} + \tfrac{1}{1-M} - 1 - M(1-M)\big)\,, \tag{C.3}$$

$$\begin{aligned}\chi_1(M) \;=\;& -\tfrac{9}{2\pi^2}\big(\tfrac{1}{M^3} + \tfrac{1}{(1-M)^3}\big) - \big(\tfrac{33}{4\pi^2} + \tfrac{n_f}{18\pi^2}\big)\tfrac{1}{M^2} \\ & -\big(\tfrac{33}{2\pi^2} - \tfrac{4n_f}{9\pi^2}\big)\tfrac{1}{(1-M)^2} - \tfrac{103n_f}{108\pi^2}\big(\tfrac{1}{M} + \tfrac{1}{1-M}\big) \\ & +\tfrac{11}{8} + \tfrac{n_f}{108} - \tfrac{143}{12\pi^2} + \tfrac{47n_f}{162\pi^2} + \tfrac{27\zeta(3)}{2\pi^2} + M\big(-\tfrac{33}{4\pi^2} + \tfrac{n_f}{2\pi^2}\big)\,,\end{aligned} \tag{C.4}$$

$$\begin{aligned}\chi_2(M) \;=\;& \tfrac{27}{2\pi^3}\big(\tfrac{1}{M^5} + \tfrac{1}{(1-M)^5}\big) + \big(\tfrac{99}{4\pi^3} + \tfrac{n_f}{\pi^3}\big)\tfrac{1}{M^4} + \big(\tfrac{495}{4\pi^3} - \tfrac{5n_f}{\pi^3}\big)\tfrac{1}{(1-M)^4} \\ & +\big[\tfrac{1167}{16\pi^3} + \tfrac{35n_f}{18\pi^3} + \tfrac{n_f^2}{108\pi^3} - \tfrac{9}{2\pi}\big]\tfrac{1}{M^3} + \big[\tfrac{1893}{16\pi^3} + \tfrac{23n_f}{9\pi^3} - \tfrac{7n_f^2}{36\pi^3} - \tfrac{9}{2\pi}\big]\tfrac{1}{(1-M)^3} \\ & +\big[\tfrac{1653}{16\pi^3} + \tfrac{377n_f}{432\pi^3} - \tfrac{5n_f^2}{648\pi^3} + \tfrac{99}{16\pi} + \tfrac{5n_f}{24\pi} - \tfrac{243\zeta(3)}{4\pi^3}\big]\tfrac{1}{M^2} \\ & +\big[\tfrac{1653}{16\pi^3} - \tfrac{5049}{8(33-2n_f)\pi^3} + \tfrac{881n_f}{144\pi^3} + \tfrac{933n_f}{8(33-2n_f)\pi^3} - \tfrac{211n_f^2}{648\pi^3} \\ & -\tfrac{19n_f^2}{4(33-2n_f)\pi^3} + \tfrac{99}{16\pi} + \tfrac{5n_f}{24\pi} - \tfrac{243\zeta(3)}{4\pi^3}\big]\tfrac{1}{(1-M)^2} \\ & +\big[\tfrac{121}{192} - \tfrac{11n_f}{144} + \tfrac{n_f^2}{432} + \tfrac{73091}{96\pi^3} - \tfrac{6125n_f}{648\pi^3} + \tfrac{11n_f^2}{1944\pi^3} - \tfrac{389}{16\pi} - \tfrac{11\dot g_{1-1}}{4\pi} \\ & +\tfrac{8n_f}{27\pi} + \tfrac{\dot g_{1-1}n_f}{6\pi} - \tfrac{87\pi}{80} - \tfrac{1683\zeta(3)}{8\pi^3} + \tfrac{457n_f\zeta(3)}{108\pi^3}\big]\big(\tfrac{1}{M} + \tfrac{1}{1-M}\big)\,.\end{aligned} \tag{C.5}$$

The expression of the NNLO kernel in asymmetric variables can be obtained by inverting eq. (6.46), with the result

$$\begin{aligned}\chi_2^\Sigma \;=\;& \big(-\tfrac{9}{2\pi} + \tfrac{1167}{16\pi^3} - \tfrac{11n_f}{12\pi^3} + \tfrac{n_f^2}{108\pi^3}\big)\tfrac{1}{M^3} + \big(\tfrac{863}{16\pi^3} + \tfrac{33}{4\pi} - \tfrac{54\zeta(3)}{\pi^3} + \tfrac{235n_f}{432\pi^3} \\ & +\tfrac{2n_f}{9\pi} - \tfrac{5n_f^2}{648\pi^3}\big)\tfrac{1}{M^2} + \big(\tfrac{121}{192} + \tfrac{73091}{96\pi^3} - \tfrac{87\pi}{80} - \tfrac{389}{16\pi} - \tfrac{11\dot g_{1-1}}{4\pi} - \tfrac{1287\zeta(3)}{8\pi^3} \\ & -\tfrac{11n_f}{144} + \tfrac{8n_f}{27\pi} - \tfrac{6125n_f}{648\pi^3} + \tfrac{\dot g_{1-1}n_f}{6\pi} + \tfrac{133n_f\zeta(3)}{108\pi^3} + \tfrac{n_f^2}{432} + \tfrac{11n_f^2}{1944\pi^3}\big)\tfrac{1}{M} \\ & +\tfrac{54}{(1-M)^5\pi^3} + \big(\tfrac{1683}{8\pi^3} - \tfrac{31n_f}{4\pi^3}\big)\tfrac{1}{(1-M)^4} \\ & +\big(-\tfrac{9}{2\pi} + \tfrac{1893}{16\pi^3} + \tfrac{65n_f}{12\pi^3} - \tfrac{7n_f^2}{36\pi^3}\big)\tfrac{1}{(1-M)^3} \\ & +\big(\tfrac{33}{8\pi} + \tfrac{2137}{16\pi^3} - \tfrac{135\zeta(3)}{2\pi^3} + \tfrac{7n_f}{36\pi} + \tfrac{3811n_f}{432\pi^3} - \tfrac{211n_f^2}{648\pi^3}\big)\tfrac{1}{(1-M)^2} \\ & +\big(\tfrac{121}{192} + \tfrac{73091}{96\pi^3} - \tfrac{389}{16\pi} - \tfrac{87\pi}{80} - \tfrac{11\dot g_{1-1}}{4\pi} - \tfrac{1287\zeta(3)}{8\pi^3} - \tfrac{11n_f}{144} + \tfrac{8n_f}{27\pi} \\ & -\tfrac{6125n_f}{648\pi^3} + \tfrac{\dot g_{1-1}n_f}{6\pi} + \tfrac{133n_f\zeta(3)}{108\pi^3} + \tfrac{11n_f^2}{1944\pi^3} + \tfrac{n_f^2}{432}\big)\tfrac{1}{1-M}\,.\end{aligned} \tag{C.6}$$

Finally, the NNLO kernel for the evolution of the integrated parton density can be obtained from the unintegrated one through eq. (6.23). The difference in asymmetric

variables is given by

$$\begin{aligned}\chi_2^i(M)-\chi_2^u(M) &= \big(-\tfrac{55n_f}{18\pi^3}+\tfrac{5n_f^2}{27\pi^3}\big)\tfrac{1}{M^3}+\tfrac{3(-33+2n_f)}{2\pi^3}\tfrac{1}{(1-M)^3}\\ &\quad+\tfrac{12393-4938n_f+206n_f^2}{648\pi^3}\tfrac{1}{M^2}+\tfrac{-15147+1182n_f-16n_f^2}{108\pi^3}\tfrac{1}{(1-M)^2}\\ &\quad+\tfrac{1}{3888\pi^3}\big[-703890+37974n_f+284n_f^2+29403\pi^2\\ &\quad-1584n_f\pi^2-12n_f^2\pi^2+96228\zeta(3)-5832n_f\zeta(3)\big]\tfrac{1}{M}\\ &\quad-\tfrac{24543+705n_f-109n_f^2}{324\pi^3}\tfrac{1}{1-M}\,. \end{aligned} \tag{C.7}$$

Bibliography

[1] M. E. Peskin, D. V. Schroeder "*An Introduction to Quantum Field Theory*", Addison-Wesley, (1995).

[2] V. R. Barger, R. J. N. Phillips "*Collider Physics*", Addison-Wesley, (1987)

[3] R. K. Ellis, W. J. Stirling, B. V. Webber "*QCD and Collider Physics*", Cambrige University Press, (1996)

[4] W. A. Bardeen, A. J. Buras, D. W. Duke and T. Muta, Phys. Rev. D **18** (1978) 3998.

[5] S. Alekhin *et al.*, arXiv:hep-ph/0601012.

[6] J. R. Forshaw, D. A. Ross "*Quantum Chromodynamics and the Pomeron*", Cambrige University Press, (1996)

[7] R. P. Feynman, Phys. Rev. Lett. **23** (1969) 1415.

[8] J. D. Bjorken and E. A. Paschos, Phys. Rev. **185** (1969) 1975.

[9] H. J. Rothe "*Lattice Gauge Theories. An Introduction*", World Scientific.

[10] Y. L. Dokshitzer, Sov. Phys. JETP **46** (1977) 641 [Zh. Eksp. Teor. Fiz. **73** (1977) 1216].

[11] V. N. Gribov and L. N. Lipatov, Sov. J. Nucl. Phys. **15** (1972) 438 [Yad. Fiz. **15** (1972) 781].

[12] G. Altarelli and G. Parisi, Nucl. Phys. B **126** (1977) 298.

[13] G. Curci, W. Furmanski and R. Petronzio, Nucl. Phys. B **175** (1980) 27.

[14] W. Furmanski and R. Petronzio, Phys. Lett. B **97** (1980) 437.

[15] S. Moch, J. A. M. Vermaseren and A. Vogt, Nucl. Phys. B **688** (2004) 101 [arXiv:hep-ph/0403192].

[16] A. Vogt, S. Moch and J. A. M. Vermaseren, Nucl. Phys. B **691** (2004) 129 [arXiv:hep-ph/0404111].

[17] A. Vogt, Comput. Phys. Commun. **170** (2005) 65 [arXiv:hep-ph/0408244].

[18] A. J. Buras, Rev. Mod. Phys. **52** (1980) 199.

[19] J. C. Collins and D. E. Soper, Ann. Rev. Nucl. Part. Sci. **37** (1987) 383.

[20] A. Donnachie and P. V. Landshoff, Phys. Lett. B **296** (1992) 227 [arXiv:hep-ph/9209205].

[21] C. Augier *et al.* [UA4/2 Collaboration], Phys. Lett. B **316** (1993) 448.

[22] V. S. Fadin, E. A. Kuraev and L. N. Lipatov, Phys. Lett. B **60** (1975) 50.

[23] E. A. Kuraev, L. N. Lipatov and V. S. Fadin, Sov. Phys. JETP **44** (1976) 443 [Zh. Eksp. Teor. Fiz. **71** (1976) 840].

[24] E. A. Kuraev, L. N. Lipatov and V. S. Fadin, Sov. Phys. JETP **45** (1977) 199 [Zh. Eksp. Teor. Fiz. **72** (1977) 377].

[25] I. I. Balitsky and L. N. Lipatov, Sov. J. Nucl. Phys. **28** (1978) 822 [Yad. Fiz. **28** (1978) 1597].

[26] A. H. Mueller, Nucl. Phys. B **415** (1994) 373.

[27] A. H. Mueller and B. Patel, Nucl. Phys. B **425** (1994) 471 [arXiv:hep-ph/9403256].

[28] V. S. Fadin and L. N. Lipatov, JETP Lett. **49** (1989) 352 [Yad. Fiz. **50** (1989 SJNCA,50,712.1989) 1141].

[29] V. S. Fadin, R. Fiore and M. I. Kotsky, Phys. Lett. B **387** (1996) 593 [arXiv:hep-ph/9605357].

[30] V. S. Fadin, M. I. Kotsky and R. Fiore, Phys. Lett. B **359** (1995) 181.

[31] V. S. Fadin, L. N. Lipatov Nucl. Phys. B **406** (1993) 259.

[32] V. S. Fadin, M. I. Kotsky, L. N. Lipatov Phys. Lett. B **415** (1997) 97.
V. S. Fadin, M. I. Kotsky, L. N. Lipatov Phys. Atom. Nucl. **61** (1998) 641.

[33] V. S. Fadin, R. Fiore, A. Flachi, M. I. Kotsky Phys. Lett. B **422** (1998) 287.
V. S. Fadin, R. Fiore, A. Flachi, M. I. Kotsky Phys. Atom. Nucl. **62** (1999) 999

[34] V. S. Fadin, L. N. Lipatov Phys. Lett. B **429** (1998) 127.

[35] G. Camici and M. Ciafaloni, Phys. Lett. B **412** (1997) 396 [Erratum-ibid. B **417** (1998) 390] [arXiv:hep-ph/9707390].

[36] M. Ciafaloni and G. Camici, Phys. Lett. B **430** (1998) 349 [arXiv:hep-ph/9803389].

[37] V. Del Duca and E. W. N. Glover, JHEP **0110** (2001) 035 [arXiv:hep-ph/0109028].

[38] J. Bartels and C. Bontus, Phys. Rev. D **61** (2000) 034009 [arXiv:hep-ph/9906308].

[39] J. Bartels, L. N. Lipatov and A. S. Vera, arXiv:0802.2065 [hep-th].

[40] V. Del Duca and E. W. N. Glover, arXiv:0802.4445 [hep-th].

[41] S. Marzani, R. D. Ball, P. Falgari and S. Forte, Nucl. Phys. B **783** (2007) 143 [arXiv:0704.2404 [hep-ph]].

[42] M. Ciafaloni, Nucl. Phys. B **296** (1988) 49.

[43] S. Catani, F. Fiorani and G. Marchesini, Nucl. Phys. B **336** (1990) 18.

[44] S. Catani, M. Ciafaloni and F. Hautmann, Nucl. Phys. B **366** (1991) 135.

[45] S. Catani, M. Ciafaloni and F. Hautmann, Published in DESY HERA Workshop 1991:0690-711

[46] S. Catani, F. Hautmann Nucl. Phys. B **427** (1994) 475.

[47] J. C. Collins and R. K. Ellis, Nucl. Phys. B **360** (1991) 3.

[48] R. D. Ball and R. K. Ellis, JHEP **0105** (2001) 053 [arXiv:hep-ph/0101199].

[49] G. Camici and M. Ciafaloni, Phys. Lett. B **386** (1996) 341 [arXiv:hep-ph/9606427].

[50] G. Camici and M. Ciafaloni, Nucl. Phys. B **496** (1997) 305 [Erratum-ibid. B **607** (2001) 431] [arXiv:hep-ph/9701303].

[51] R. D. Ball, Nucl. Phys. B **796** (2008) 137 [arXiv:0708.1277 [hep-ph]].

[52] T. Jaroszewicz, Phys. Lett. B **116** (1982) 291.

[53] R. D. Ball and S. Forte, Phys. Lett. B **351** (1995) 313 [arXiv:hep-ph/9501231].

[54] R. D. Ball and S. Forte, Phys. Lett. B **359** (1995) 362 [arXiv:hep-ph/9507321].

[55] R. D. Ball and S. Forte, Phys. Lett. B **405** (1997) 317 [arXiv:hep-ph/9703417].

[56] R. D. Ball and S. Forte, Phys. Lett. B **465** (1999) 271 [arXiv:hep-ph/9906222].

[57] G. Altarelli, R. D. Ball, S. Forte Nucl. Phys. B **575** (2000) 313.

[58] G. Altarelli, R. D. Ball, S. Forte Nucl. Phys. B **599** (2001) 383.

[59] G. Altarelli, R. D. Ball, S. Forte Nucl. Phys. B **621** (2002) 359.

[60] G. Altarelli, R. D. Ball, S. Forte Nucl. Phys. B **674** (2003) 459.

[61] G. Altarelli, R. D. Ball, S. Forte Nucl. Phys. Proc. Suppl. **135** (2004) 163.

[62] R. D. Ball, S. Forte Nucl. Phys. B **742** (2006) 158.

[63] G. Altarelli, R. D. Ball and S. Forte, Nucl. Phys. B **742** (2006) 1 [arXiv:hep-ph/0512237].

[64] G. Altarelli, R. D. Ball and S. Forte, arXiv:0802.0032 [hep-ph].

[65] E. Eriksen, Journal of Math. Phys. **Vol.9-5** (1968) 790.

[66] P. Falgari, Laurea Thesis Milan University, April 2005.

[67] S. Marzani, Laurea Thesis Milan University, April 2005.

[68] M. Dittmar *et al.*, arXiv:hep-ph/0511119.

[69] M. Ciafaloni, D. Colferai and G. P. Salam, Phys. Rev. D **60** (1999) 114036 [arXiv:hep-ph/9905566].

[70] M. Ciafaloni, D. Colferai and G. P. Salam, JHEP **9910** (1999) 017 [arXiv:hep-ph/9907409]. PHRVA,D60,114036;

[71] M. Ciafaloni, D. Colferai, G. P. Salam and A. M. Stasto, Phys. Rev. D **68** (2003) 114003 [arXiv:hep-ph/0307188].

[72] M. Ciafaloni, D. Colferai, G. P. Salam and A. M. Stasto, JHEP **0708** (2007) 046 [arXiv:0707.1453 [hep-ph]].

[73] C. D. White and R. S. Thorne, Phys. Rev. D **75** (2007) 034005 [arXiv:hep-ph/0611204].

[74] G. P. Salam, JHEP **9807** (1998) 019 [arXiv:hep-ph/9806482].

[75] L. N. Lipatov, Sov. Phys. JETP **63** (1986) 904 [Zh. Eksp. Teor. Fiz. **90** (1986) 1536].

[76] J. S. Schwinger, Phys. Rev. **82** (1951) 664.

[77] S. D. Drell and T. M. Yan, Phys. Rev. Lett. **25** (1970) 316 [Erratum-ibid. **25** (1970) 902].

[78] G. Altarelli, R. K. Ellis and G. Martinelli, Nucl. Phys. B **157** (1979) 461.

[79] R. Hamberg, W. L. van Neerven and T. Matsuura, Nucl. Phys. B **359** (1991) 343 [Erratum-ibid. B **644** (2002) 403].

[80] J. Blumlein and V. Ravindran, Nucl. Phys. B **716** (2005) 128 [arXiv:hep-ph/0501178].

[81] B. Humpert and W. L. van Neerven, Nucl. Phys. B **184** (1981) 225.

[82] W. N. Bailey "*Generalised Hypergeometric Series*", Cambridge University Press (1935).

[83] J. Alcaraz *et al.* [LEP Collaborations and ALEPH Collaboration and DELPHI Collaboration an], arXiv:0712.0929 [hep-ex].

[84] J. R. Ellis, M. K. Gaillard and D. V. Nanopoulos, Nucl. Phys. B **106** (1976) 292; M. A. Shifman, A. I. Vainshtein, M. B. Voloshin and V. I. Zakharov, Sov. J. Nucl. Phys. **30** (1979) 711 [Yad. Fiz. **30** (1979) 1368].

[85] D. Graudenz, M. Spira and P. M. Zerwas, Phys. Rev. Lett. **70** (1993) 1372.

[86] M. Spira, A. Djouadi, D. Graudenz and P. M. Zerwas, Nucl. Phys. B **453** (1995) 17.

[87] R. Bonciani, G. Degrassi and A. Vicini, JHEP **0711** (2007) 095.

[88] M. Kramer, E. Laenen and M. Spira, Nucl. Phys. B **511** (1998) 523.

[89] A. Djouadi, M. Spira and P. M. Zerwas, Phys. Lett. B **264** (1991) 440.

[90] K. G. Chetyrkin, B. A. Kniehl and M. Steinhauser, Phys. Rev. Lett. **79** (1997) 2184 [arXiv:hep-ph/9706430]. K. G. Chetyrkin, B. A. Kniehl and M. Steinhauser, Nucl. Phys. B **510** (1998) 61 [arXiv:hep-ph/9708255].

[91] S. Dawson, Nucl. Phys. B **359** (1991) 283.

[92] C. Anastasiou and K. Melnikov, Nucl. Phys. B **646** (2002) 220;

[93] R. V. Harlander and W. B. Kilgore, Phys. Rev. Lett. **88** (2002) 201801;

[94] V. Ravindran, J. Smith and W. L. van Neerven, Nucl. Phys. B **665** (2003) 325.

[95] S. Moch and A. Vogt, Phys. Lett. B **631** (2005) 48.

[96] S. Catani, D. de Florian, M. Grazzini and P. Nason, JHEP **0307** (2003) 028.

[97] F. Hautmann, Phys. Lett. B **535** (2002) 159.

[98] A. V. Lipatov and N. P. Zotov, Eur. Phys. J. C **44** (2005) 559 [arXiv:hep-ph/0501172].

[99] V. Del Duca, W. Kilgore, C. Oleari, C. Schmidt and D. Zeppenfeld, Nucl. Phys. B **616** (2001) 367.

[100] R. S. Pasechnik, O. V. Teryaev and A. Szczurek, Eur. Phys. J. C **47** (2006) 429.

[101] L. Lewin "*Polylogarithms and associated functions*", Elsevier North Holland, (1981)

[102] S. Marzani, R. D. Ball, V. Del Duca, S. Forte and A. Vicini, Nucl. Phys. B **800** (2008) 127 [arXiv:0801.2544 [hep-ph]].

[103] A. D. Martin, R. G. Roberts, W. J. Stirling and R. S. Thorne, Eur. Phys. J. C **28** (2003) 455.

[104] C. Anastasiou, L. J. Dixon and K. Melnikov, Nucl. Phys. Proc. Suppl. **116** (2003) 193 [arXiv:hep-ph/0211141].

[105] C. Anastasiou, K. Melnikov and F. Petriello, Phys. Rev. Lett. **93** (2004) 262002 [arXiv:hep-ph/0409088].

[106] M. Ciafaloni, D. Colferai JHEP **0509**(2005) 069.

[107] M. Ciafaloni, D. Colferai, G. P. Salam, A. M. Stasto Phys. Lett. B **635**(2006) 320.

[108] R. K. Ellis, D. A. Ross and A. E. Terrano, Nucl. Phys. B **178** (1981) 421.

[109] D. A. Kosower and P. Uwer, Nucl. Phys. B **563** (1999) 477 [arXiv:hep-ph/9903515].